Kinetic investigation of the hydrolytic hydrogenation of oligosaccharides to sorbitol

Von der Fakultät für Mathematik, Informatik und Naturwissenschaften der RWTH Aachen University zur Erlangung des akademischen Grades einer Doktorin der Naturwissenschaften genehmigte Dissertation

vorgelegt von

M. Sc. Chem. Eng.
Leila Negahdar
aus Hamedan

Berichter:
Universitätsprofessor Dr. Regina Palkovits
Universitätsprofessor Dr. Marcel Liauw

Tag der mündlichen Prüfung: 12.12.2014

ACKNOWLEDGMENT

First and foremost, I would like to express my sincerest gratitude to my doctoral advisor, professor Regina Palkovits for her constant encouragement and support which made this work possible. She has been a great mentor. Her advice on research and numerous other academic matters has been invaluable.

I'm thankful to professor Marcel Liauw who kindly accepted the refereeing of this dissertation and provided valuable advice.

I would like to thank Dr. Stefan Palkovits for his valuable suggestions on numerous occasions.

This has been a delightful journey together with colleagues, coworkers whose companionship and support is most appreciated. My many thanks go to Elke Biener, Peter Hausoul, Irina Delidovich, Jens Oltmanns, Kai Schute, Florian Krebs, Steffen Heddrich, Philipp Grande and Stephan Sibirtsev.

My special thanks go to Noah Avraham for the time and effort she put into the measurements.

Last but not least, I would like to thank my family and friends for their presence and support.

ABSTRACT

The rare characteristics of sorbitol as a promising intermediate in biomass to biofuel conversion have attracted much research. Nevertheless, adequate understanding of the mechanism and kinetics of its reactions is still missing, mostly because of the complex molecular structure of the polysaccharides that are involved. This dissertation is the tale of our research on the kinetics and mechanism of sorbitol production through hydrolytic hydrogenation of oligosaccharides. Preceding research on this topic is almost entirely based on the controversial hypothesis that conversion of polysaccharides to sorbitol passes through a consecutive hydrolysis to monosaccharides followed by hydrogenation to sorbitol. Our research, on the other hand, reveals two competing reaction pathways, namely hydrolysis of oligosaccharides, and its hydrogenation to reduced form. More interestingly, at lower reaction temperatures the hydrogenation pathway becomes considerably dominant which is contrary to the widely accepted premise.

To overcome the molecular complexity of polysaccharides, we settled for model-molecules such as disaccharides and trisaccharides which have simple

structure and sufficiently resemble the polysaccharides. Most of our effort has been directed towards selective hydrolysis-hydrogenation of these model molecules over a catalytic system composed of molecular acids and supported metal catalysts.

Kinetic study of disaccharides showed that at lower reaction temperatures, the hydrogenation pathway is dominant whereas at higher reaction temperatures, direct hydrolysis of disaccharides becomes favorable. Analysis of kinetic data confirmed the hydrolysis reaction as the rate determining step. Kinetic investigation of trisaccharides also indicated that the hydrogenation proceeds faster than hydrolysis. At the same time, a facilitated hydrolysis of reduced trisaccharides compared with non-reduced counterpart was observed.

The study was extended to include oligosaccharides with longer chains, up to heptasaccharides, using the same underlying kinetic model. Despite growing complexity of the reaction network, the same kinetic selectivities i.e. the hydrogenation over hydrolysis as well as facile hydrolysis of reduced compounds were confirmed. Overall, a direct hydrogenation of oligosaccharides to reduced forms followed by hydrolysis appears as a superior sorbitol production pathway.

Contents

Nomenclature

η_e	external catalyst effectiveness factor
η_i	internal catalyst effectiveness factor
μ_L	dynamic viscosity of the liquid (kg $m^{-1}s^{-1}$)
ϕ	Weisz modulus
ρ_L	density of the liquid (kg m^{-3})
ρ_p	bulk density of catalyst particle (g cm^{-3})
ρ_{cat}	catalyst bulk density(kg m^{-3})
C_a	Carberry number
C_b	concentration in bulk liquid (mol m^{-3})
$C^*_{H_2}$	hydrogen solubility in liquid (cm^3 g^{-1})
D_e	effective diffusion coefficient (m^2 s^{-1})

D_k Knudsen diffusivity ($m^2\ s^{-1}$)

d_p catalyst particle diameter (m)

d_s stirring diameter (m)

DP degree of polymerization

E_a activation energy (k J mol^{-1})

H_{H_2} Henry constant (Pa l mol^{-1})

k_i reaction rate coefficient (s^{-1})

K_La volumetric gas–liquid mass transfer coefficient (s^{-1})

$k_{i,0}$ pre-exponential constant (s^{-1})

K_{Ls} liquid–solid mass transfer coefficient (s^{-1})

N_p power number

N_s stirring speed (s^{-1})

P_0 pressure at initial state before absorption (Pa)

P_1 pressure before saturation state (Pa)

P_2 pressure after absorption state (Pa)

r_p catalyst particle redius (m)

r_{obs} observed reaction rate (mol $m^{-3}\ s^{-1}$)

V_L volume of liquid (m^3)

a liquid–solid interface area ($m^2\ m^{-3}$)

C concentration (mol l^{-1})

D diffusion coefficient (m^2 s^{-1})

disac. disaccharide

K adsorption constant (m^3 m^3 $kg_{cat}{}^{-1}$)

n reaction order

P pressure (Pa)

P(n) oligosaccharide with length n

R ideal gas constant (Pa m^3 mol^{-1} K^{-1})

R(n) reduced oligosaccharide with length n

Re Reynolds number

re-disac. reduced disaccharide

re-trisac. reduced trisaccharide

Sc Schmidt number

Sh Sherwood number

T temperature (K)

t time (min)

trisac. trisaccharide

x conversion

List of Figures

List of Tables

CHAPTER 1

INTRODUCTION

The socioeconomic impact of energy consumption and supply is unquestionably immense. Also, the ongoing environmental crisis has made it imperative to find alternative energy resources. Finding clean renewable energy is now a global research endeavor [1, 2, 3]. Among various alternatives, biomass is a highly promising source of energy which is renewable and potentially sustainable. Lignocellulose and starch-base materials are the most abundant source of biomass, representing about 40–50% of dry weight of plants. They can be chemically altered to valuable fuels and platform chemicals such as glycerol, 3-hydroxypropionic acid, sorbitol, levulinic acid, xylitol, glucaric acid, bioethanol, acetic acid, D-lactic acid, etc [4, 5, 6].

These biopolymers (cellulose and starch) are composed of sugar chains joined by hydrogen bonding. In starch the glucose units are connected via α-1,4-glycosidic bonds (amylose), while in cellulose the glucose units are connected via β-1,4-glycosidic bonds (Figure 1.1) [7].

Cellulose chains in primary plant cell walls have degrees of polymerization ranging from 5000 to 7500 glucose units, and in wood and cotton-based materials

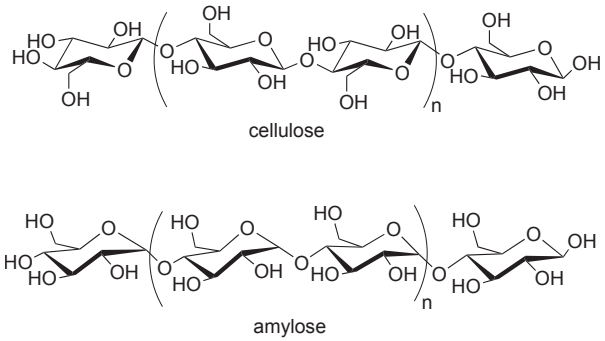

Figure 1.1: Structure of cellulose and amylose.

between 10000–15000. The basic repeating unit of cellulose is cellobiose, the β-(1-4) linked disaccharide of D-glucopyranose. Cellulose is insoluble in water and most conventional solvents. It has a crystalline structure and harsh conditions such as high temperatures or high acid concentrations are needed to deconstruct the polymer and release the monomers from the tightly associated chains [8].

Starch is composed of two kinds of polysaccharides; amylose and amylopectin. The amylose has linear glucose linkages and amylopectin has both linear and about 5% branched linkages. Starch is insoluble in water and has partially crystalline structure. Depending on the source of the starch the degree of polymerization varies between 300–4000 in amylose and 104–105 in amylopectin with the repeating unit maltose, an α-(1-4) linked disaccharide of D-glucopyranose [9].

In order to make polysaccharides accessible to further transformations, depolymerization process is necessary. The depolymerization is the process of converting polysaccharides into mono- and oligosaccharides that are soluble in an aqueous environment. To date a variety of depolymerization methods have been developed, mostly including pre-hydrolysis with acid or alkaline solution, dissolution in ionic liquids, or applying a mechanocatalytic depolymerisation by milling in the presence of acids [10, 11, 12, 13, 14]. A depolymerization under

optimal conditions allows to reduce the degree of polymerization of polysaccharides significantly. Acid hydrolysis is among the oldest and prevalent pretreatment techniques. Two different methods are widely used for acid hydrolysis of polysaccharides. The first method uses a high concentration of acids and low operation temperatures. The major drawbacks of this method are the high cost of acid recovery and the need for expensive construction materials. In the second method, a highly diluted acid at high operation temperatures is utilized. This method is more favorable and most frequently applied [15, 16].

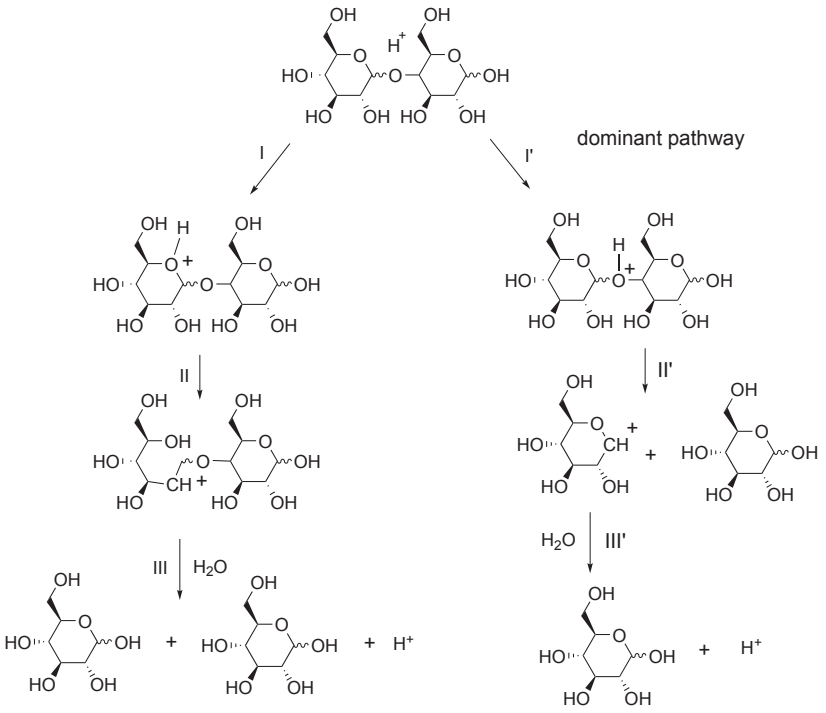

Figure 1.2: Acid hydrolysis mechanism, depicted from [17].

During acid hydrolysis, the glycosidic bonds of polysaccharides are cleaved to yield sugar oligomers. Acid hydrolysis of polysaccharides typically occurs via protonation of the glycosidic bond to form a conjugated acid, leading to cleavage of the glycosidic bond along with addition of a water molecule to release both

glucose or oligomers and a hydrogen ion (Figure 1.2) [18].

Hydrolysis of polysaccharides is a complex process involving multiple reaction steps and transfer phenomena. Typically, the hydrolysis includes a sequence of first-order reactions: the hydrolysis of polysaccharides to oligosaccharides and subsequently, to monosaccharides, followed by further degradation of monosaccharides. However, understanding the kinetics and mechanisms of hydrolysis of polysaccharides is of great importance while depolymerization via hydrolysis paves the way for further catalytic transformation.

1.1. ACID HYDROLYSIS KINETICS

Kinetics of polysaccharide hydrolysis especially cellulose have been widely studied. The majority of kinetic studies proposed a lumped model in which the polymer and all oligomers were considered as one substrate. Whereas some models took into account the formation of oligomers as intermediate. The kinetics of hydrolysis reaction were also investigated by using depoymerization concepts and model compounds. A brief overview of kinetic models described in the literature for hydrolysis of linear polysaccahrides will be discussed in the following sections.

1.1.1. CONVENTIONAL KINETIC MODEL

Various kinetic studies on the acid catalyzed hydrolysis of polysaccharides have been reported in literature. The first systematic kinetic study on biomass hydrolysis was reported by Saeman in 1945 [19]. Hydrolysis was assumed to be pseudo homogeneous first order and to follow two consecutive reactions:

$$\text{cellulose} \xrightarrow{k_1} \text{glucose} \xrightarrow{k_2} \text{degradation products} \tag{1.1}$$

The reaction rate equations describing cellulose and glucose concentrations are as follows:

$$\frac{dC_{cellulose}}{dt} = -k_1 C_{cellulose} \tag{1.2}$$

$$\frac{dC_{glucose}}{dt} = k_1 C_{cellulose} - k_2 C_{glucose} \tag{1.3}$$

the reaction rate constants (k_i) follow an Arrhenius temperature dependence with including acid concentration as shown as following equation:

$$k_i = k_{0,i}[A]^m e^{\frac{-E_a}{RT}}, \tag{1.4}$$

where $k_{0,i}$ is the pre-exponential factor, [A] is acid concentration, and m is an empirical exponent.

Numerous kinetic studies on biomass hydrolysis between 1945 and 1990 applied the kinetic model developed earlier by Saeman. A literature overview of kinetics of acid hydrolysis of polysaccharides at different acid concentrations and temperatures is presented in the Table 1.1. The apparent activation energies of different sources of polysaccharides vary in a broad range of 105-188 kJ mol^{-1}. For example higher activation energies have been determined for kraft and filter paper, whereas lower ones are obtained for sugarcane and wheat straw. This indicated that the simple kinetic model for hydrolysis cannot be applied on the entire range of temperatures and acid concentrations.

Since the first kinetic model proposed by Saeman, several modifications were added to include additional factors. The most recent modified model for dilute acid hydrolysis of cellulose includes the presence of soluble oligomeric intermediates which were found in non-negligible quantities during hydrolysis at high temperatures and low acid concentrations. The conversion of oligomers to glucose is two to three times faster compared to the hydrolysis of cellulose to soluble oligomers; therefore, oligomer formation initially was not recognized [22]. Abatzoglou et al. reported the presence of oligomers in significant amounts in the

Substrate	Temp./° C	Acid conc.	E_a/kJ mol^{-1}	Reference
Inulin	7-100	pH 2-4.2	109	[20]
Sugarcane bagasse	100-128	2-6 wt%	109	[21]
α-cellulose	220-240	0.2-1 wt%	177	[22]
Kraft paper	180-240	0.2-1 wt%	188	[23]
Douglas fir	170-190	0.4-1 wt%	179	[19]
Arabinogalactan	80-100	1 M, pH 1	135	[24]
Solka-floc	180-240	0.5-2 wt%	177	[25]
Filter paper	200-240	0.4-1.5 wt%	178	[26]
Paper refuse	180-240	0.2-1 wt%	137	[23]
Municipal solid wastes	200-240	1.3-4.4 wt%	171	[27]
Poplar	140-160	0.49 wt%	176	[28]
Sunflower residues	110-140	0.5-6 wt%	101	[29]
Corn straw	95-160	0.6-1.2 wt%	130	[28]
Switchgrass	160-189	0.6-1.2 wt%	169	[28]
Hardwood	170-190	4.41-12.2 wt%	165	[30]
Corn cobs	140-170	0.47-1.95 wt%	148	[31]
Microcrystalline cellulose	25-40	30-70 wt%	127	[32]
Wheat straw	95-160	0.5 wt%	105	[33]

Table 1.1: Literature overview on the kinetics of polysaccharides hydrolysis.

initial stages of a diluted acid hydrolysis of cellulose. Therefore, the Saeman model was modified according to equation 1.5 :

$$\text{cellulose} \xrightarrow{\alpha k_1} \text{oligosaccharides} \underset{\gamma k_2}{\overset{\beta k_1}{\leftrightarrows}} \text{glucose} \xrightarrow{k_2} \text{degradation products} \quad (1.5)$$

In their proposed mechanism, three possibilities were considered: (1) the reaction of oligomers to glucose is equilibrium; (2) the hydrolysis of oligomers to glucose is not in equilibrium; and (3) there are no repolymerization reactions

from glucose to oligomers. The third model was in agreement with experimental data. They suggested two-step reactions in which the reaction of cellulose to oligomers is catalyzed in a first stage followed by the oligomer to glucose reaction in a second stage under milder conditions. Including oligomers as intermediate appeared to be important in distinguishing the performance of hydrolysis and also helped to explain the deviations of models from experimantal data.

Also, kinetic model proposed by Samean predicted only glucose yields up to 60-65% during acid hydrolysis of cellulose [19]. Some kinetic models have been proposed to explain this yield by considering the possibility of hydrolysis of a part of cellulose which might be responsible for the observed limited yield. Conner et al. incorporated a reaction with two fractions of cellulose, one more easily hydrolyzed than the other and also transformation of glucose into possible products (Figure 1.3). The results of this model indicate that the degradation of glucose is a main reason for the low glucose yields observed during acid hydrolysis [34].

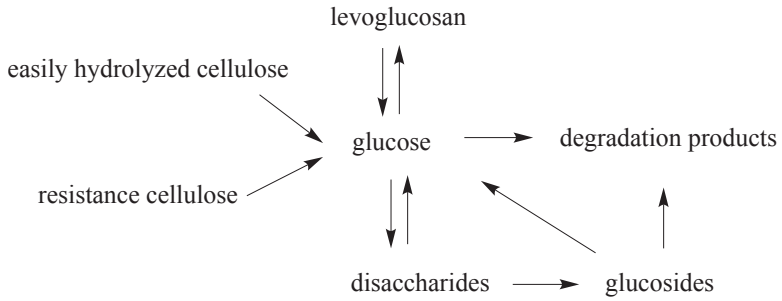

Figure 1.3: Modified kinetic model for cellulose hydrolysis including two fractions, depicted from [34].

Another important modification concerns a parasitic pathway during hydrolysis. Mok and Antal reported that a portion of cellulose or insoluble oligomers cannot be hydrolyzed to glucose. Their proposed mechanism led addition of

a parasitic pathway competing with acid-catalyzed hydrolysis. Based on these observations, another reaction network was suggested (Figure 1.4) [35].

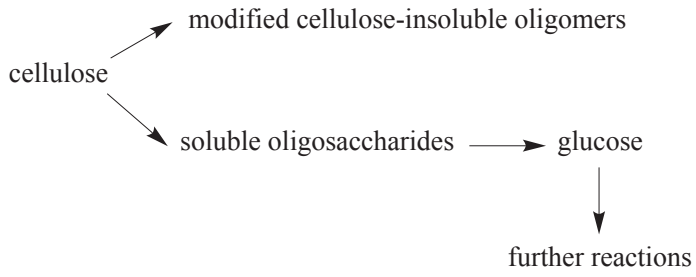

Figure 1.4: Modified kinetic model for cellulose hydrolysis including parasitic pathway, depicted from [35].

This model implies that low glucose yields are not necessarily only due to glucose degradation or reversible reactions instead a parallel pathway should be incorporated into the kinetic model to enable an accurate predication of the glucose yields.

Bouchard et al. applied thermogravimetric analysis, differential scanning calorimetry, and diffuse reflectance to study the chemical structure of remaining cellulose after hydrolysis [36]. They found that there is a significant change

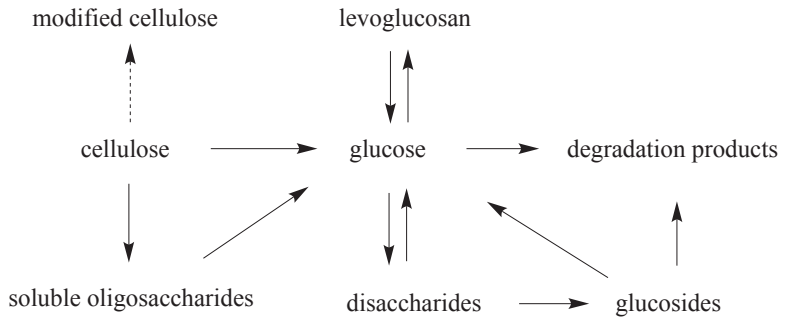

Figure 1.5: Modified kinetic model for cellulose hydrolysis including modified cellulose, depicted from [36].

in the chemical structure compared to unhydrolyzed cellulose. Therefore, the remaining cellulose is modified during hydrolysis and cannot be analytically identified. According to this observation they suggested to consider a new kinetic pathway for cellulose degradation facilitating the prediction of conversion and sugar yields (Figure 1.5).

Several studies reported that the neutralizing capacity of the used substrate should be included in the kinetics [28, 36, 37]. Cahela et al. founded that minerals in the substrate would neutralize up to 70 % of the acid [37]. Therefore, in the rate equation the molar hydronium ion [H_3O^+] was replaced by acid concentration (Eq. 1.6) [38].

$$k_i = k_{0,i}[H_3O^+]^m e^{\frac{-E_a}{RT}} \tag{1.6}$$

Conner et al. defined the molar hydronium ion [H_3O^+] in which the acid concentration was calculated from the neutralizing capacity of the substrate and the concentration of the used acid (Eq. 1.7) [34].

$$[H_3O^+] = \text{molar of acid} - \text{molar of cations} \tag{1.7}$$

Another correlation was suggested by Malester et al. applying pH as a measure of acidity as follows [27]:

$$k_i = k_0 \; exp(\frac{-E_a}{RT} - 2.303 \; pH) \tag{1.8}$$

Replacing weight percent of acid concentration by pH or [H_3O^+] showed more accurate kinetic constants obtained from kinetic modeling.

1.1.2. DEPOLYMERIZATION KINETIC MODEL

The acid hydrolysis of polysaccharides specially cellulose has been studied applying kinetics of depolymerization considering variation of the molecular weight

distribution. Unfortunately, little work has been reported so far with regard to the use of depolymerization models in polysaccharides hydrolysis. Before Saeman reporting his first-order kinetic model, depolymerization models based on random and nonrandom scission of long polymer chains were reported by Simha in 1941 [39]. The kinetics of degradation were investigated according to two aspects: (1) a determination of the distribution of all possible chain lengths at different stages of the reaction; (2), the change of average molecular weight with time. The average degree of polymerization ($\overline{DP}$) was defined by following equation:

$$\overline{DP} = 1 - exp(-kt) \tag{1.9}$$

From the results of this model, cellulose hydrolysis was best described with the assumption of a faster bond cleavage at the ends of chains faster compared to internal glycosidic bonds.

In most depolymerization studies, the hydrolysis process is characterized by following the evolution of the chain scissions and the degree of polymerization with time utilizing a kinetic model derived from the first or pseudo-zero order Ekenstam's equation [40, 41]:

$$\frac{1}{DP} - \frac{1}{DP_0} = kt \ , \tag{1.10}$$

where DP_0 is the initial value of the degree of polymerization and DP is degree of polymerization at a certain time t. These studies are usually supported by experimental data. However, since the scission of bonds is not a variable easy to determine, the degradation of the polymer is often studied by monitoring the weight loss [42, 43].

In many depolymerization studies, a single step first order models was preferred compared to multistep reactions. For example in case of multistep kinetic

models, the formation of other intermediates in the mixture will be considered. Such intermediates are difficult to identify or quantify. On the other hand, a high number of parameters should be considered which makes the model complex. Nevertheless, most reports suggested a single step model of depolymerization by taking the scission of the glycosidic bonds into account to simulate the weight loss behavior during hydrolysis [42, 44].

Significant insights into the kinetics and mechanisms of the depolymerization of linear polysaccharides have been achieved by advanced of analytical methods such as gel permeation chromatography (GPC) which enabled the determination of the molecular weight distribution [45].

Hydrolysis of amorphous cellulose in cotton-based paper was studied using GPC to obtain a more detailed picture of the course of reaction. The progress of the molecular weight distribution in the course of the reaction indicated that the hydrolysis proceeded in several stages. In stage I, the amorphous chains will be broken once causing a large decrease of the degree of polymerization. Stage II, the amorphous chains will be broken again in the region near to the end of amorphous segments producing free oligomers. During stage III, most of hydrolysis will occurred on very short amorphous segments. Kinetic analysis showed that hydrolysis of intact amorphous regions of cellulose is slow and can be described by a first order reaction [46].

Another approach to analysis the depolymerization kinetics of polysaccharides is using a Monte Carlo model. The basis of this method is to construct a kinetic model based on probability. In this approach the reaction rate constants will be consider as "probabilities per unit time". Thus, depolymerization in term of the scission of the chain will happen with a certain probability [47].

$$Prob_i = 1 - e^{k_i \Delta t}, \qquad i = 1, 2 \tag{1.11}$$

The polymer will be considered as a Markov chain, a group of parallel subsystems, each being composed of a single bond (Figure 1.6). It should be noted that this method does not estimate the reaction rate constants rather than using known values to predict the progress of depolymerization. In fact, in the Monte Carlo approach kinetic information obtained from a model compound will be used to predict the course of depolymerization.

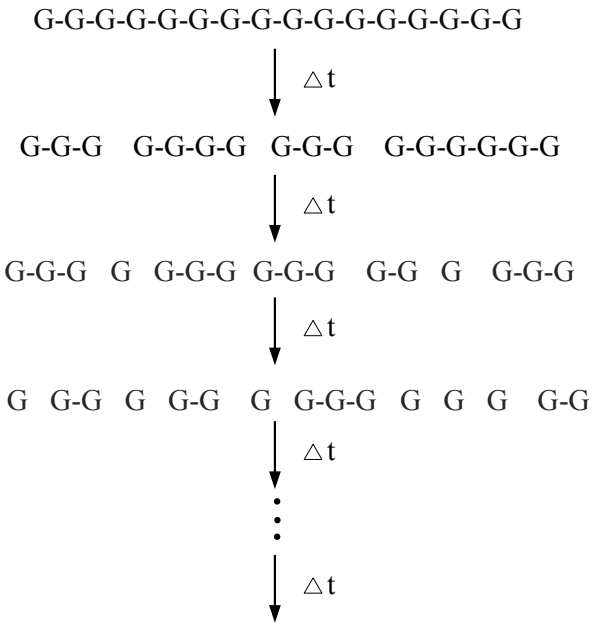

Figure 1.6: Monte Carlo depolymerization scheme; G(glucose unit), depicted from [48].

Different assumptions have been applied to the depolymerization model of linear polysaccharides when using the Monte Carlo method [39, 49]:

1. The rate of cleavage is the same for all bonds and is independent of the position in the chain.

2. There is a preferential cleavage at the ends of the chain.

3. There is a progressive change in the rate of cleavage as a function of the distance from the ends of the chains.

Acid hydrolysis of glycosidic bonds in polysaccharide has been described by using Monte Carlo method. In this study, a Monte Carlo procedure was developed to simulate amylose depolymerization using kinetic information obtained from cellobiose hydrolysis. The simulation permitted to foresee the time evolution of product distribution upon substrate depolymerization [47]. Dadach et al. simulated the acid hydrolysis of cellulose at high temperatures using a Monte Carlo method. For the simulation, kinetic information related to hydrolysis of cellobiose and morphological aspects of cellulose including crystalline, semi-amorphous, and amorphous zones have been considered. In the model both cleavage of a glycosidic bond and the degradation of glucose were assumed to be two irreversible reactions in series. The simulation indicated that for all temperatures, the overall glucose disappearance rate constant was higher than the experimental constant obtained from degradation of pure glucose. These results showed that the reversible reactions from glucose will increase during acid hydrolysis of cellulose [48].

1.1.3. KINETICS WITH MODEL COMPOUNDS

Kinetic studies with model compounds is performed with the aim to obtain more detailed kinetic information for optimizing the reaction condition and catalyst performance. In a kinetic study reported by Bobleter et al., cellobiose as model compound of cellulose was used to investigate the behavior of hydrothermal and diluted acid hydrolysis. The region where acidic hydrolysis turns into hydrothermolysis was subject of special interest. This region was best analyzed at relatively high temperatures and low acid concentrations. The experimental

results suggested a first order kinetic:

$$\text{cellobiose} \xrightarrow{k_1} \text{glucose} \xrightarrow{k_2} \text{degradation products} \tag{1.12}$$

Their results showed that reaction rate constants for the glucose formation and glucose degradation (k_1/k_2) have little dependency on temperature. Dependency of acid concentration on the reaction rate was investigated. At pH 2–3, the rate of hydrolysis was proportional to the acid concentration but, pH between 3 and 4.7 had no influence on the reaction rate. The analysis with Zucker-Hammett plot for acid hydrolysis and hydrothermolysis also showed a deviation of the hydrolysis rate in the pH 3–4.7. From these observations, they concluded that the hydrothermolysis follows a reaction mechanism different from acidic hydrolysis [50].

Another study compared hydrothermolysis with acidic hydrolysis of carbohydrates. The hydrothermolysis of cellobiose in the range 180 – 249 °C has been carried out. Kinetic analysis of the reaction showed that 60% of cellobiose was converted into glucose, and 40% into other products. The results indicated that, during hydrothermolysis, cellobiose is involved in at least one parallel reaction pathway. The proposed reaction network is as follows:

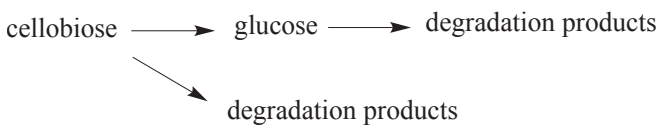

Figure 1.7: Kinetic model for cellobiose hydrolysis including parallel pathway, depicted from [51].

Interpretation of the kinetic data pointed out that the possibility of cellobiose hydrolysis to glucose is 50% higher than the simultaneous reaction path of cellobiose to degradation products (see Figure 1.7). Their study on pH-dependency

of hydrothermolysis also showed that hydrothermolysis differs from acidic hydrolysis and it is not dependent on pH, at least in the range from 3-7 [51].

Acid hydrolysis of cellobiose was discussed by Moiser et al. with the aim to characterize the optimum pH region for cellulose hydrolysis. Results showed that acid catalyzed hydrolysis is proportional to $[H_3O^+]$ concentration and varies for different acids. For example, carboxylic acids did not catalyze the degradation of glucose while sulfuric acid catalyzed this degradation. Therefore, overall yields of glucose obtained from cellobiose and cellulose are higher for the carboxylic acid, maleic acid, when compared to sulfuric acid at equivalent solution pH [16].

The kinetics of hydrolysis of oligosaccharides were studied to gain insights into the rate of hydrolysis of different bond positions and the effects of chain length on the overall hydrolysis rate. In some studies trimers were selected as model compound has been selected. The rate of acid catalyzed hydrolysis of cellotriose was investigated by Freudenberg et al. to compare the reactivity of glycosidic bonds during hydrolysis.

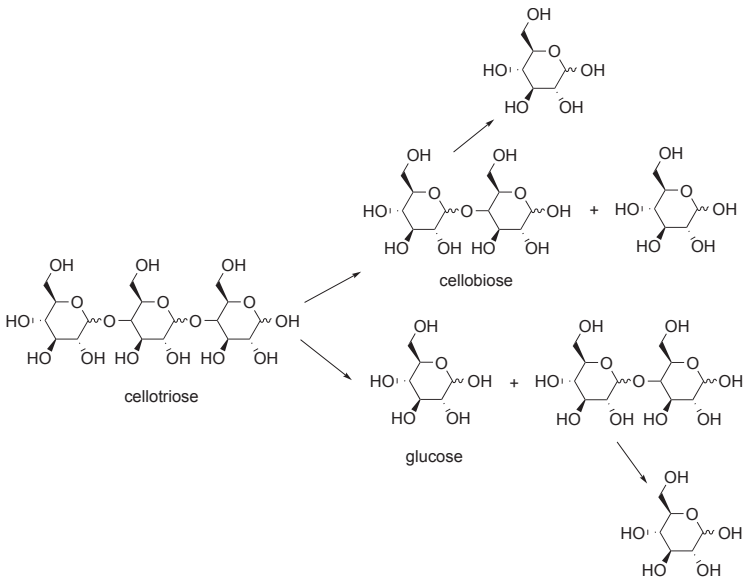

Figure 1.8: Kinetic model for cellotriose hydrolysis, depicted from [52].

In this study the change in the reduction potential of acid solution with time was used as a measure of the hydrolysis. The proposed reaction network is summarized in Figure 1.8. Their study indicated that the specific rates of hydrolysis of two glycosidic bonds are equal but different from the rate for cellobiose [52].

In another study reported by Feather and Harris, cellotriose was labeled specifically at one end. Labeled cellotriose (cellotriose-1-^{14}C) was partially hydrolyezed using sulfuric acid at different temperatures. Their investigation pointed out that the glycosidic bond adjacent to the nonreducing end of cellotriose is hydrolyzed at about 1.5 times faster than the bond adjacent to the reducing end, and at a rate nearer to that for cellobiose [53].

In addition, the rate constants for hydrolysis of the individual glycosidic bonds of maltotriose and maltohexaose have been determined by radioactively labeling the reducing D-glucose residue. The hydrolysis was described by using two rate constants for hydrolysis of the reducing and non reducing end of the oligomer (Figure 1.9). The obtained data emphasized that the rate constant for hydrolysis of the non- reducing end of the chain (k_1) is 1.8 times compared to the value for the other glycosidic bonds (k_2) [54].

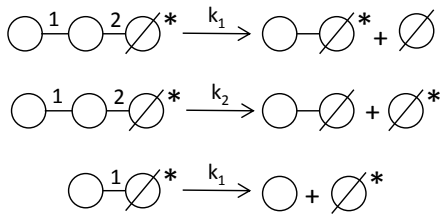

Figure 1.9: Kinetic model for maltotriose hydrolysis, depicted from [54].

Amylose has been labeled on either reducing or non-reducing end with D-glucose ^{14}C to determine the reactivity of different bonds. This study confirmed that the terminal bonds are preferentially hydrolyzed and their rate of hydrol-

ysis is faster [55]. The depolymerization of oligosaccharides with a degree of polymerization between 2-7 has been studied to determine the influence of the chain length on the rate of hydrolysis. From the kinetic results different explanations for the differences in rates of hydrolysis have been suggested in literature such as (1) the bonds of both reducing and nonreducing terminal residues are hydrolyzed at a higher rate than others, (2) the bond at the reducing end is hydrolyzed at higher rate than others, (3) the rate of hydrolysis decreases from the terminal bonds towards the interior bonds, (4) all bonds in oligosaccharides are hydrolyzed at the same rate and this rate is dependent on chain length [55].

1.2. HYDROLYTIC HYDROGENATION OF POLYSACCHARIDES

Recently, the production of biofuels and value-added chemicals from polysaccharides has gained much attraction. Special attention has been devoted to the conversion of polysaccharides into sorbitol. Sorbitol has several application areas [11]. It is used as precursor in food and pharmaceutical industry and as platform chemical for the synthesis of chemical compounds such as isosorbide, sorbitan, glycerol, L-sorbose, ethylene glycol, propylene glycol, etc [56, 57]. Further transformation of sorbitol into alkanes as well as efficient aqueous phase reforming for hydrogen generation has been demonstrated (Figure 1.10) [58]. Additionally, sorbitol has been selected as one of the top 12 value-added products from biomass by the US Department of Energy because of its potential to be used as source for fuels production Sorbitol can be produced selectively from hydrolysis-hydrogenation of polysaccharides. From literature, polysaccharides can be hydrolyzed into glucose and subsequently hydrogenated into sorbitol. Generally, the conversion of polysaccharides to sorbitol necessitates acid and metal catalysts, for hydrolysis and hydrogenation, respectively. Molecular acids

can be used together with supported metal catalysts as catalytic system. It is reported that catalytic systems containing molecular acids such as H_2SO_4, HCl or heteropoly acids combined with supported metal catalysts like Pt, Pd and Ru could efficiently catalyze the conversion of cellulose to sorbitol [5, 59, 60, 61]. Recently, the hydrogenation of the mechanocatalytic pre-hydrolysis of cellulose over Ru/C yielded up to 94% of sorbitol [10]. Sorbitol can also be produced selectively e.g. via hydrogenation of a hydrolysed starch solution in the presence of catalysts such as Raney nickel or Ru/C [62, 63]. However, the conversion of

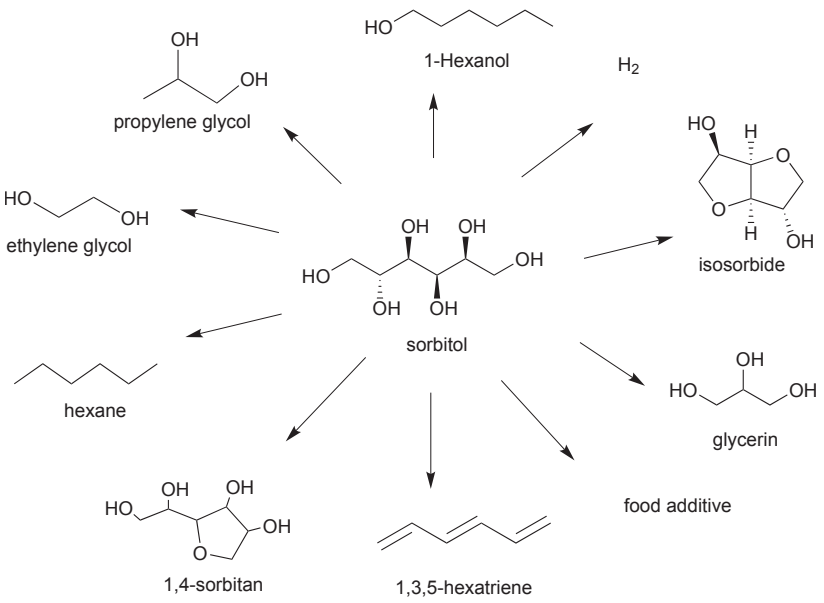

Figure 1.10: Products obtained from sorbitol.

polysaccharides to sorbitol involves both hydrolysis and hydrogenation reactions. Acid hydrolysis is homogeneous while hydrogenation is mostly heterogeneously catalyzed reaction and takes place on the surface of a solid catalyst. Therefore, hydrogenation and hydrolysis exhibit different kinetics and mechanism and should be considered separately.

1.3. HYDROGENATION REACTION KINETICS

In kinetic study of heterogeneous catalyzed reactions, more factors need to be considered than when dealing with homogeneous catalyzed reactions. For a solid-catalyzed reaction, the rate depends on the reactant concentrations on the catalyst surface [64]. Therefore, the rate will be defined per unit surface area of catalyst. Since the surface area is not as easily or accurately determined, instead the mass of the catalyst will be used. The mechanisms of heterogeneously catalyzed reactions can in principle be described by a sequence of reaction steps. Reaction on the surface includes several steps:

- Diffusion of reactants to the external surface of the catalyst and into the pores
- Adsorption of reactants on the active sites of catalyst
- Reaction on the surface between adsorbed reactants or between adsorbed species and a reactant in the fluid phase
- Desorption of the products
- Diffusion of products out of the catalyst pores into the fluid

All the steps assumed to have equal rate when the system is at steady state. Typically, it is assumed that the overall reaction rate is controlled by one step. Therefore, knowing which step limits the rate is key to develop a kinetic model [65]. For reactions on the surface, the Langmuir isotherm will be used to describe adsorption of reactant on the unoccupied site of a catalyst s which can be denote as $A + s \longrightarrow A_s$. The vacant sites of the catalyst is expressed as (1 - θ), where θ is the fraction of occupied sites. Then, the rate of adsorption and desorption of

reactant will be defined as follows:

$$r_{ads,A} = k_1 C_A(1-\theta)$$
$$r_{des,A} = k_2\theta \tag{1.13}$$

At equilibrium the rates of adsorption and desorption are equal:

$$k_1 C_A(1-\theta) = k_2\theta \tag{1.14}$$

The ratio of the adsorption and desorption rate constants (k_1/k_2) is the equilibrium constant (K_A). The Langmuir isotherm equation will be defined as following equation:

$$\theta = \frac{K_A C_A}{1 + K_A C_A} \tag{1.15}$$

The use of Langmuir isotherms to interpret kinetic data was proposed by Hinshelwood [66]. In this model, surface reaction rates are assumed to depend on the fraction of sites covered by different species. Thus for a simple reaction where the products are not adsorbed or are very weakly adsorbed, the kinetic model will be express as follows:

$$A_s \longrightarrow B + s$$
$$r = k\theta_A = \frac{kK_A C_A}{1 + K_A C_A} \tag{1.16}$$

The reaction kinetic model will be further simplified under some special reaction conditions. For example at low concentration of reactant A, the reaction would appear first order and zero order at very high concentration. For a reaction between two molecules that are competitively adsorbed on the same type of sites of the catalyst, the reaction rate depends on the probability that the molecules are on the sites. The reaction rate will be defined as the product of the coverages:

$$A_s + B_s \longrightarrow C_s + D_s$$

$$r = k\theta_A\theta_B = \frac{kK_AC_AK_BC_B}{(1 + K_AC_A + K_BC_B + K_CC_C + K_DC_D)^2} \tag{1.17a}$$

Another model to consider is the reaction of adsorbed molecules of A with molecules of B from the fluid phase. This model was proposed by Rideal and Eley as an alternative to the Langmuir–Hinshelwood models. The reaction rate is assumed to be proportional to the fraction of the surface covered by A and the concentration of B in the fluid:

$$A_s + B \longrightarrow C$$

$$r = k\theta_AC_B = \frac{kK_AC_AC_B}{1 + K_AC_A} \tag{1.18}$$

It predicts that the reaction is first order in B, the reactant from the fluid phase, and varying order to the reactant A [65]. Assuming that no product is adsorbed and a non-competitive adsorption of reactants occurs, the model will be modified to Langmuir–Hinshelwood–Hougen–Watson kinetics [67]:

$$A_s + B_s \longrightarrow C + D$$

$$r = k\theta_A\theta_B = \frac{kK_AC_AK_BC_B}{1 + K_AC_A} \tag{1.19}$$

In hydrogenation, the mode of hydrogen adsorption is important for the formulation of the rate equation. Hydrogen can adsorb dissociatively or it can appear on the catalyst surface in molecular form. The latter case is mostly reported [68].

1.4. SCOPE AND OUTLINE

As mentioned before, sorbitol is a platform chemical which can be produced selectively via the hydrolytic hydrogenation of polysaccharides. Several studies

have focused on the design of catalytic systems that convert polysaccharides to sorbitol in order to maximize productivity. However, only a few mechanistic investigations are available and a complete kinetic model describing the catalytic conversion of polysaccharides to sorbitol is still missing. Mechanistic studies and reaction kinetics can provide an insight into the reaction pathways and help to identify the key intermediate compounds of the reaction network. Such studies allow for a quantitative description of the influence of reaction conditions on reaction rates and the selectivity of the desired products. Therefore, a kinetic analysis facilitates the improvement of catalytic performance and the rationalizing of process development. The aim of this work is to gain insights into the reaction mechanism and kinetics of the catalytic conversion of polysaccharides to sorbitol. Polysaccharides have a complex molecular structure rendering a comprehensive kinetic study of their transformation difficult. To overcome this complexity, we investigated the hydrolytic hydrogenation of simpler molecules with the same monomeric unit and shorter chain length, namely; disaccharides, trisaccharides, and oligosaccharides. Recent reports on the catalytic conversion of cellulose to sugar alcohols indicated that heteropoly acids (silicotungstic acid) together with Ru/C can efficiently convert cellulose to sorbitol with yields up to 81% [61]. Therefore, in the presented study the same catalytic conditions were applied to have optimum reaction conditions. In order to study the kinetics of this heterogeneously catalyzed reaction, it is crucial to verify mass transfer limitations. In chapter 2, the absence of mass transfer limitations was verified by applying experimental investigations as well as literature criteria. Chapter 3 focuses on the reaction mechanism and kinetics of a catalytic conversion of disaccharide to sorbitol. Possible reaction pathways and key intermediate compounds of this reaction are investigated and kinetic models covering different reaction temperatures are developed. In chapter 4, trisacchrides were chosen

as model compounds of polysaccharides to gain further insights concerning the significance of hydrogenation-hydrolysis sequences within the overall reaction networks. A systematic kinetic analysis has been carried out providing a quantitative interpretation of the reaction pathways. A detailed kinetic study and modeling of the transformation of oligosaccharide to sorbitol is carried out in chapter 5. Based on basic stochastic assumptions, the choice of reaction mechanism and kinetics is justified. Kinetic rate constants are estimated for the kinetic model to closely resemble the experiments. The experimental results confirm the hypothesized reaction pathways and selectivities. Chapter 6 concludes this work and addresses some possible extensions.

CHAPTER 2

TRANSPORT ANALYSIS

Portions of this chapter have been published in "L. Negahdar, J. U. Oltmanns, S. Palkovits, and R. Palkovits, Kinetic investigation of the catalytic conversion of cellobiose to sorbitol, Applied Catalysis B: Environmental, 147(0):677–683, 2014".

In the reaction kinetic analysis, it is necessary to verify the absence of mass transfer limitations and examine the influence of reaction conditions on the selectivity of products. In the catalytic heterogeneous reactions with a gas–liquid–solid system, mass transfer plays an important role. The overall reaction rate of these multiphase catalytic processes could be limited by mass transport. In the case of three-phase catalytic hydrogenation, the following mass transfer processes should be considered (Figure 2.1): gas–liquid mass transfer, transport of the dissolved gas and dissolved reactants from the liquid bulk to the outer surface of the catalyst particles (external transport) and transport inside the solid particles (internal diffusion).

The absence of mass transfer limitations are typically examined by varying the stirring speed or the catalyst particle size. To study the effect of external mass transfer resistance, the stirring speed is increased until the reaction rate

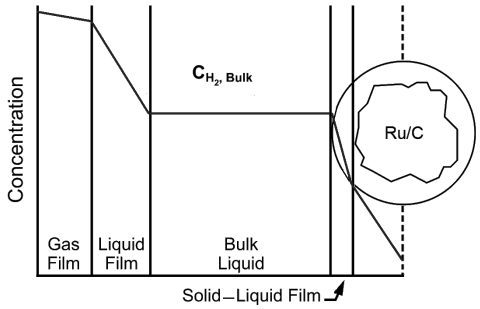

Figure 2.1: Schematic illustration of the mass transfer in the three phase hydrogenation reactions.

remains constant [69]. Therefore, to check whether gas–liquid mass transfer is controlling the reaction the stirrer speed was varied between 600 and 1200 rpm. There was a negligible difference in the reaction rates indicating the absence of gas–liquid mass transfer limitations (Figure B.1). Variation of the particle size can be applied to check for the existence of internal diffusion resistance. Usually small catalyst particles are used in order to eliminate internal diffusion resistance. For small catalyst particle of Ru/C (19 μm) an internal mass transfer resistance can be excluded.

Additionally literature criteria can be used to verify the absence of mass transfer limitations. Criteria based on the observed rate reaction have been applied to verify the absence of mass transport limitations. Experiments are performed in the intrinsic kinetic regime if the ratio of the observed rate to the rate that would be observed in the absence of diffusional limitations does not deviate more than 5 % (2.1) [70].

$$\frac{rate_{(observed)}}{rate_{(maximum)}} = 1 \pm 0.05 \tag{2.1}$$

For the analysis described in this section, initial reaction rates have been used to estimate the highest limitations. The results are discussed in the following

section.

2.1. MASS TRANSFER EFFECTS

The absence of external mass transfer can be checked using the Carberry number being a dimensionless number representing the ratio of the observed reaction rate to the maximum transfer rate (Eq. 2.2). In general, for first order reactions the absence of transfer limitations is verified if the value of the resulting effectiveness factor is above 0.95 (Eq. 2.3) [70].

$$Ca_{(G-L)} = \frac{r_{obs}}{K_{La} C^*_{H_2}} \tag{2.2}$$

$$\eta_e = (1 - Ca)^n \tag{2.3}$$

To calculate a Carberry number for gas to liquid mass transfer according to equation 2.2 the maximum transfer rate of H_2 was calculated by using the volumetric gas-liquid mass transfer coefficient and the hydrogen solubility in water. The hydrogen solubility ($C^*_{H_2}$) was taken based on data published by Pray et al. [71]. The volumetric gas-liquid mass transfer coefficient (k_La) was calculated using the pressure step method (Figure B.3) [72]. To verify the absence of a liquid-solid mass transfer limitation a Carberry type equation can be used which contains a liquid-solid mass transfer coefficient (k_{LS}) (Eq. 2.4).

$$Ca_{(L-S)} = \frac{r_{obs}}{K_{LS} C_{C_b}} \tag{2.4}$$

The required liquid–solid mass transfer coefficient was estimated by a typical correlation of the Sherwood number (Sh) for slurry reactors which includes Reynolds (Re) and Schmidt (Sc) numbers (Eq. 2.5) [73].

$$Sh = \frac{K_{LS} d_p}{D} = 2 + 0.4 Re^{1/4} Sc^{1/3} \tag{2.5}$$

The detailed calculations to verify the absence of external mass transfer limitation can be found in the appendix B. Table 2.1 shows the calculated results indicating with an effectiveness factor η above 0.95 that external mass transfer limitations can be neglected.

T(K)	P(MPa)	$Ca_{(G-L)}$	$\eta_{(G-L)}$	$Ca_{(L-S)}$	$\eta_{(G-L)}$	ϕ_{H_2}	η_{H_2}
393	5	0.0037	0.99	0.0063	0.99	0.0142	0.99

Table 2.1: Evaluation of the absence/presence of transport limitations.

In case of internal diffusion, the Weisz-Prater criterion being the ratio of the observed reaction rate and the maximum effective rate of diffusion was used to evaluate the absence of internal diffusion limitations (Eq. 2.6) [74].

$$\phi = (r_p)^2 \left(\frac{n+1}{2}\right) \frac{r_{obs}\rho_p}{D_e C_b} \tag{2.6}$$

If the resulting value of Weisz correlation is $\phi << 1$, then diffusion phenomena are not significant and the observed reaction rate is equal to intrinsic reaction rate. From Table 1 the calculated results show effectiveness factor η above 0.95 in all cases indicating that mass transfer limitations can be neglected for the used reaction conditions and it can be assumed that the experiments are carried out in the intrinsic regime.

2.2. REACTION PARAMETER EFFECTS

The effects of reaction parameters were studied to have first insights into the potential kinetic model which could follow the experimental results. Therefore, effects of reaction parameters such as initial substrate concentration and system pressure were studied. The effect of the initial concentration of the saccharides was studied with 2, 5, and 10 wt % substrate solutions at 393 K and 4 MPa.

Substrate concentration did not have a significant effect on the selectivity of sorbitol at the experimental range, when the catalyst-to-substrate ratio is kept constant. Figure 2.2 shows the influence of the initial saccharide concentration on the selectivity of sorbitol. However, it should be noted that in highly concentrated saccharide solutions the low solubility of hydrogen may cause diffusion limitations. A dependency of the initial reaction rate on the initial concentra-

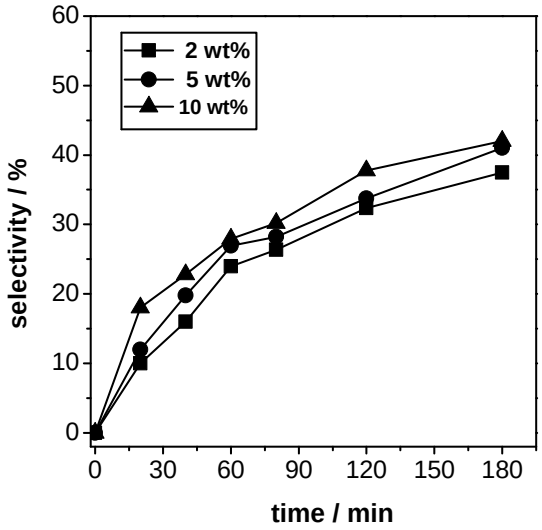

Figure 2.2: Effect of the initial cellotriose concentration on the sorbitol selectivity at 393 K and 4 MPa.

tion can provide insight into the order of reaction. Figure 2.3 shows that the reaction is first order with respect to the substrate concentration in the operation range used. An increased hydrogen pressure has a positive effect on the reaction rate. In the studied pressure range, Henry's law is valid leading to a hydrogen concentration in the solution proportional to the applied hydrogen pressure. Investigating the effect of the hydrogen pressure on the initial rate of saccharide the hydrogen pressure dependency approaches a saturation situation at pressures above 3.5 MPa. Furthermore, this effect can be described by clas-

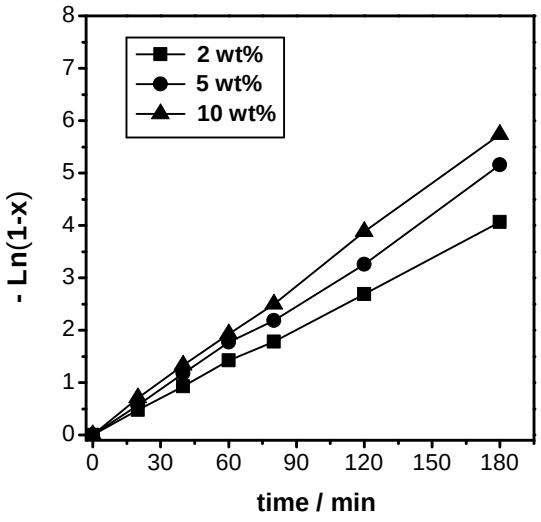

Figure 2.3: Effect of initial cellotriose concentration on the initial reaction rate at 393 K and 4 MPa; (x=conversion).

sical Langmuir–Hinshelwood kinetics. In the lower pressure range, an apparent first order dependency and at higher concentration zero order can be observed (Figure B.2)

Based on the aforementioned experimental observations a kinetic control of the reaction can safely be assumed at a stirrer speed above 750 rpm, a hydrogen pressure above 3.5 MPa and low concentrations of the saccharide in solution. The kinetic modeling of the reaction network was therefore undertaken under these experimental conditions.

2.3. REACTION KINETIC MEASUREMENTS

Experiments were performed in a batch-type high-pressure autoclave reactor. Typically, oligosaccharide (2 mmol), 5 wt.% Ru/C (0.1 g) and heteropoly acid (HPA, silicotungstic acid) (0.2 g) were added into a Teflon-lined stainless steel reactor precharged with H_2O (20 cm^3). The reactor was flushed several times

with N_2 and H_2 at room temperature. The reactor was pressurized with H_2 and then preheated to the defined temperature. The reaction was operated at a pressure of 3.5-5 MPa, a temperature range of 393-463 K, a stirring speed of 800 rpm and for 3 h. The time zero was set at beginning of the isothermal reaction stage. The reactor was equipped with a sampling valve and the progress of the reaction was monitored by periodically taking sample. Samples were filtered through a 25 μm nylon filter and were analyzed off-line using an HPLC (High pressure liquid chromatography).

CHAPTER 3

DISACCHARIDES

Portions of this chapter have been published in "L. Negahdar, J. U. Oltmanns, S. Palkovits, and R. Palkovits, Kinetic investigation of the catalytic conversion of cellobiose to sorbitol, Applied Catalysis B: Environmental, 147(0):677–683, 2014".

The aim of this chapter is to gain insights into the reaction mechanism and kinetics of the catalytic conversion of linear polysaccharides (cellulose and starch) to sorbitol. Because of the complex structure of polysaccharides, disaccharides as simple model compounds of these polymers were chosen for a detailed kinetic investigation. Disaccharides represent the basic repeating unit of linear polysaccharides and consist of two glucose monomers linked by a $\alpha/\beta(1\text{–}4)$ glycosidic bonds (Figure 3.1). In the following, kinetics and reaction pathways of

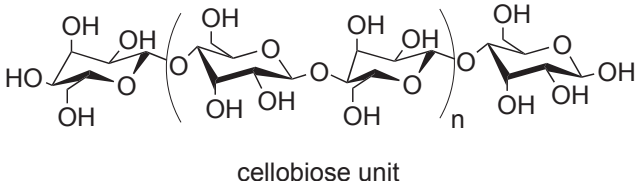

Figure 3.1: Structure of cellulose and cellobiose.

the hydrolytic hydrogenation of disaccharides to sorbitol applying a catalytic system consisting of heteropoly acids and a supported ruthenium catalyst (5 wt.% Ru/C) will be discussed.

3.1. MECHANISTIC STUDY

Several studies have reported the hydrolytic hydrogenation of polysaccharides to sorbitol to follow a cleavage of the glycosidic (C–O–C) bonds via hydrolysis and consecutive hydrogenation of glucose to sorbitol (Figure 3.2) [75, 76, 77].

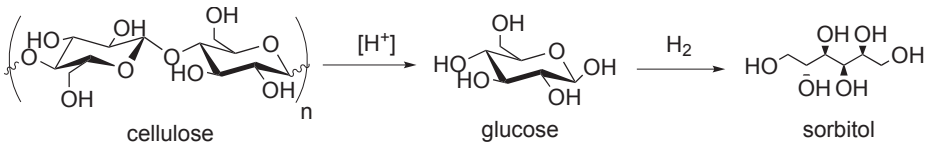

Figure 3.2: Reaction pathway for hydrolytic hydrogenation of cellulose.

However, the experimental results of the conversion of disaccharides (cellobiose or maltose) to sorbitol indicate an additional reaction pathway to occur. In the presence of a molecular acid and a supported metal catalyst, the disaccharide either undergoes hydrolysis to glucose or as an alternative pathway proceeds through a hydrogenation of the C–O bond at the reduced end of the disaccharide leading to cellobitol (3-β-D-glucopyranosyl-D-glucitol) or maltitol (3-α-D-glucopyranosyl-D-glucitol). In a subsequent reaction, the reduced disaccharide can undergo hydrolysis to sorbitol and glucose. The proposed reaction pathways of the conversion of a disaccharide are illustrated in Figure 3.3.

Only few studies discuss the formation of reduced disaccharides during the catalytic transformation of disaccharides to sorbitol [78, 79, 80]. For example, Kuo et al. reported the formation of cellobitol under neutral and basic conditions applying ruthenium nanoclusters in the ionic liquid 1-butyl-3-

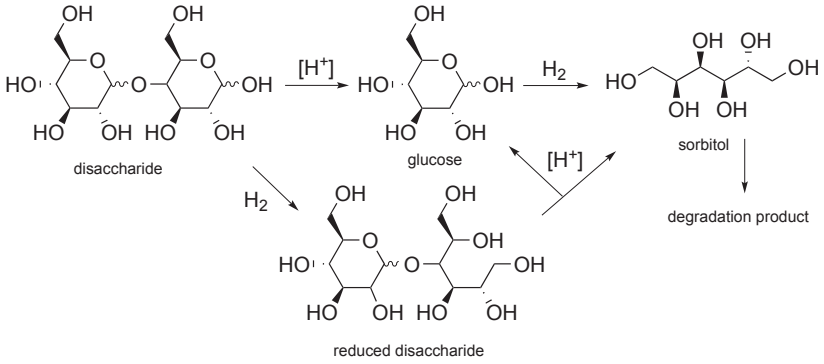

Figure 3.3: Proposed reaction pathways for the conversion of disaccharides with HPA and Ru/C.

methylimidazolium chloride [81]. However, they concluded that the formation of cellobitol was not related to sorbitol formation. Instead, sorbitol was formed via direct hydrogenolysis of the β(1,4)-glycosidic bond of cellobiose under such conditions delivering sorbitol and dideoxyhexitol. A first study discussing cellobitol as intermediate in the transformation of cellobiose to sorbitol has been presented by Wang et al. [82]. They observed cellobitol in the conversion of cellobiose over carbon nanotube-supported Ru catalysts in neutral aqueous solutions and concluded that the formation of cellobitol followed by hydrolysis is the main pathway for sorbitol formation. Recently, Makkee et al. investigated the reaction mechanism of the transformation of cellobiose into sorbitol in aqueous $ZnCl_2$ with Ru/C as hydrogenation catalyst [83]. Their experimental data pointed towards a competition of two reaction pathways, (1) via cellobitol formation followed by hydrolysis and (2) via hydrolysis of cellobiose and subsequent hydrogenation. Under the presented reaction conditions path (1) was kinetically most important. Nevertheless, they suggested that various parameters such as reaction temperature, catalyst loading as well as the addition of mineral acids may influence the relative contribution of both pathways.

The plot of selectivity as a function of elapsed time at different reaction temperatures was used to have further information on the product distribution. Figure 3.4 shows time resolved product selectivity courses at different reaction temperatures for cellobiose as starting material. Selectivity is defined as molar ratio of the respective product with regard to the consumed amount of disaccharides ($n_{disaccharide,0} - n_{disaccharide,t}$) at time t.

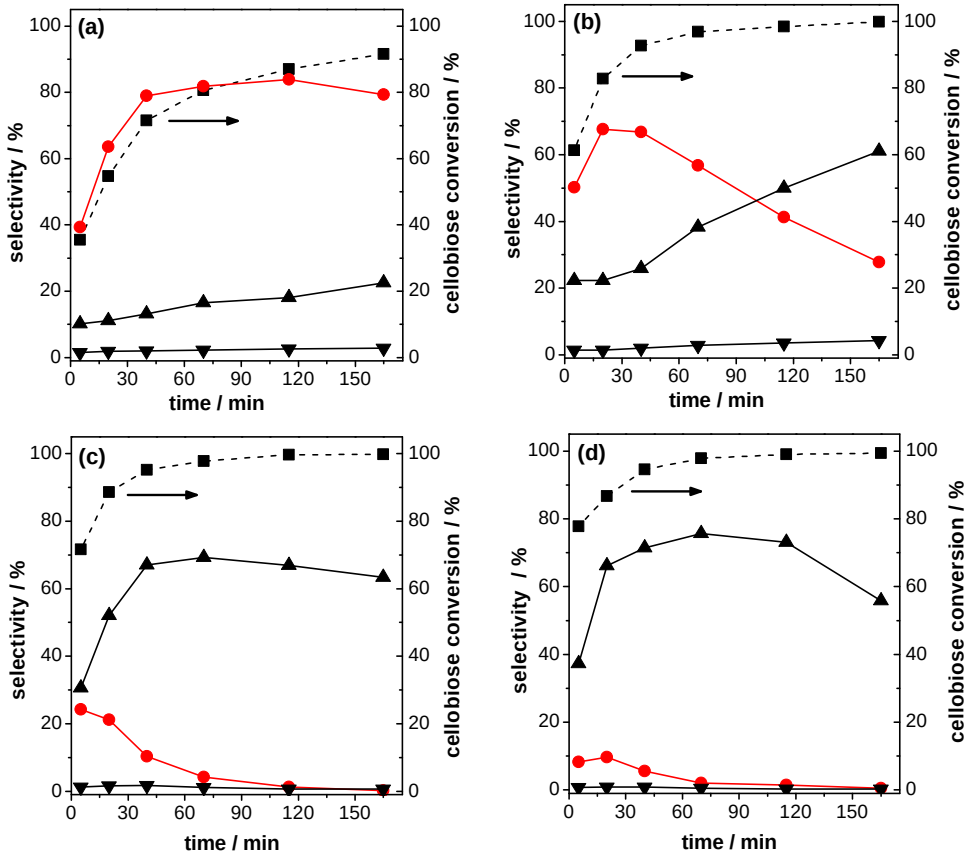

Figure 3.4: Selectivity of cellobitol (•), glucose (▾), sorbitol (▴) and cellobiose conversion (▪) as a function of elapsed time (a) 393, (b) 413, (c) 433 and (d) 443 K , Reaction conditions: cellobiose, 1.17 mmol; Ru/C, 0.1 g; HPA, 0.175 g; H_2O, 20 cm^3; H_2, 5 MPa; time, 2.5 h.

At moderate temperatures of 393 K cellobitol is the main product with a maximum selectivity of 81 %. Increasing the reaction temperature up to 443 K decreases the cellobitol selectivity to less than 1 % after 1.25 h reaction time while the selectivity of sorbitol rises to a maximum of 75 %. These observations suggest a simultaneous hydrolysis of cellobitol to sorbitol and glucose. However, comparing both time resolved data sets of the cellobiose conversion with HPA and Ru/C the presence of two competing reaction pathways with different intermediate substrates becomes obvious. At lower temperatures of up to 413 K the hydrogenation of the C–O bond at the reduced end of cellobiose seems to be dominant while for higher temperatures direct hydrolysis of cellobiose becomes favorable. For maltose as substrate, an analogous observation could be made. Maltitol, the hydrogenation product of maltose is the major product and present in yields up to 82 % after 1.3 h at 393 K (Figure 3.5).

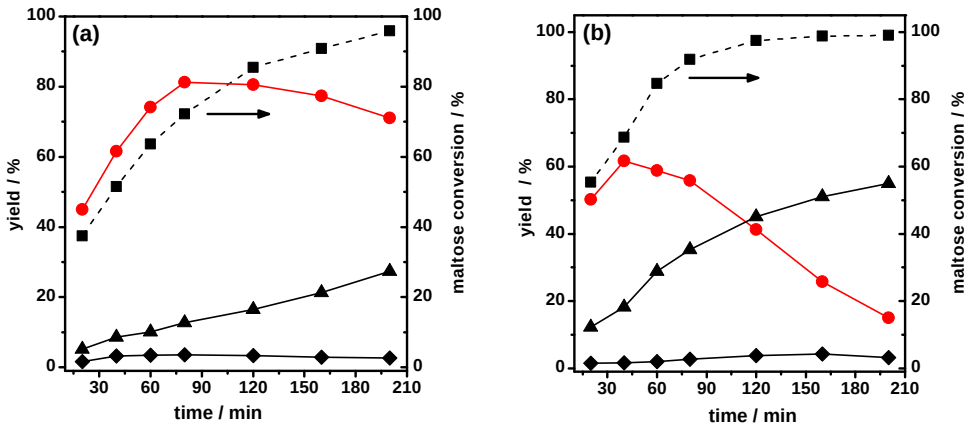

Figure 3.5: Yeild of maltiitol (•), sorbitol (▲), glucose (◆) and maltose conversion (■) as a function of elapsed time. Reaction conditions: maltose, 1.17 mmol; Ru/C, 0.1 g; HPA, 0.175 g; H_2O, 20 cm^3; H_2, 5 MPa; (a) 393 and (b) 413 K.

Dependent on the reaction conditions, the reduced disaccharide seems to

play a key role as an intermediate compound in the hydrolytic hydrogenation of disaccharides. To gain insights into these reaction pathways, a kinetic investigation determining reaction rates and main activation energies appears necessary. In line, reduced disaccharides were synthesized and isolated. For example, cellobitol can be produced selectively in neutral water at 433 K with yield of 99 % after ca. 2 h (Figure 3.6). At higher temperatures such as 463 K, reduced disaccharides undergo consecutive reactions to sorbitol and further degradation reactions via dehydration as well as C–C and C–O bond cleavage occur.

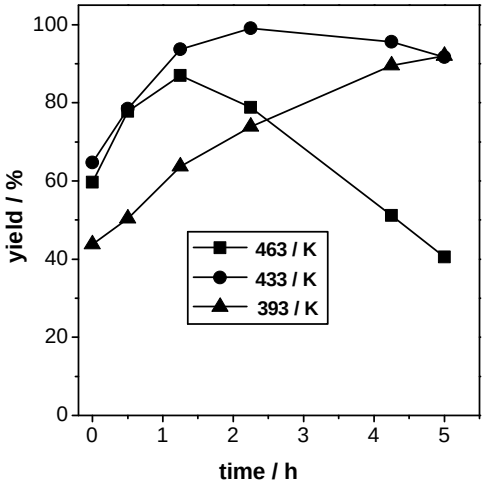

Figure 3.6: Yield of cellobitol as a function of elapsed time. Reaction conditions: cellobiose, 1.17 mmol; Ru/C, 0.1 g; H_2O, 20 cm^3; H_2, 5 MPa.

When the hydrogenation activity is sufficiently high, the degradation product from glucose was not observed. Under all mentioned reaction conditions only a low yield of glucose was observed as the hydrogenation of glucose to sorbitol takes place on the metal catalyst with high selectivity and rate [84]. The previous investigation on sorbitol dehydration under the same reaction condition is in agreement with the observed side products such as sorbitan, isosorbide and other degradation products [85]. Under this reaction condition, the carbon balance

was closed and there was no humin formation [59].

3.2. KINETIC MODELING

Figure 3.7 illustrates the possible reaction pathways of the catalytic conversion of disaccharides to sorbitol. The pathway can be divided into two main catalytic reactions including hydrolysis of disaccharide (k_1) or reduced disaccharide (k_3) and hydrogenation of disaccharide (k_2) or of glucose (k_4). Possible side reactions of sorbitol to by-products are further hydrogenolysis (k_7 and k_8) and dehydration reactions (k_5 and k_6). The kinetics of hydrolysis of polysaccharides

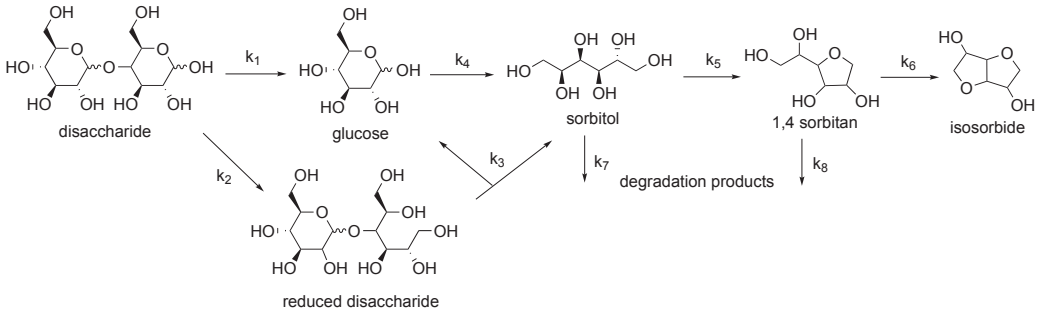

Figure 3.7: Schematic illustration of the reaction network for the catalytic conversion of disaccharides to sorbitol.

is assumed to be pseudo first order [23, 26, 25]. The reaction rate constants follow a modified form of the Arrhenius equation including temperature effects (T) and the hydronium ion concentration of the acid in solution (Eq. 3.1).

$$k_i = k_{i,0}[H_3O^+]^m e^{\frac{-E_a}{RT}}, \qquad i = 1, 2 \tag{3.1}$$

Herein k_0 represents the pre-exponential factor (s^{-1}), $[H_3O^+]$ is the hydronium ion concentration in solution, and m is an empirical exponent [16].

For the development of our kinetic models for the hydrogenation reactions, it is assumed that no catalyst deactivation is taking place during the reaction

and the adsorption of the solvent and the products on the catalyst surface is negligible. For hydrogenation reactions the Langmuir–Hinshelwood–Hougen–Watson (LHHW) model can be assumed with a non-competitive adsorption of hydrogen and disaccharide or glucose at different sites of the catalyst (Eq. 3.2) [86].

$$r = \frac{kK_{disac.}C_{disac.}K_{H_2}P_{H_2}}{1 + K_{disac.}C_{disac.}} \tag{3.2}$$

On the basis of the preliminary kinetic analysis, some simplifications can be made. At the selected operation conditions, a large excess of hydrogen and a low concentration of disaccharide and glucose is present in solution leading to the assumption of the reaction to be pseudo first order (Eq. 3.3).

$$r = k_2 C_{disac.} \tag{3.3}$$

The constant k_2 is a lumped parameter including the intrinsic rate constant as well as adsoprtion constant. The dehydration reactions are also assumed to be first-order [85, 87]. Based on the reaction network illustrated in scheme 2 the following ordinary differential equations (ODEs) can be proposed for the individual components as a function of time (3.4 - 3.9):

$$\frac{dC_{disac.}}{dt} = -k_1 C_{disac.} - \rho_{cat} k_2 C_{disac.} \tag{3.4}$$

$$\frac{dC_{re-disac.}}{dt} = \rho_{cat} k_2 C_{disac.} - k_3 C_{re-disac.} \tag{3.5}$$

$$\frac{dC_{glucose}}{dt} = 2k_1 C_{disac.} + k_3 C_{re-disac.} - \rho_{cat} k_4 C_{glucose} \tag{3.6}$$

$$\frac{dC_{sorbitol}}{dt} = \rho_{cat}\left(k_4 C_{glucose} - k_7 C_{sorbitol}\right) + k_3 C_{re-disac.} - k_5 C_{sorbitol} \tag{3.7}$$

$$\frac{dC_{sorbitan}}{dt} = k_5 C_{sorbitol} - \rho_{cat} k_8 C_{sorbitan} - k_6 C_{sorbitan} \tag{3.8}$$

$$\frac{dC_{isosorbide}}{dt} = k_6 C_{sorbitan} \tag{3.9}$$

where C_i's represent the species' concentrations, k_i's are the apparent rate constants and ρ_{cat} is the catalyst bulk density.

Matlab was used for the numerical integration of the ODEs and parameter estimations and moreover to compare the experimental data with the proposed kinetics. The Matlab codes are given in appendix C. The rate constants were estimated at different temperatures (393–463 K). Figures 3.8, 3.9, and 3.10 show the curve fitting for the experimental data at different reaction temperatures.

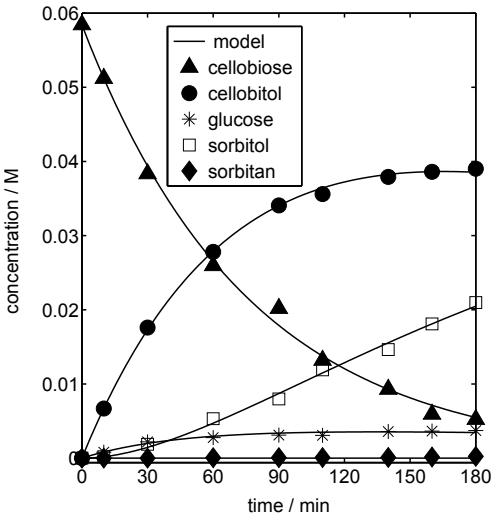

Figure 3.8: Fit of the kinetic model (Eqs. (3.4-3.9)) to the experimental data; Reaction conditions: cellobiose, 1.17 mmol; Ru/C, 0.1 g; H_2O, 20 cm^3; H_2, 5 MPa at 393 K.

3.3. RESULTS AND DISCUSSION

Table 3.1 summarizes the estimated values of the reaction rate constants and the corresponding activation energies for the transformation of cellobiose. At temperatures below 463 K the rate constant k_2 (cellobiose to cellobitol) is significantly higher compared to the rate constant k_1 (cellobiose to glucose) indi-

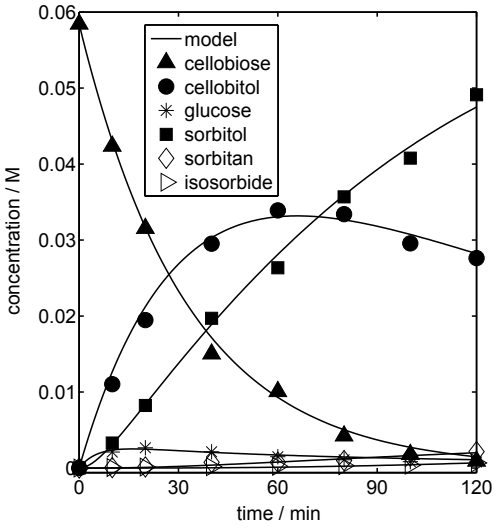

Figure 3.9: Fit of the kinetic model (Eqs. (3.4-3.9)) to the experimental data; Reaction conditions: cellobiose, 1.17 mmol; Ru/C, 0.1 g; H_2O, 20 cm^3; H_2, 5 MPa at 413 K.

cating the hydrogenation step to proceed faster than hydrolysis. With increasing reaction temperature, the rate constants of both reaction pathways become comparable and both reactions compete with each other. Additionally, at temperatures below 463 K the rate constants of both hydrolysis steps (k_1 and k_3) are lower compared to the ones of the hydrogenation reactions (k_2 and k_4) reflecting the fact that hydrolysis is the rate-determining step independent of the reaction pathway. Nevertheless, a previous transformation of cellobiose to cellobitol appears to facilitate subsequent hydrolysis resulting in a superior rate constant for the hydrolysis of cellobitol k_3 compared to cellobiose k_1. Overall, the reaction rate constant k_4 for the hydrogenation of glucose to sorbitol is the highest compared with the other ones emphasizing a fast hydrogenation of glucose and explaining the low glucose concentrations detected under most reaction conditions. The rate constants of the subsequent dehydration of sorbitol to sorbitan (k_5) and further to isosorbide (k_6) are small under the selected reaction

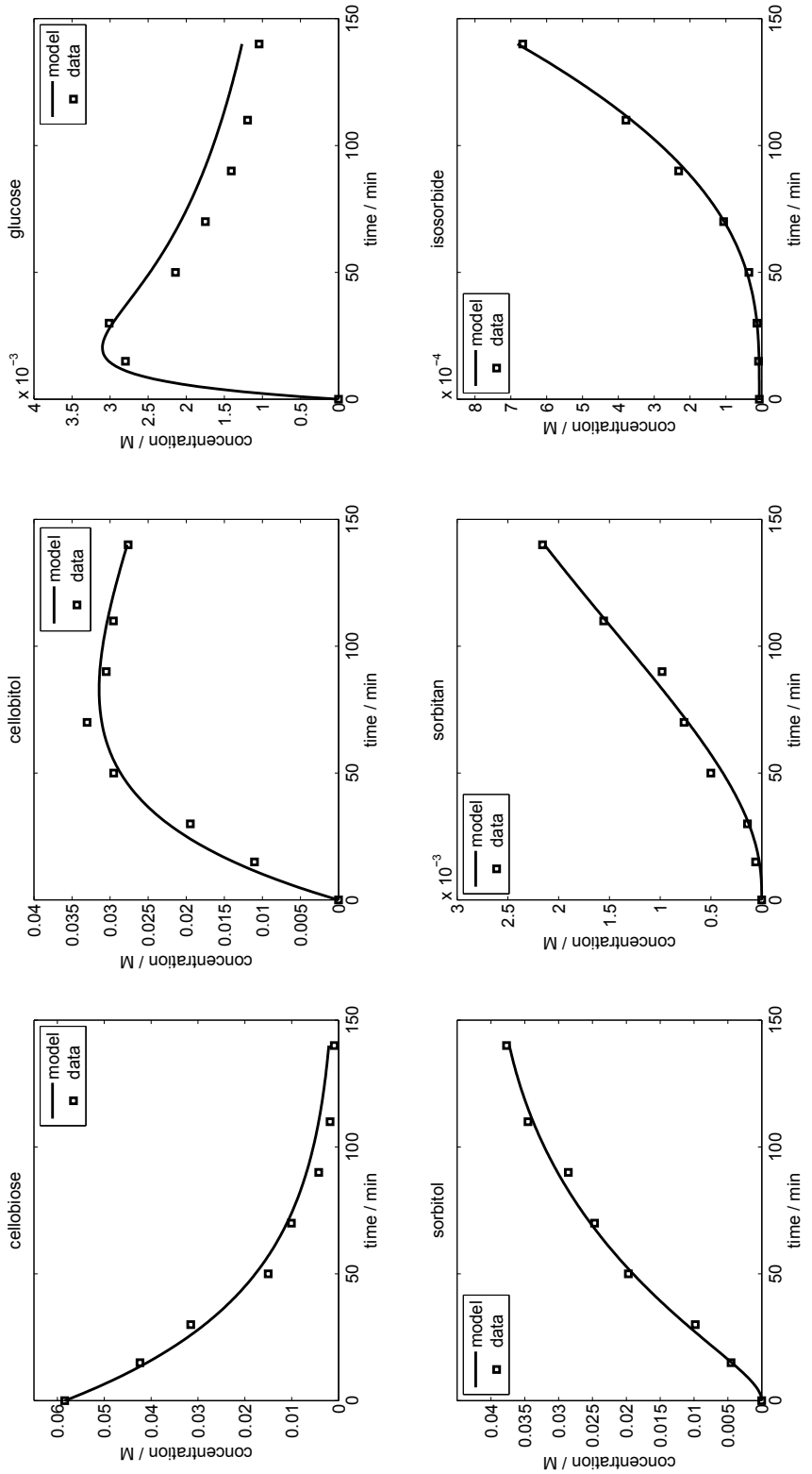

Figure 3.10: Fit of the kinetic model (Eqs. (3.4-3.9)) to the experimental data; Reaction conditions: cellobiose, 1.17 mmol; Ru/C, 0.1 g; H_2O, 20 cm^3; H_2, 5 MPa at 423 K.

conditions. These low concentrations hampered a kinetic modeling of further degradation reactions of sorbitan and isosorbide (k_7 and k_8). Nevertheless, values for k_5 and k_6 as well as the corresponding activation energies are in well agreement with a previous investigation focusing on the dehydration of sorbitol [85]. Figure 3.11 shows the the Arrhenius diagram of the reaction rate constants

Reaction T(K)	393	423	443	463	E_a [kJ mol^{-1}]	R^2
$k_1(10^{-2}min^{-1})$	0.014	0.319	1.013	2.98	115	0.98
$k_2(10^{-2}min^{-1})$	0.119	0.717	2.183	3.76	76	0.98
$k_3(10^{-2}min^{-1})$	0.032	0.551	1.785	3.51	103	0.97
$k_4(10^{-2}min^{-1})$	0.203	1.911	3.574	4.74	69	0.92
$k_5(10^{-2}min^{-1})$		0.010	0.024	0.48	164	0.93
$k_6(10^{-2}min^{-1})$		0.001	0.027	0.084	178	0.94

Table 3.1: Kinetic parameters for the catalytic conversion of cellobiose to sorbitol.

of the conversion of cellobiose to sorbitol. Estimation of the activation energy of cellobiose hydrolysis E_1 yields a value of 115 kJ mol^{-1} which is in good agreement with the respective literature data (108-119 kJ mol^{-1}) [16, 88, 89]. The activation energy E_3 for the hydrolysis of cellobitol was determined to be 103 kJ mol^{-1} which is lower than E_1 pointing out that the hydrolysis of cellobitol is easier compared to cellobiose under the used reaction conditions. The activation energy for the hydrogenation of glucose E_4 was estimated to 69 kJ mol^{-1} being also in good agreement with reported data ranging from 55-71 kJ mol^{-1} [86]. An activation energy E_2 of 76 kJ mol^{-1} can be determined for the hydrogenation of cellobiose to cellobitol corresponding well to the data for glucose hydrogenation. For the modified Arrhenius equation (Eq. 3.1), the values of the empirical exponent m were estimated to be 1.02 and 0.96 respectively. Table 3.2 shows

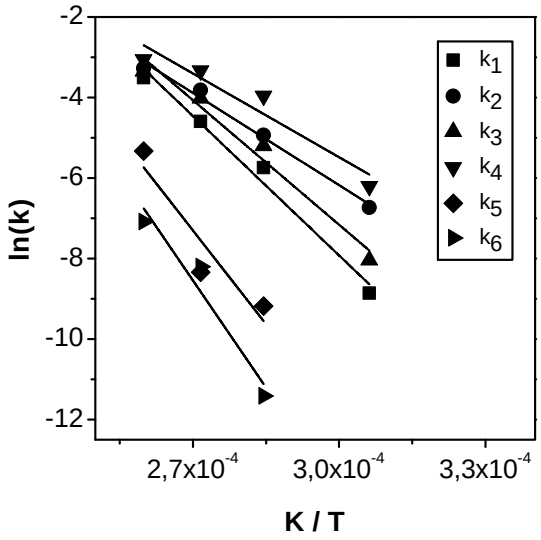

Figure 3.11: Arrhenius diagram of the reaction rate constants for the estimation of activation energies of the catalytic conversion of cellobiose to sorbitol.

the estimated values of reaction rate constants and activation energies for the catalytic conversion of maltose to sorbitol. The fit of experimental data to the

Reaction T(K)	393	413	433	E_a [kJ mol^{-1}]	R^2
$k_1(10^{-2}min^{-1})$	0.08	0.72	2.02	110	0.95
$k_2(10^{-2}min^{-1})$	0.45	1.87	3.3	70	0.94
$k_3(10^{-2}min^{-1})$	0.15	1.01	2.77	99	0.97
$k_4(10^{-2}min^{-1})$	0.61	2.35	3.5	61	0.96

Table 3.2: Kinetic parameters for the catalytic conversion of maltose to sorbitol.

kinetic model for hydrolytic hydrogenation of maltose is shown in the Figure 3.12. Similar to cellobiose, a comparable observation for maltose was obtained. Comparing the activation energy of hydrolysis of maltose (E_1) estimated to be 110 kJ mol^{-1} with hydrogenation (E_2) with the value of 70 kJ mol^{-1} emphasize that hydrogenation of maltose takes place faster than its hydrolysis. The acti-

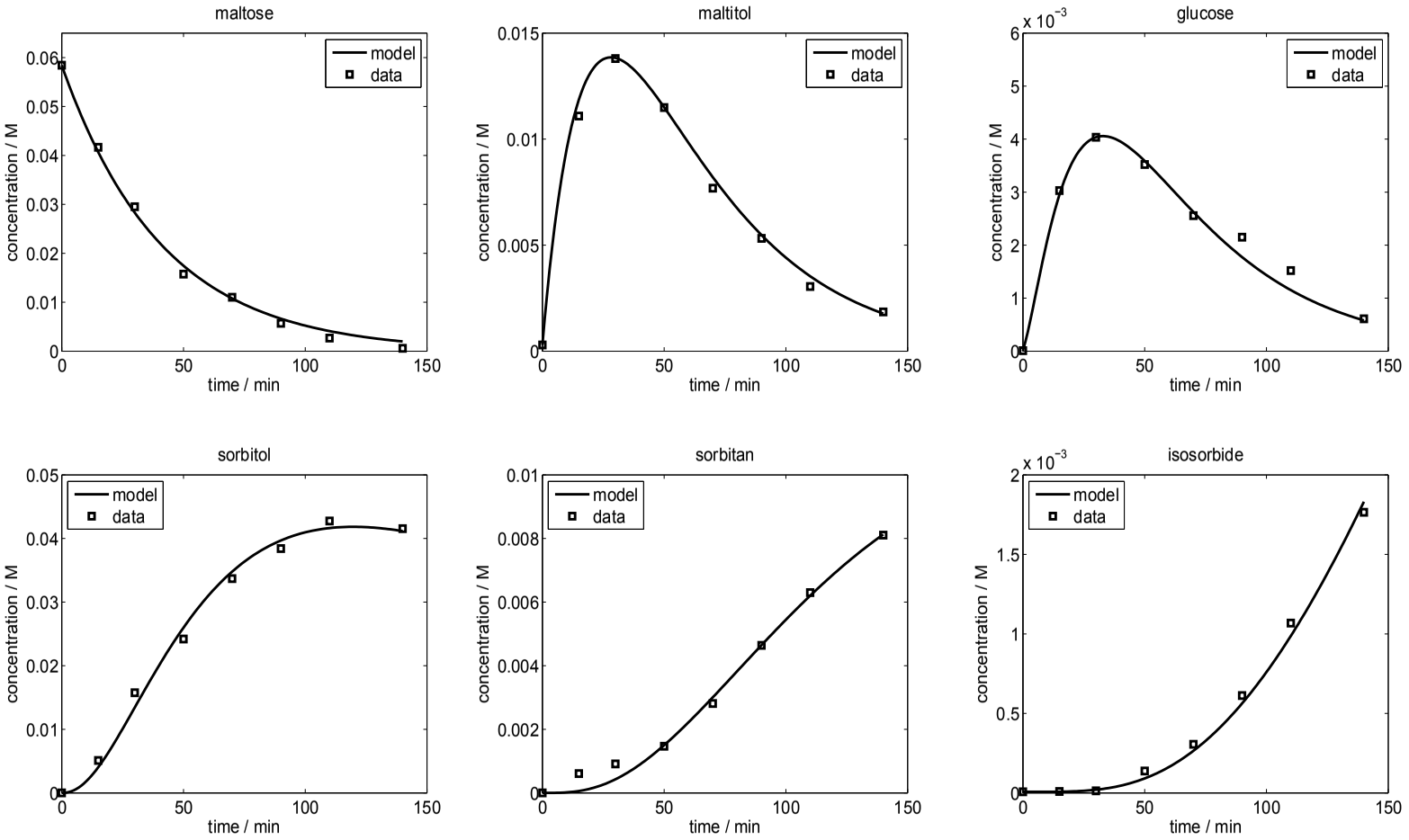

Figure 3.12: Fit of the kinetic model (Eqs. (3.4-3.9)) to the experimental data; Reaction conditions: maltose, 1.17 mmol; Ru/C, 0.1 g; H_2O, 20 cm^3; H_2, 5 MPa at 433 K.

vation energy of hydrolysis and hydrogenation reactions for maltose is slightly higher than cellobiose. From literature, the rate of hydrolysis of oligosaccharides depends on the type of glycosidic bond. For example it has been reported that the α(1–4) glycosidic bond in maltose are cleaved more readily than the β(1–4) glycosidic linkage in cellobiose. This observation was explained to be because of conformational effects and some factors relative to solubility of sugars [90, 49]. Therefore, the estimated activation for hydrolysis of maltose is somewhat smaller than cellobiose.

Analysis of the reaction network emphasizes two reaction pathways delivering sorbitol based on disaccharide. Considering the fact that subsequent dehydration and hydrogenolysis of sorbitol need to be suppressed to achieve a high selectivity of sorbitol, a preferential transformation via the reduced disaccharide formation appears interesting. The facilitated hydrolysis of the reduced form enables a reaction under neutral or weakly acidic reaction conditions at rather low reaction temperatures. Therefore, under optimum reaction condition a controlled sorbitol production via the selective hydrogenolysis of disaachride or oligosaccharide could be possible.

3.4. SUMMARY

Our mechanistic study on the hydrolytic hydrogenation of disaccharides to sorbitol confirms two competing reaction pathways starting from disaccharides. The substrate either undergoes hydrolysis to glucose or hydrogenation to the reduced form (3-α/β-D-glucopyranosyl-D-glucitol). Reduced disaccharide can then be further hydrolyzed to glucose and sorbitol. Reduced disaccharide can be produced selectively with up to 99 % yield utilizing a Ru/C catalyst in neutral water and appropriate reaction conditions. The study confirms indeed that

both pathways occur and their relative contribution strongly depends on the selected reaction conditions. Kinetic parameters of both reaction pathways were obtained from the proposed model with non-linear regression analysis. The results emphasize hydrolysis as rate determining step independent of the reaction pathway. Overall, a selective transformation of disaccharides to sorbitol proceeding via a reduced disaccharide formation appears more efficient. Especially at lower reaction temperature, this reaction pathway dominates and overall lower activation energies together with higher rate constants can be observed.

CHAPTER 4

TRISACCHARIDES

Portions of this chapter have been submitted in "L. Negahdar, P. J. C. Hausoul, S. Palkovits, and R. Palkovits, Direct cleavage of sorbitol from oligosaccharides via a sequential hydrogenation–hydrolysis pathway, Applied Catalysis B: Environmental, 160:460–464, 2015."

In the pervious chapter, an investigation on the hydrolytic hydrogenation of disaccharides as model molecules of polysaccharides confirmed a direct hydrogenation to reduced disaccharides followed by hydrolysis as alternative reaction pathway. The kinetic analysis revealed that this reaction pathway can contribute significantly to sorbitol formation. Consequently the question arises if a selective formation of sorbitol via hydrogenation followed by hydrolysis should also be considered for oligo- and polysaccharides, respectively.

In this regard, trisaccharides including cellotriose based on cellulose, and maltotriose based on starch were investigated to gain further insights concerning the significance of hydrogenation-hydrolysis sequences within the overall reaction networks. A systematic kinetic analysis has been carried out providing a quantitative interpretation of the reaction pathways paving the way for a novel view on the transformation of oligosaccharides and potentially polysaccharides

into sorbitol.

4.1. REACTION NETWORK ANALYSIS

In the presence of a supported metal catalyst (Ru/C) and a molecular acid in form of a heteropoly acid, the catalytic conversion of both trisaccharides, cellotriose and maltotriose, respectively, proceeds via the described sequence of steps illustrated in Figure 4.1. A direct hydrolysis of the studied trisaccha-

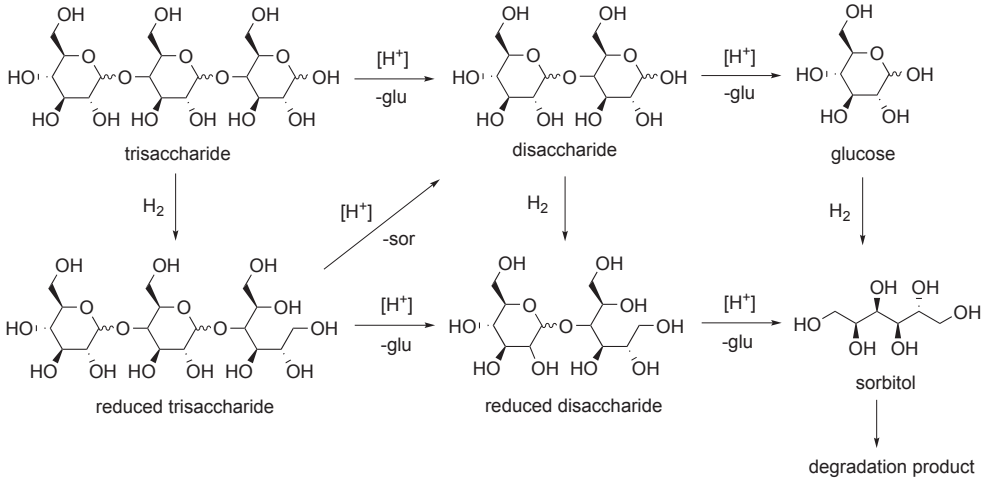

Figure 4.1: Reaction network for a catalytic conversion of trisaccharides to sorbitol; glu=glucose, sor=sorbitol.

rides (cellotriose or maltotriose) to the corresponding disaccharides (cellobiose or maltose) and glucose as well as a hydrogenation to the reduced trisaccharides (cellotriitol or maltotriitol) were observed. In line, experiments using reduced trisaccharides as substrate were performed. The hydrolysis of reduced trisaccharides yields either a disaccharide and sorbitol or a reduced disaccharide (cellobitol or maltitol) and glucose. In subsequent transformations, the disaccharide can be either hydrolysed to glucose or hydrogenated to the reduced form which can

be further hydrolysed to glucose and sorbitol.

One has to mention that trisaccharides exhibit two slightly different glycosidic bonds which can be hydrolysed. A facilitated hydrolysis at the reducing end of oligosaccharides has been discussed by Feather and Harris. They concluded that the glycosidic bond adjacent to the non-reducing end of the cellotriose which is controlled by a D-glycopyranose structure is hydrolysed faster than the bond adjacent to the reducing end which is controlled by a more bulky glycone containing two D-glycopyranose residues [53]. Another study by Freudenberg et al. suggested that the two glycosidic bonds in cellotriose are hydrolysed at the same rate and this rate differs from that of cellobiose [52]. Nevertheless, the interpretation of the hydrolysis rate of two glycosidic bonds in cellotriose based on different measurements remains uncertain. Cleaving either of the two glycosidic bonds in cellotriose yields the same products, glucose and cellobiose. Therefore, in this study the cleavages of the glycosidic bond at the reducing or non-reducing ends of cellotriose are not distinguished.

Analysing the yield of the described intermediates and final products as function of elapsed time at different reaction temperatures enables further insights on the course of the reaction. Figure 4.2 shows the time evolution of products yield at different reaction temperatures for conversion of cellotriose to sorbitol. The product distribution at different reaction temperatures illustrates a significant contribution of a prior hydrogenation of the substrate to the reduced form. This effect is favoured at lower reaction temperatures. Cellotriitol, the hydrogenation product of cellotriose, is the major product with maximum selectivity of 69 % at 393 k. As the reaction temperature increases the yield of cellotriitol decreases. At the same time, yield of the target product, sorbitol increases reaching a maximum of 74 % at 443 K. Cellobiose presents a potential reaction intermediate and is simultaneously converted via two catalytic pathways: (1) hydrogenation

to cellobitol and (2) hydrolysis to glucose. At lower reaction temperatures, cellobitol has a higher yield which again points out the preferential hydrogenation of cellobiose over its hydrolysis. This observation can be related to the direct

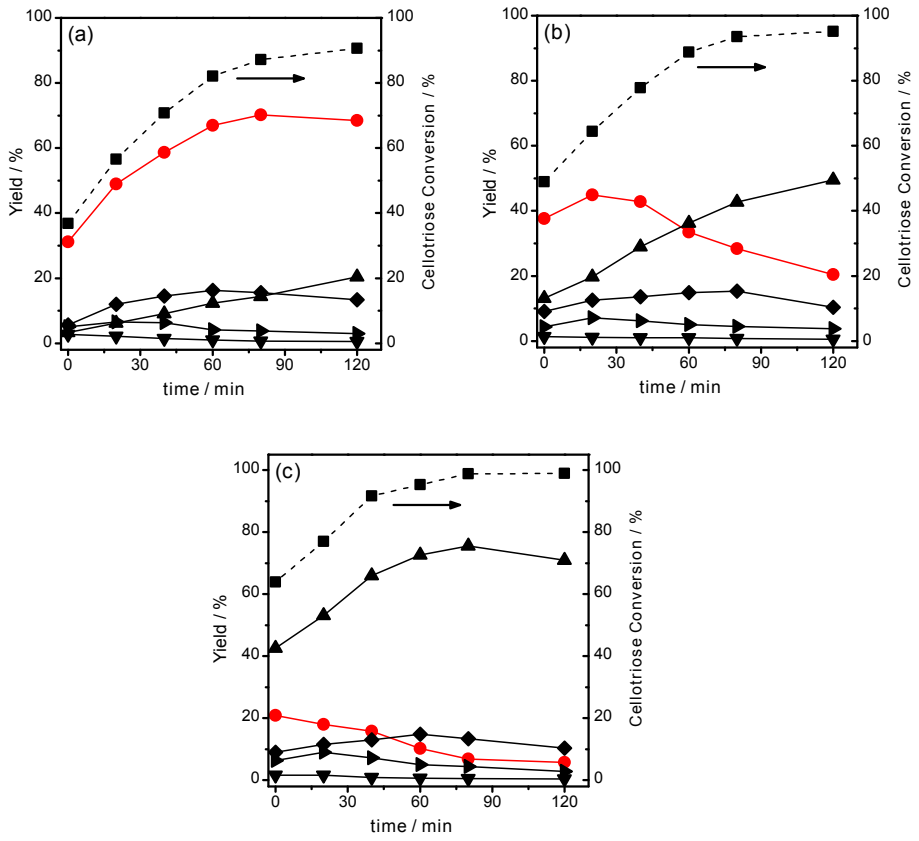

Figure 4.2: Time course study for cellotriose, yield of cellotriitol (•), cellobiose (▸), cellobitol (◆), sorbitol (▲), glucose (▾) and cellotriose conversion (■); Reaction conditions: cellotriose, 2 mmol; Ru/C, 0.1 g; HPA, 0.175 g; H_2O, 20 cm^3 and 4 MPa H_2 at (a) 393, (b) 413 and (c) 433 K.

formation of sorbitol based on hydrolysis of cellotriitol and maltotriitol together with a fast hydrogenation of glucose to sorbitol. Cellobiose presents a potential reaction intermediate and is simultaneously converted via two catalytic pathways: (1) hydrogenation to cellobitol and (2) hydrolysis to glucose. In line, only

low concentrations of cellobiose were detected. At lower reaction temperatures an accumulation of cellobitol can be observed indicating a facilitated hydrogenation of cellobiose compared to hydrolysis. Overall, these findings suggest that the hydrogenation of substrates and intermediates proceeds faster compared to hydrolysis. Unlike a simple hydrolysis to glucose, both trisaccharides, cellotriose and maltotriose, are mainly converted via hydrogenation-hydrolysis sequences. Under the applied reaction condition, no side reactions based on glucose, e.g. via dehydration, were observed and degradation products from sorbitol were negligible. In the described temperature range, carbon-balances could be closed and no humin formation was observed.

4.2. REACTION KINETIC MODELING

The reaction network for cellotriose consists of hydrolysis and hydrogenation pathways (Figure 4.3). Cellotriose is discussed comprehensively and major differences and consistencies are elucidated to translate the observations to other oligo- and polysaccharides. The hydrolysis reactions include the hydrolysis of

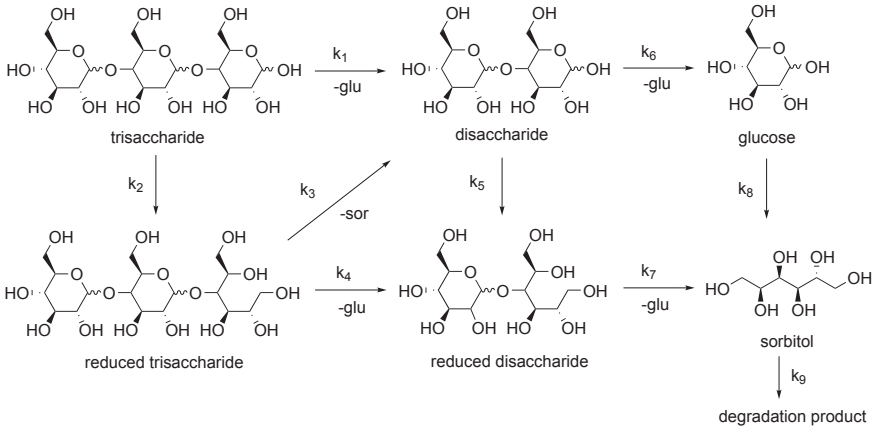

Figure 4.3: Reaction network for a catalytic conversion of trisaccharides to sorbitol; glu=glucose, sor=sorbitol.

cellotriose (k_1), cellotriitol (k_3, k_4), cellobiose (k_6) and cellobitol (k_7). The hydrogenation reactions comprehend the hydrogenation of cellotriose (k_2), cellobiose (k_5) and glucose (k_8). As mentioned previously, for hydrolysis of cellotriose, the cleavage of bonds is not distinguished assuming that each type of linkage hydrolyses at the same rate regardless of where it occurs. Therefore, the rate constant is the sum of the rate constants for the hydrolysis of both bonds. Based on time-resolved analysis of the reaction progress, kinetic modelling has been carried out. For hydrolysis, a pseudo first order kinetic was assumed [23, 26, 25, 19]. For hydrogenation, a Langmuir–Hinshelwood mechanism has been assumed. Due to the large excess of H_2 and a low concentration of oligosaccharides in the solution this rate equation has been simplified and treated as pseudo first order reaction [86]. The reaction parameters were estimated by minimizing the least-squares (LS) objective function, defined as the sum of squares of the residuals. The rate constants were correlated by the Arrhenius equation including temperature dependency. All kinetic data were estimated in the temperature range from 373 to 433 K. The concentrations of any compound as function of time in the reaction network are represented as follows:

$$\frac{dC_{trisac.}}{dt} = -k_1 C_{trisac.} - \rho_{cat} k_2 C_{trisac.} \tag{4.1}$$

$$\frac{dC_{re-trisac.}}{dt} = \rho_{cat} k_2 C_{trisac.} - k_3 C_{re-trisac.} - k_4 C_{re-trisac.} \tag{4.2}$$

$$\frac{dC_{disac.}}{dt} = k_1 C_{trisac.} + k_3 C_{re-trisac.} - \rho_{cat} k_5 C_{disac.} - k_6 C_{disac.} \tag{4.3}$$

$$\frac{dC_{re-disac.}}{dt} = k_4 C_{re-trisac.} + \rho_{cat} k_5 C_{disac.} - k_7 C_{re-disac.} \tag{4.4}$$

$$\frac{dC_{glucose}}{dt} = k_1 C_{trisac.} + k_4 C_{re-trisac.} + 2k_6 C_{disac.} + k_7 C_{re-disac.} - \rho_{cat} k_8 C_{glucose} \tag{4.5}$$

$$\frac{dC_{sorbitol}}{dt} = k_7 C_{re-disac.} + \rho_{cat} k_8 C_{glucose} + k_3 C_{re-trisac.} - k_9 C_{sorbitol} \tag{4.6}$$

where C_i's represent the species' concentrations, k_i's are the apparent rate constants and ρ_{cat} is the catalyst bulk density.

4.3. RESULTS AND DISCUSSION

Figures 4.4 and 4.5 show the curve fitting for cellotriose hydrolytic hydrogenation to sorbitol at different reaction temperatures. The apparent rate constants and activation energies for hydrolysis and hydrogenation steps of cellotriose and maltotriose are summarized in Table 4.1. Below 433 K the rate constant k_2 is significantly higher than the rate constant k_1 confirming a fast hydrogenation to reduced trisaccharides. The rate constant k_3 is slightly higher compared to k_4 indicating that the hydrolysis of the glycosidic bond close to the reducing end is easier than that for the glycosidic bond adjacent to the non-reducing end.

Reaction T(K)	393	413	433	E_a [kJ mol^{-1}]	R^2
$k_1(10^{-1}min^{-1})$	0.0015	0.017	0.101	147	0.95
$k_2(10^{-1}min^{-1})$	0.022	0.146	0.315	94	0.94
$k_3(10^{-1}min^{-1})$	0.0036	0.040	0.156	133	0.93
$k_4(10^{-1}min^{-1})$	0.0023	0.027	0.116	139	0.94
$k_5(10^{-1}min^{-1})$	0.0617	0.283	0.601	80	0.96
$k_6(10^{-1}min^{-1})$	0.0062	0.061	0.235	128	0.91
$k_7(10^{-1}min^{-1})$	0.0092	0.087	0.265	119	0.94
$k_8(10^{-1}min^{-1})$	0.109	0.357	0.810	71	0.93

Table 4.1: Kinetic parameters for the catalytic conversion of cellotriose to sorbitol.

In case of disaccharides similar to trisaccharides the hydrogenation reaction is notably faster compared to hydrolysis at lower temperatures. Additionally, the rate constant for hydrolysis of reduced disaccharide k_7 is higher than the

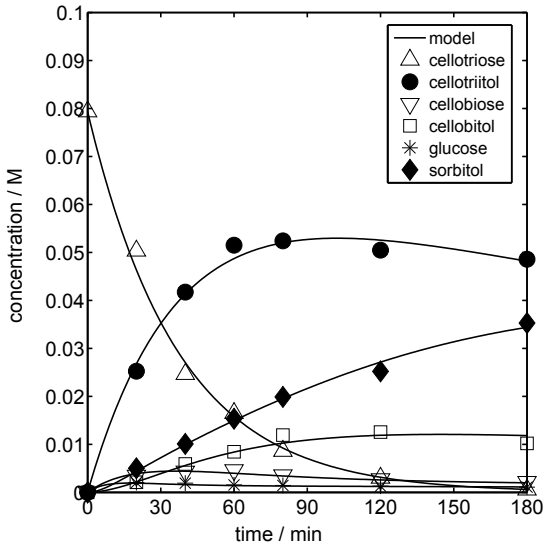

Figure 4.4: Fit of the kinetic model to the experimental data at 393 K; Reaction conditions: cellotriose, 2 mmol; Ru/C, 0.1 g; HPA, 0.2 g; H_2O, 20 cm^3 and 4 MPa H_2.

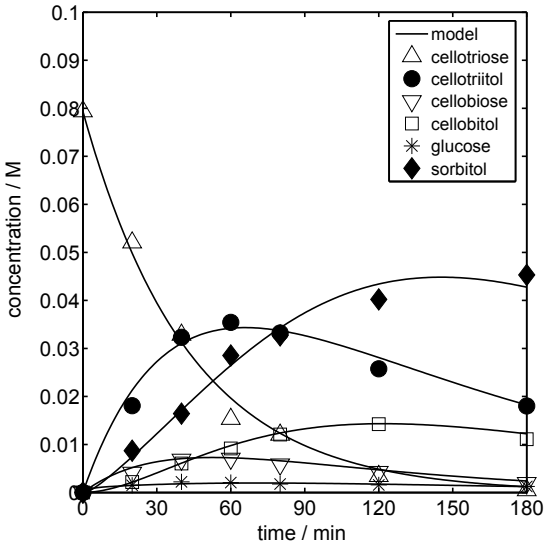

Figure 4.5: Fit of the kinetic model to the experimental data at 413 K; Reaction conditions: cellotriose, 2 mmol; Ru/C, 0.1 g; HPA, 0.2 g; H_2O, 20 cm^3 and 4 MPa H_2.

rate constant for hydrolysis of the disaccharide k_6 confirming again a facilitated hydrolysis after hydrogenation. A closer look on the observed activation energies strengthens this interpretation. The activation energies E_3 and E_4 for the hydrolysis of a reduced trisaccharide compared to E_1 for the hydrolysis of trisaccharides emphasising again a facilitated hydrolysis after hydrogenation.

Activation energies E_2, E_5 and E_8 for the hydrogenation reactions were estimated being in good agreement with our previous report and literature values [91]. Obviously, activation energies for hydrogenation increase with increasing chain length. Together with decreasing reaction rate constants, one may conclude on a facilitated hydrogenation of shorter saccharides. A comparable trend can be observed for hydrolysis. Comparing hydrolysis of di- and trisaccharides, activation energies increase ($E_6 < E_1$) and reaction rate constants decrease ($k_6 > k_1$). This observation is in well agreement with a decrease of the hydrolysis rate constant of cellodextrin with an increase of the degree of polymerization (DP) [52, 92].

Hydrolysis of oligosaccharides is affected by geometric constrains such as the anomeric configuration of the glycosidic linkages (α or β), the position of linkage such as (1-4), (1-6), the presence of functional groups in the molecule and the intensity of inter- and intra-molecular interactions [90, 49]. Therefore, the estimated kinetic constants for cellotriose and maltotriose has slightly different values (Table 4.2 and Table 4.1).

The present study confirms a tremendous effect of oligosaccharide hydrogenation. To rationalise the obtained results the ratios of reaction rate constants for hydrogenation versus hydrolysis of cellotriose and maltotriose (Table 4.2) were summarized (Figures 4.7 and 4.8). Despite a facilitated hydrolysis of α-1,4-glycosidic bonds in maltose and maltotriose, hydrogenation remains to be superior to hydrolysis especially at lower temperatures. The dominant character

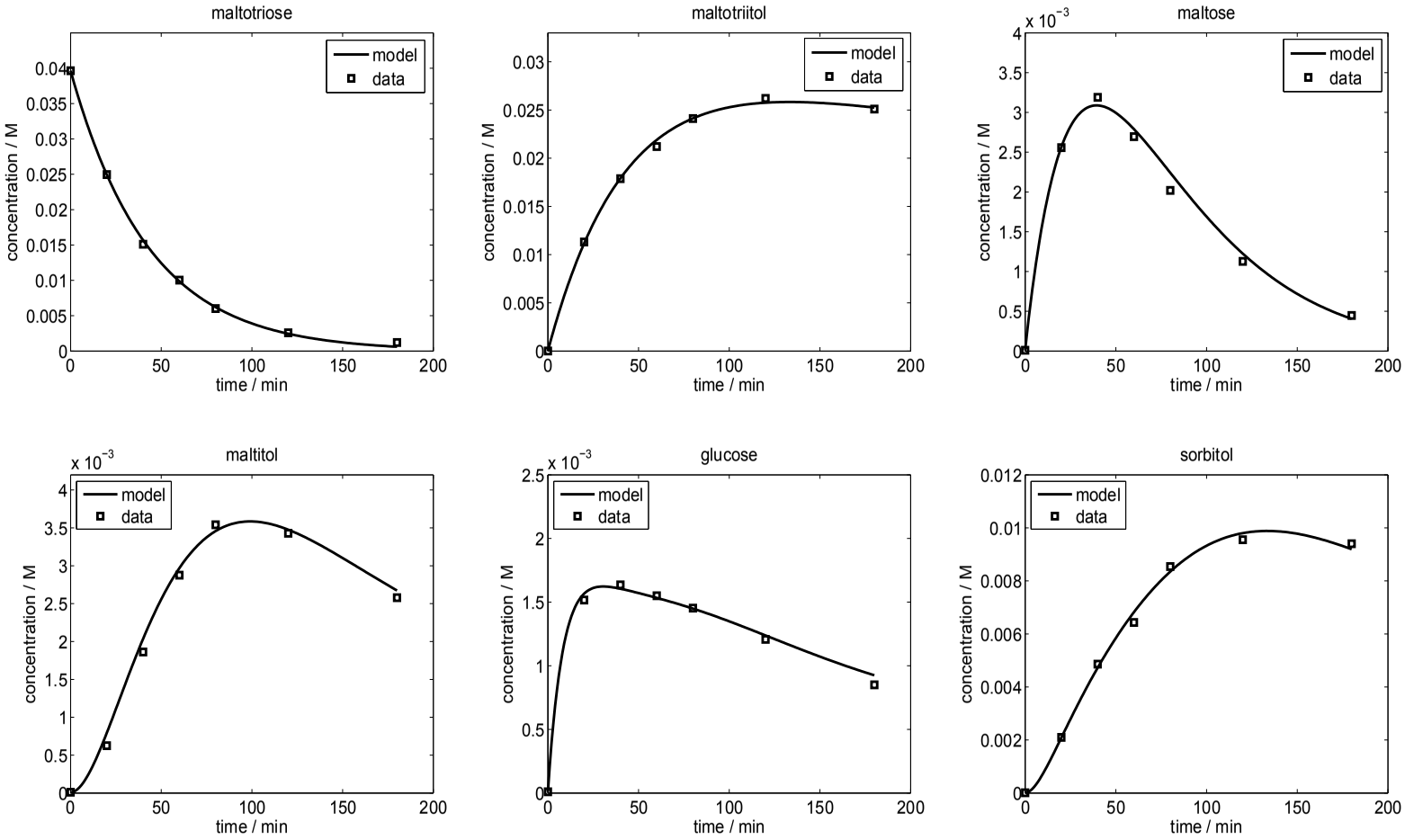

Figure 4.6: Fit of the kinetic model to the experimental data at 413 K; Reaction conditions: maltotriose, 2 mmol; Ru/C, 0.1 g; HPA, 0.2 g; H_2O, 20 cm^3 and 4 MPa H_2.

Reaction T(K)	393	413	433	E_a [kJ mol^{-1}]	R^2
$k_1(10^{-1}min^{-1})$	0.0025	0.035	0.101	131	0.97
$k_2(10^{-1}min^{-1})$	0.0612	0.26	0.653	84	0.98
$k_3(10^{-1}min^{-1})$	0.0075	0.102	0.201	117	0.96
$k_4(10^{-1}min^{-1})$	0.0041	0.071	0.141	126	0.97
$k_5(10^{-1}min^{-1})$	0.108	0.418	0.985	77	0.98
$k_6(10^{-1}min^{-1})$	0.011	0.103	0.281	112	0.97
$k_7(10^{-1}min^{-1})$	0.021	0.184	0.352	101	0.98
$k_8(10^{-1}min^{-1})$	0.26	0.81	1.51	62	0.98

Table 4.2: Kinetic parameters for the catalytic conversion of maltotriose to sorbitol.

of hydrogenation is even more pronounced for longer oligomers. Comparing the ratio of k_2/k_1 versus k_5/k_6, a maximum decrease from 24 to 10 and 15 to 10 for maltotriose and cellotriose, respectively, becomes obvious (Figure 4.7).

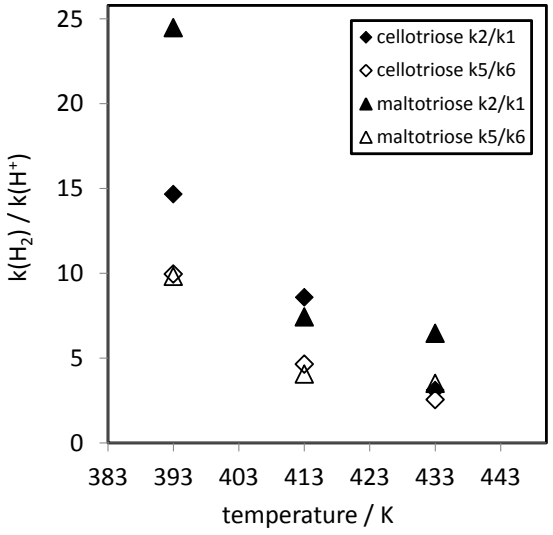

Figure 4.7: Kinetic selectivity of hydrogenation versus hydrolysis at various reaction temperatures (Table 4.2 and Table 4.1).

For all temperatures, the kinetic selectivity of hydrogenation versus hydrolysis is more pronounced for the investigated trisaccharides compared to the corresponding disaccharides.

The kinetic selectivity for hydrolysis of reduced compounds with regard to hydrolysis of the corresponding saccharide adds to the described effects (Figure 4.8). For all compounds, temperatures and positions in the reaction network, hydrolysis after hydrogenation is accelerated. Indispensable of (α-1,4) or (β-1,4) glycosidic linkages, a facilitated hydrolysis after hydrogenation occurs. Important to note, the trend is even more distinct for hydrolysis of longer oligosaccharides (k_7/k_6 vs. k_3/k_1 for cellotriose and maltotriose). From a structural point of view, these data emphasize an accelerated hydrolysis of oligosaccharides in open ring structures compared to hydrolysis of the close structure. A progressive

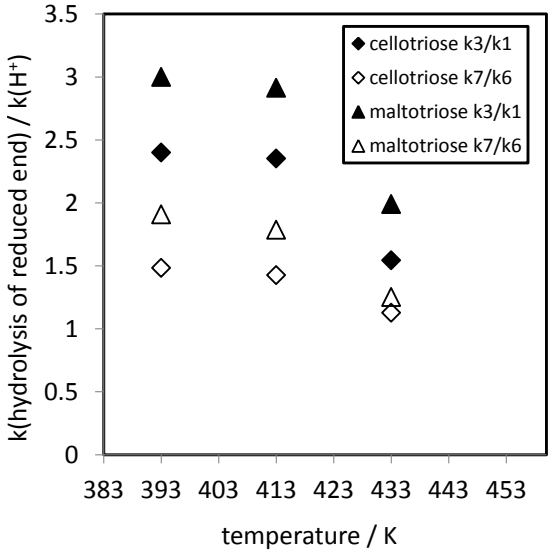

Figure 4.8: Kinetic selectivity of hydrogenation versus hydrolysis at various reaction temperatures (Table 4.2 and Table 4.1).

decrease of the rate constants with increasing size of the oligosaccharide can be observed. Together with overall higher rate constants for hydrolysis of reduced

compounds, a sequential hydrogenation followed by hydrolysis to release sorbitol could even present an important reaction pathway in case of longer oligosaccharides. However, it should be noted that the presented kinetic analysis can only support the proposed reaction network but not confirm the reaction sequence.

4.4. SUMMARY

Trisaccharides have been studied as substrates for the formation of sorbitol. Hydrogenation of such oligosaccharides followed by a facilitated hydrolysis of the terminal sorbitol unit could be observed. A time-resolved study and kinetic analyses emphasise this reaction pathway to be preferred at low reaction temperatures and for longer oligomers. The kinetic selectivity of hydrogenation versus hydrolysis increases with oligomer size reaching a ratio of 24 and 15 at 393 K for maltotriose and cellotriose, respectively. Our observations clearly confirm the significance of the described pathway of sorbitol production. Especially at lower temperatures and with increasing oligomer size, a preferential hydrogenation and hydrolysis of the terminal sorbitol unit can be observed.

CHAPTER 5

OLIGOSACCHARIDES

This chapter is based on the hypothesis that hydrogenation of long-chain oligosaccharides increases the rate of hydrolysis to a considerable extent and presents a significant alternative pathway in sorbitol formation. To this end, maltodextrin (DP 2-7) has been chosen as model of oligosaccharides while the mixture of cellodextrin is hardly available. The theoretical background of this work is prevalent in chemical process literature and is mostly based on the works of Gillespie [93, 94, 95], McQuarrie [96], Gibson & Bruck [97], and Renken [98].

5.1. KINETICS OF LONG CHAIN OLIGOSACCHARIDES

Three different methodologies are used to model the kinetics of long chain oligomers. First, the process can be treated as a statistical problem using mathematical method such as Markov chain theory. Second, the stochasticity of the process can be treated by preforming simulation. For example using Monte Carlo method, to compute the evaluation of the reacting system. Third, using a deterministic approach in which population balance will be used to express the

kinetics of reaction. In some cases, deterministic approach can be cumbersome and difficult to implement. For example, for macromolecules such as lignin with complicated distribution of reactive moieties and physical characteristics, Monte Carlo simulation is often more convenient because it renders the physical structure of the reactant explicit. Therefore, choice of methodology to simulate the kinetics depends on the condition of system. In the following section, theoretical background and a detailed justification of the choice of methodology will be discussed.

5.1.1. STOCHASTIC CHEMICAL KINETICS

Chemical kinetics deals mainly with the question of *how long* it takes for a chemical reaction to reach equilibrium that is when the reaction completes in the sense that the time averages of reactant populations becomes constant. Depending on reactant populations, a chemical process can be viewed as either *deterministic* or *stochastic*. Closely related to this, it can also be viewed as either *continuous* or *discrete*. In principle, all chemical reactions are stochastic and discrete. They are discrete because they take place among individual molecules whose populations must be quantified as integers. On the one hand, a chemical reaction takes place at such small scales that *quantum indeterminacy* cannot be overlooked. This means, no matter how elementary a single reaction is, one cannot know for sure whether it occurs or not, or predict when, if it does. In this manner, one can only speak of probability of such an event. This in turn, makes the reactant populations indeterminate i.e. stochastic.

5.1.2. CHEMICALLY REACTING SYSTEMS

A chemically reacting system is an agglomerate of molecules confined within non-permeable thermodynamic walls. It is also taken to be *well-stirred* so that

all observable quantities of the system have a homogeneous spatial distribution. This makes certain that a single reaction is equally likely anywhere inside the system. To simplify the matters further, it is presumed that a chemically reacting system keeps its temperature and pressure constant through contact with proper surroundings. Again since such a system is well-stirred, its state can be completely specified with its molecular populations $\mathbf{X}(t) = (X_1(t), X_2(t), \ldots, X_N(t))$ of the N chemical species $\{S_1, S_2, \ldots, S_N\}$ of which it is composed. The X_i's are whole numbers. We suppose that the chemical process $\mathbf{X}(t)$ is realized through M chemical reactions $\{R_1, R_2, \ldots, R_M\}$. The stoichiometric coefficient of the i^{th} chemical component in the j^{th} reaction is ν_{ij}. There are $N \times M$ such coefficients which form a matrix $\boldsymbol{\nu}$. The collective coefficients of a reaction R_j is called *state change vector*, written as $\boldsymbol{\nu}_j = (\nu_{1j}, \nu_{2j}, \ldots, \nu_{Nj})$. If at time t the reaction R_j takes place, the state vector $\mathbf{X}$ changes as $\mathbf{X}(t + \Delta t) = \mathbf{X}(t) + \boldsymbol{\nu}_j$.

Stochasticity

We already explained why a chemical process is essentially stochastic. Stochasticity, in quantitative terms, means that the state $\mathbf{X}$ is a random vector composed of random variables X_i, $i = 1, \ldots, N$. The time dependency of $\mathbf{X}(t)$ is the principle. We perceive time as being divided into past, present, and future. One could raise the question as to whether the future state(s) of a system can be predicted based on its present state only, and independent of its past. If such is the case, the $\mathbf{X}(t)$ is called a Markov process. A Markov process is, in short, a memoryless stochastic process. If $\mathbf{X}(t)$ indicates a Markov chemical process, we are entitled to defining the conditional probability density function

$$P(\mathbf{x}, t|\mathbf{x}_0, t_0) \equiv \mathrm{Prob}\{\mathbf{X}(t) = \mathbf{x}, \text{ given that } \mathbf{X}(t_0) = \mathbf{x}_0\}, \tag{5.1}$$

where $\mathbf{X}(t_0) = \mathbf{x}_0$ is the initial condition. For its determination, it is sufficient to know the propensity function of the Markov chemical process. The idea is the direct proportionality between the reaction R_j and the elapsed time Δt. The coefficient of this proportionality depends on molecular populations and is called propensity function.

Assumption 1. *If at any instant t the molecular populations of a Markov chemical process are given, $\mathbf{X}(t) = \mathbf{x}$, the probability that any reaction R_j will occur somewhere inside the system Ω within the next time interval of length Δt, is equal to $a_j(\mathbf{x})\,\Delta t$. The $a_j(\mathbf{x})$ is called propensity function.*

Quantum mechanics predicts that for every possible reaction R_j inside a chemically reacting system Ω there exists a constant c_j, such that $c_j\,dt$ equals the probability that a molecule in Ω takes part in the reaction within the next infinitesimal time dt. From definitions, it is clear that the propensity function a_j is proportional to c_j. If R_j is unimolecular, for instance, $a_j(x) = xc_j$, where x is the number of reactant molecules. For a bimolecular reaction we have $a_j(x, y) = xyc_j$. If the bimolecular reaction has a single reactant, i.e. $2\mathrm{A} \to \mathrm{B}$, the propensity $a_j(x) = x(x-1)c_j$.

To establish the connection between probability density and propensity function, let us observe a Markov chemical process within a small time interval $[t, t + \Delta t)$. If Δt is assumed equal to the characteristic time between two consecutive reactions, there are two possible ways for the system to proceed within this time interval. Either one single reaction takes place or no reaction takes place. Since these two possibilities are mutually exclusive, the sum of their probabilities makes up the $P_{\mathbf{x}}(t + \Delta t)$. The probability that one reaction occurs, equals the sum of conditional probabilities of all M possible reactions $P_{\mathbf{x}}(t + \Delta t) = \Delta t \sum_{j=1}^{M} a_j(\mathbf{x} - \boldsymbol{\nu}_j)\, P_{\mathbf{x}-\boldsymbol{\nu}_j}(t)$. The probability that nothing happens,

on the other hand, is the complement to the event that all reactions take place $P_{\mathbf{x}}(t+\Delta t) = \left[1 - \Delta t \sum_{j=1}^{M} a_j(\mathbf{x})\right] P_{\mathbf{x}}(t)$. Adding up the two values we obtain the increment formula

$$P_{\mathbf{x}}(t+\Delta t) = P_{\mathbf{x}}(t) + \Delta t \left[\sum_{j=1}^{M} a_j(\mathbf{x}-\boldsymbol{\nu}_j)\, P_{\mathbf{x}-\boldsymbol{\nu}_j}(t) - a_j(\mathbf{x})\, P_{\mathbf{x}}(t)\right] \tag{5.2}$$

This is called the *chemical master equation (CME)*. It can also be written in the form of a *differential-difference* equation

$$\frac{dP_{\mathbf{x}}(t)}{dt} = \sum_{j=1}^{M} a_j(\mathbf{x}-\boldsymbol{\nu}_j)\, P_{\mathbf{x}-\boldsymbol{\nu}_j}(t) - a_j(\mathbf{x})\, P_{\mathbf{x}}(t) \tag{5.3}$$

This is not at variance with discreteness of the chemical process, because the time derivative operates on the probability function and molecular populations appear in difference terms and factors only.

In principle, the chemical master equation is all that is needed to determine the probability densities of the random vector of molecular populations $\mathbf{X}$. However, it becomes complex as the number of reaction pathways and their molecularity grow. Notice that the chemical master equation is a highly coupled system of stochastic partial differential-difference equations. This means even if analytical solutions were available, in realistic situations, one would settle for their numerical solutions. But then again, due to the presence of numerous conditional probabilities, even a numerical algorithm would be overly complex.

For multi-molecular reactions with many pathways an alternative formulation exists which is formally different than, but logically equivalent to the chemical master equation. This alternative is called *stochastic simulation algorithm (SSA)* (see [95]). We will see that the chemical master equation is adequate for our purposes, since all the reactions in our experiment follow a pseudo first-order kinetics. We will also show that due to macroscopic molecular populations the stochasticity effects are negligible.

5.1.3. BIMOLECULAR REACTIONS

Let us focus on a simple chemically reacting system composed of three species A, B, and C with random populations $X(t), Y(t)$, and $Z(t)$, respectively, and with a single bimolecular reaction $A + B \to C$. The initial populations are given as $X(0) = x_0$, $Y(0) = y_0$, and $Z(0) = z_0$, and the state change vector $\nu = (-1, -1, 1)$. Since the process takes place through a single chemical reaction, the number of probability functions required to formulate the chemical master equation reduces to one. In case when $Y(0) > X(0)$, the chemical master equation (5.3) takes on the following form

$$\frac{dP_x(t)}{dt} = c(x+1)(w_0 + x + 1)P_{x+1}(t) - cx(w_0 + x)P_x(t) \tag{5.4}$$

where $w_0 = y_0 - x_0$ and constant c has already been introduced through its relation to the propensity function, as $a_j(x, y) = xyc_j$.

However, if the bimolecular reaction takes place in a large system (macroscopic), some simplifications can be made which set the stage for our model. We will see that the above formulation demonstrates the deterministic behavior of a thermodynamic system as its limiting case.

Deterministic kinetics as limiting case of stochastic kinetics

The reactions we are interested in, hydrogenation and hydrolysis of long-chain oligosaccharides are bimolecular:

$$P_n + \mathrm{H_2O} \xrightarrow{\mathrm{HPA}} P_{n-m} + P_m \tag{5.5a}$$

$$R_n + \mathrm{H_2O} \xrightarrow{\mathrm{HPA}} P_{n-m} + R_m \tag{5.5b}$$

$$P_n + \mathrm{H_2} \xrightarrow{\mathrm{Ru/C}} R_n \tag{5.5c}$$

where P_n and R_n are oligosaccharide and reduced oligosaccharide of length n. Therefore they conform to the kinetic formulation that we just developed (5.4).

It should be noted, however due to large reactant populations in our experiments, the stochastic effects can be neglected.

At each run of the experiment we roughly provide 10^{-3} moles of oligosaccharides which is the equivalent of 10^{20} molecules. The water in hydrolysis (5.5a) (5.5b) and hydrogen in hydrogenation (5.5c) are much more abundant than the oligosaccharides. In terms of the notation introduced in (5.4) these mean that $w_0 \gg x_0$ and $x_0 \gg 1$.

- $w_0 \gg x_0$ stands for overabundance of H_2 and H_2O, and
- $x_0 \gg 1$ stands for large (macroscopic) population of oligosaccahrides.

The first of these two assumptions, i.e. $w_0 \gg x_0$, reduces the general solution of (5.4) to a simple formulation in terms of the average and the variance of X (see [96])

$$\langle X(t)\rangle = x_0\, e^{-kt}\,,\ k = (w_0+1)c \tag{5.6a}$$

$$\langle\langle X(t)\rangle\rangle = x_0\, e^{-kt}\left(1 - e^{-kt}\right) \tag{5.6b}$$

The average value (5.6a) is clearly the solution to a first-order deterministic reaction rate equation

$$\frac{d\langle X(t)\rangle}{dt} = -k\langle X(t)\rangle\,, \quad \langle X(0)\rangle = x_0\,. \tag{5.7}$$

The bimolecular reactions (5.5) are therefore called *pseudo first-order* reactions. Hence, hydrogen and water are often omitted from reaction equations (5.5). The *reaction rate equations* like (5.7) are commonly expressed in terms of concentrations rather than molecular populations.

$$\frac{dC_A}{dt} = -kC_A\,, \quad C_A(0) = a_0\,, \tag{5.8}$$

in which C_A is the molar concentration of reactant A.

A simple standard method to measure the stochasticity of a random process $X(t)$ is the ratio of the standard deviation $\sqrt{\langle\langle X(t)\rangle\rangle}$ to its average $\langle X(t)\rangle$. Now considering the assumption $x_0 \gg 1$ and (5.6) we have

$$\lim_{x_0\to\infty} \frac{\sqrt{\langle\langle X(t)\rangle\rangle}}{\langle X(t)\rangle} = \frac{\sqrt{x_0\, e^{-kt}\,(1-e^{-kt})}}{x_0\, e^{-kt}} \propto \lim_{x_0\to\infty} \frac{1}{\sqrt{x_0}} = 0\,, \tag{5.9}$$

which implies that the stochasticity of the reaction is negligible when the polysaccharide population is macroscopic.
From the two recent results (5.7) and (5.9) we conclude that

Result 2. *Hydrogenation and hydrolysis of polysaccharides follow a deterministic pseudo first-order kinetics.*

5.2. RESULTS AND DISCUSSION

Hydrolytic hydrogenation of oligosaccharides (maltodextrin) is conducted at four different temperatures between 373 and 403 K. The concentrations of the oligosaccharides are analyzed with HPLC. The peaks in the chromatograms corresponding to maltooligomers (DP 2–7) and their reduced form can be seen in the Figure 5.1. It should be noted that the used maltodextrin is a mixture with different initial compositions of oligomers. Chromatograph shows the spectrum of reactants and products at different time intervals starting from the time when the reaction temperature is reached. Sugar oligomers appear together with their isomers in two adjacent peaks. Each gray peak belongs to the reduced form of corresponding sugar. The spectra evidently show the progress of reaction through hydrolysis and hydrogenation. Within the first 30 min the onset of reduction of oligosaccharides is observed expectedly. This is consistent with our previous analyses of di- and trisaccharides, reconfirming the dominance of hydrogenation reaction.

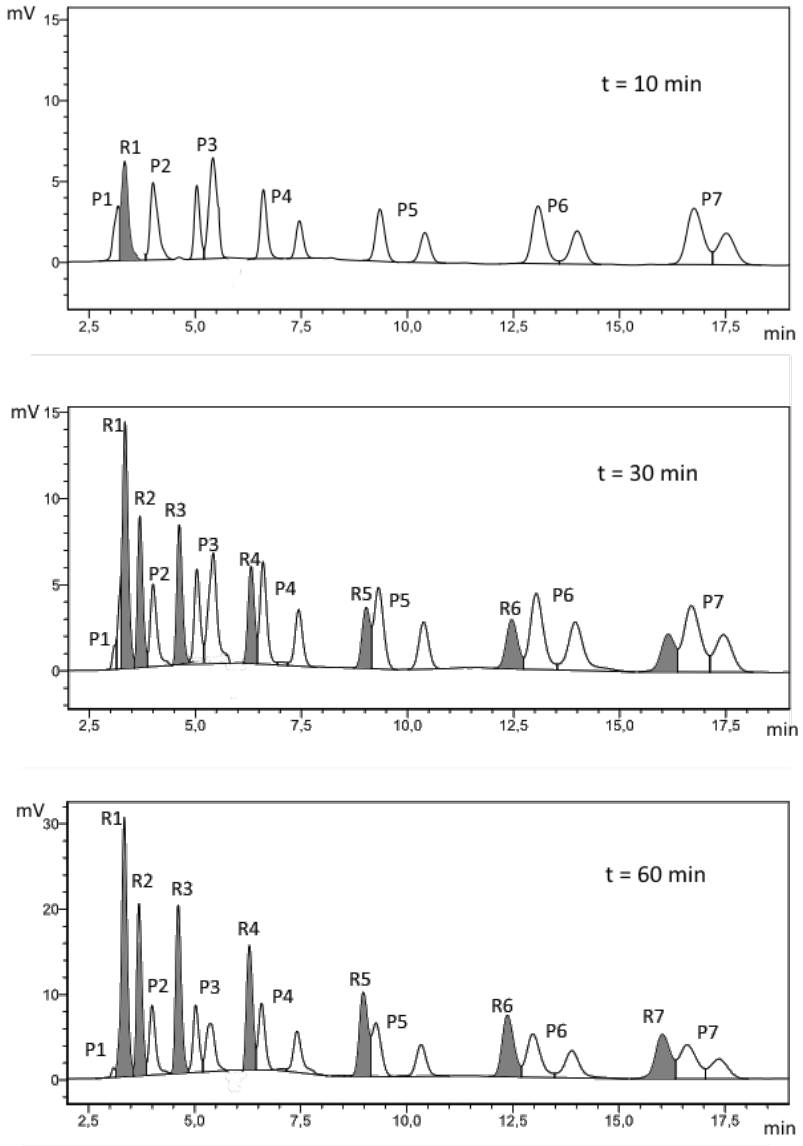

Figure 5.1: HPLC analysis of oligosaccharides; Reaction conditions: maltodextrin, 2 mmol; Ru/C, 0.1 g; HPA, 0.2 g; H_2O, 20 cm^3 and 4 MPa H_2 at 383 K, (P=oligosaccharide, R=reduced oligosaccharide).

5.2.1. MODEL FORMULATION

We formulate a kinetic model of the above experiment on the basis that two types of reactions take place, namely random hydrolysis of glycosidic bonds, and hydrogenation of reducing end of oligosaccharidic chain. We make no a priori assumption on hydrolysis rates of glycosidic bonds at different positions. This means the hydrolysis of each bond has its dedicated reaction rate equation, and we let the model decide whether they are equal or not.

These random scissions of the glycosidic bonds and reduction of terminal units of the chains are summarized in the following compact form

$$P_n \xrightarrow{k_{H^+}} P_j + P_{n-j} \qquad n = 2, \ldots, N \qquad j = 1, \ldots, \lfloor n/2 \rfloor \tag{5.10a}$$

$$P_n \xrightarrow{k_{H_2}} R_n \qquad n = 1, \ldots, N \tag{5.10b}$$

$$R_n \xrightarrow{k_{H^+}} P_j + R_{n-j} \qquad n = 2, \ldots, N \qquad j = 1, \ldots, \lfloor n/2 \rfloor, \tag{5.10c}$$

where P_n and R_n are oligosaccharide and reduced oligosaccharide of length n. Reactions (5.10a) and (5.10c) represent the hydrolysis (scission) and (5.10b) the hydrogenation (reduction). In the case of heptaoligosaccharide, the (5.10) forms a network of 14 species and 41 unimolecular reactions (Figure 5.2). Since all reactions follow the pseudo first-order rate equation (5.8), the overall kinetics of this reaction network takes the form of a first-order linear system of ordinary differential equations as we explain next.

Suppose that the reaction network is composed of N species $\{S_1, \ldots, S_N\}$, connected through M first-order reactions $\{Q_1, \ldots, Q_M\}$. We formerly introduce the $N \times M$ matrix of stoichiometric coefficients such that the element ν_{ij} is the the stoichiometric coefficient of S_i in Q_j. If the rate of the j$^{\text{th}}$ reaction is denote by r_j, the concentration of the i$^{\text{th}}$ species is given by

$$\frac{dC_i}{dt} = \sum_{j=1}^{M} \nu_{ij} r_j \tag{5.11}$$

	REACTION				MULTIPLICITY
1	P7	>>>	P6	P1	2
2	P7	>>>	P5	P2	2
3	P7	>>>	P4	P3	2
4	P7	>>>	R7		1
5	R7	>>>	P6	R1	1
6	R7	>>>	P5	R2	1
7	R7	>>>	P4	R3	1
8	R7	>>>	P3	R4	1
9	R7	>>>	P2	R5	1
10	R7	>>>	P1	R6	1
11	P6	>>>	P5	P1	2
12	P6	>>>	P4	P2	2
13	P6	>>>	P3	P3	1
14	P6	>>>	R6		1
15	R6	>>>	P5	R1	1
16	R6	>>>	P4	R2	1
17	R6	>>>	P3	R3	1
18	R6	>>>	P2	R4	1
19	R6	>>>	P1	R5	1
20	P5	>>>	P4	P1	2
21	P5	>>>	P3	P2	2
22	P5	>>>	R5		1
23	R5	>>>	P4	R1	1
24	R5	>>>	P3	R2	1
25	R5	>>>	P2	R3	1
26	R5	>>>	P1	R4	1
27	P4	>>>	P3	P1	2
28	P4	>>>	P2	P2	1
29	P4	>>>	R4		1
30	R4	>>>	P3	R1	1
31	R4	>>>	P2	R2	1
32	R4	>>>	P1	R3	1
33	P3	>>>	P2	P1	2
34	P3	>>>	R3		1
35	R3	>>>	P2	R1	1
36	R3	>>>	P1	R2	1
37	P2	>>>	P1	P1	1
38	P2	>>>	R2		1
39	R2	>>>	P1	R1	1
40	P1	>>>	R1		1

Figure 5.2: Reactions including in the kinetic modeling

Furthermore, since Q_j is first order, its rate depends linearly on concentrations of species. This can be formulated as

$$r_j = \sum_{i=1}^{N} k_{ji} C_i \,, \tag{5.12}$$

in which C_i is the concentration of species S_i. The k_{ij}'s are reaction rate constants which form an $M \times N$ matrix. The rate r_j depends only on one species concentration which largely simplifies (k_{ij}). If we now substitute (5.12) back into (5.11), we obtain

$$\frac{dC_i}{dt} = \sum_{j=1}^{M} \sum_{i=1}^{N} \nu_{ij} k_{ji} C_i \,, \quad i = \{1, 2, \ldots N\} \tag{5.13}$$

This is a linear system of N ordinary differential equations which is the foundation of our kinetic model.

5.2.2. MODEL IMPLEMENTATION

The experimental data from chromatography is a collection of concentrations of species sampled at regular time intervals. The sample data points are shown by an asterisk. For instance $C_i^*(t_n)$ will be the concentration of S_i in the sample taken at time t_n. Our objective is to find the rate constants (k_{ij}) such that the solution of (5.13) follows the sample points C_i^* as closely as possible. This is basically an optimization procedure which we implemented in MATLAB™ using the following algorithm:

1. Import the empirical concentration values and time steps $C_i^*(t_n)$.
2. Assign and initial guess for k_{ij}'s.
3. Assign the initial concentrations from step 1.
4. Solve (5.13) for $C_i(t)$, based on guess k_{ij}'s from step 2 and initial values from step 3 using finite difference method.

5. Find the least square distance between data points $C_i^*(t_n)$ from step 1 and the solution $C_i(t)$ from step 4.

6. If the distance evaluated in step 5 is smaller than a predesignated tolerance, then go to step 8, otherwise go to step 7.

7. Change the (k_{ij}) in the proper direction using the MATLAB built-in *Trust-Region-Reflective Optimization* algorithm, and go to step 4.

8. End.

The MATLAB code enclosed as appendix C is self-descriptive.

5.2.3. DATA ANALYSIS

The concentrations have been normalized to better distinguish the data points on multi-plot figures. Therefore, time profiles are given as mole fraction of the considered oligomer. Mole fraction is defined as the ratio of the mole of considered species to the total moles in the system. Figure 5.3 indicates the application of the above curve-fitting algorithm to experimental data for the given reaction conditions. The fitting is apparently successful which confirms our choice of kinetic model, i.e. first-order. Optimization was run for a wide range of initial guess for k_{ij} to make sure that the optimization is stable and the numerical results are reliable. So it is safe to assume that the reactions (5.10) take place precisely as presented. Since the reaction rate constants have been successfully estimated, we are now able to

- compare the rate of reduction and the rate of scission for each oligosaccharide P_n,

- calculate the rate of scission for each reduced oligosaccharide,

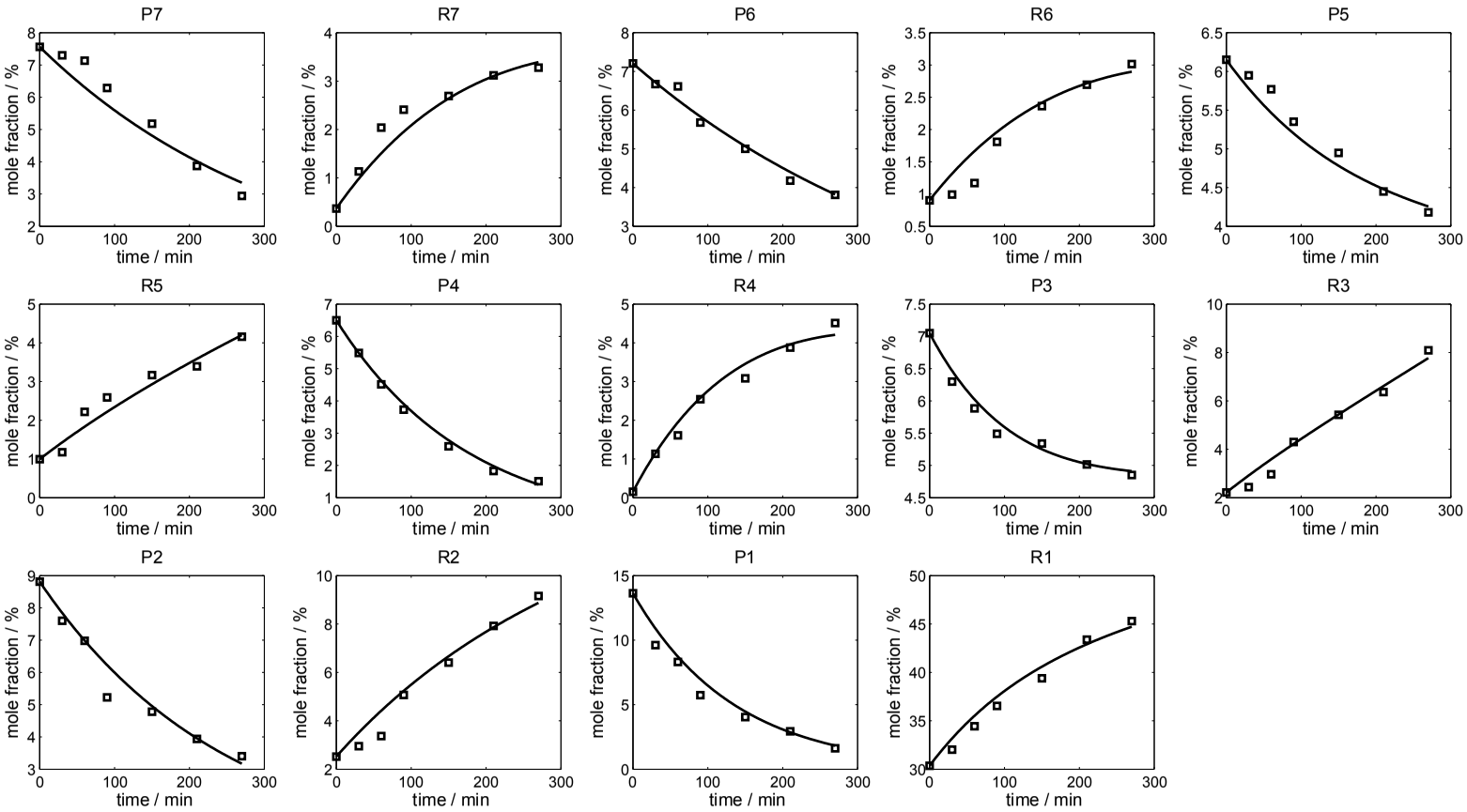

Figure 5.3: Kinetic modeling of oligosaccharides; Reaction conditions: maltodextrin, 2 mmol; Ru/C, 0.1 g; HPA, 0.2 g; H_2O, 20 cm^3 and 4 MPa H_2 at 383 K, (P=oligosaccharide, R=reduced oligosaccharide).

- compare the overall amount of scission between reduced and non-reduced compounds.

In a single instance of hydrolysis reaction (5.10a) or(5.10c) exactly one glycosidic bond is broken. This means that, the reaction rate equals the rate of scission. So for every compound, the sum of all hydrolysis reactions that have the compound as reactant, equals the rate with which the glycosidic bond are broken. In simple terms, the number of molecules that go through hydrolysis is equal to the number of broken bonds.

$$\text{scission rate of } P_n = r_{(P_n-scission)} = \left(\sum_{j=1}^{\lfloor n/2 \rfloor} k^{(j)}_{H^+,P_n} \right) P_n \,, \tag{5.14}$$

$$\text{scission rate of } R_n = r_{(R_n-scission)} = \left(\sum_{j=1}^{\lfloor n/2 \rfloor} k^{(j)}_{H^+,R_n} \right) R_n \tag{5.15}$$

The same holds for reduction (5.10b). The number of molecules which go through hydrogenation equals the number of reduced ends.

$$\text{reduction rate of } P_n = r_{(P_n-reduction)} = k_{H_2,P_n}\, P_n \tag{5.16}$$

The ratio of reduction to scission for each oligosaccharide is given by

$$\text{reduction/scission } P_n = \frac{k_{H_2,P_n}}{\sum_{j=1}^{\lfloor n/2 \rfloor} k^{(j)}_{H^+,P_n}} \,, \tag{5.17}$$

is independent of concentration.

For the simulation, the number broken bonds and the number of reduced ends in terms of mole fractions are obtained by time integration $n(t) = \int_0^t r\, dt$, of rate equations (5.14), (5.15) and (5.16).

Figure 5.4 compares scission yield versus reduction yield for each oligosaccharide. The kinetic selectivity of hydrogenation over hydrolysis for each oligosaccharide can be clearly seen. Notice that, the used maltodextrin is a mixture

with different initial compositions of oligomers. Oligomers with shorter chains have higher selectivity of hydrogenation. This is in agreement with our investigation on the kinetics of trisaccharides in which shorter chain oligomers have lower activation energies for hydrogenation indicating higher kinetic selectivity of hydrogenation.

To show the selectivity of hydrogenation over hydrolysis, , we added up all the mole numbers of reduced ends for all reacting compounds. The results are illustrated in Figure 5.5 for reaction temperatures of 383, 393, and 403 K. The overall higher kinetic selectivity of reduction over scission can be clearly observed. This kinetic selectivity will increase with increasing the reaction temperature. At temperature of 383 K, the total mole fraction of oligomers which are reduced is about 36 % and increases to 57 % at temperature of 403 K. In order to compare selectivity of hydrolysis of reduced compounds over hydrolysis of non-reduced compounds, the total mole numbers of broken bonds was added up. It can be seen that the reduced compounds will be hydrolysed in higher kinetic selectivity. Effect of temperature is higher for the hydrolysis of reduced compounds compared with non-reduced ones. At temperature of 403 K, total number of moles of reduced compound which goes through hydrolysis is about two times higher than total number of moles of non-reduced ones. This observation reconfirms the facile hydrolysis of reduced oligosaccharides.

5.3. SUMMARY

For our chemical reacting system, deterministic approach has been applied as a more convenient approach. Kinetic modeling was used to compare the rate of scission versus the rate of reduction for each oligosaccharide. Analysis of data showed the higher kinetic selectivity of hydrogenation over hydrolysis for each

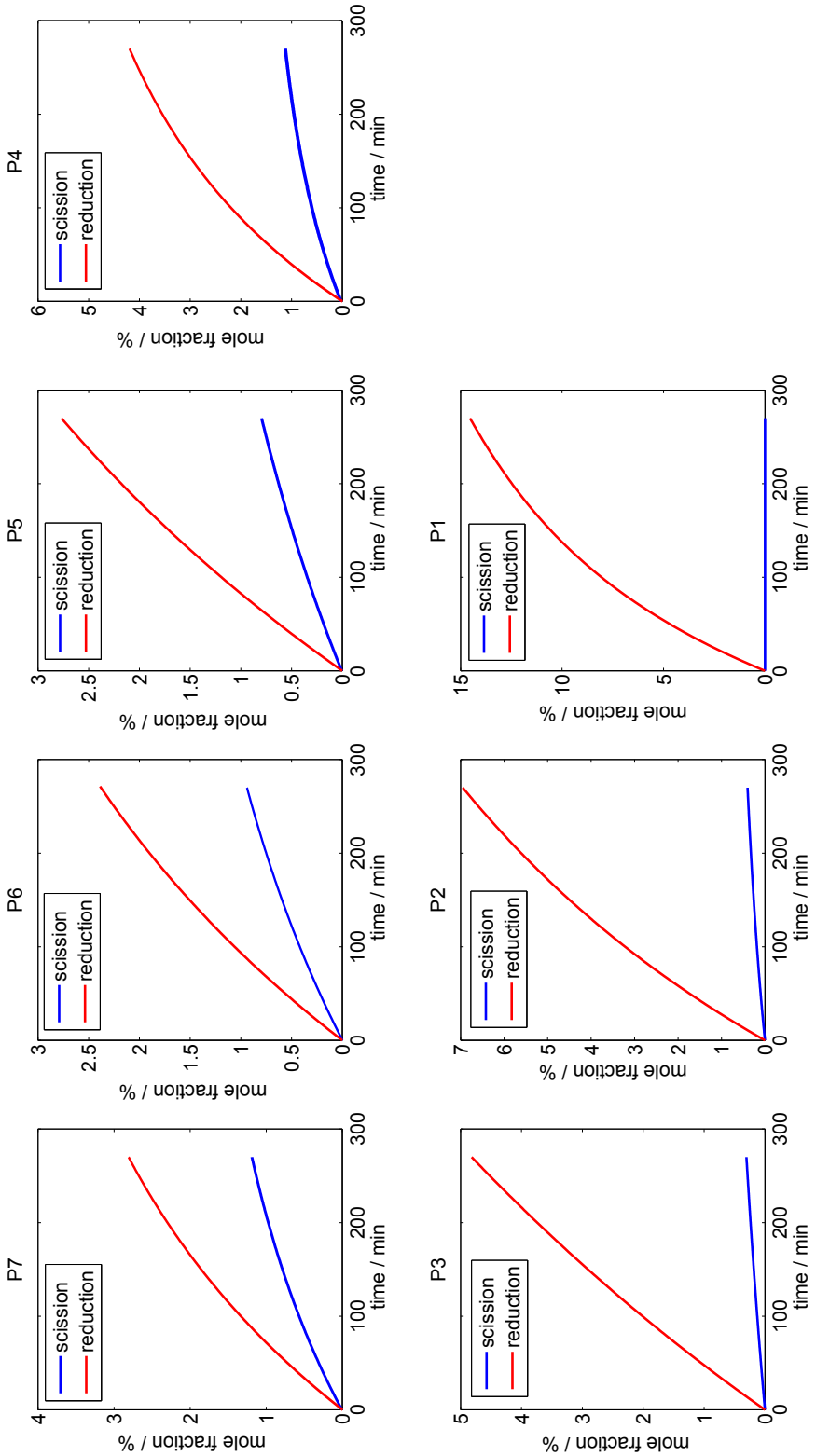

Figure 5.4: Scission versus reduction of oligosaccharides; Reaction conditions: maltodextrin, 2 mmol; Ru/C, 0.1 g; HPA, 0.2 g; H_2O, 20 cm^3 and 4 MPa H_2 at 383 K, (P=oligosaccharide).

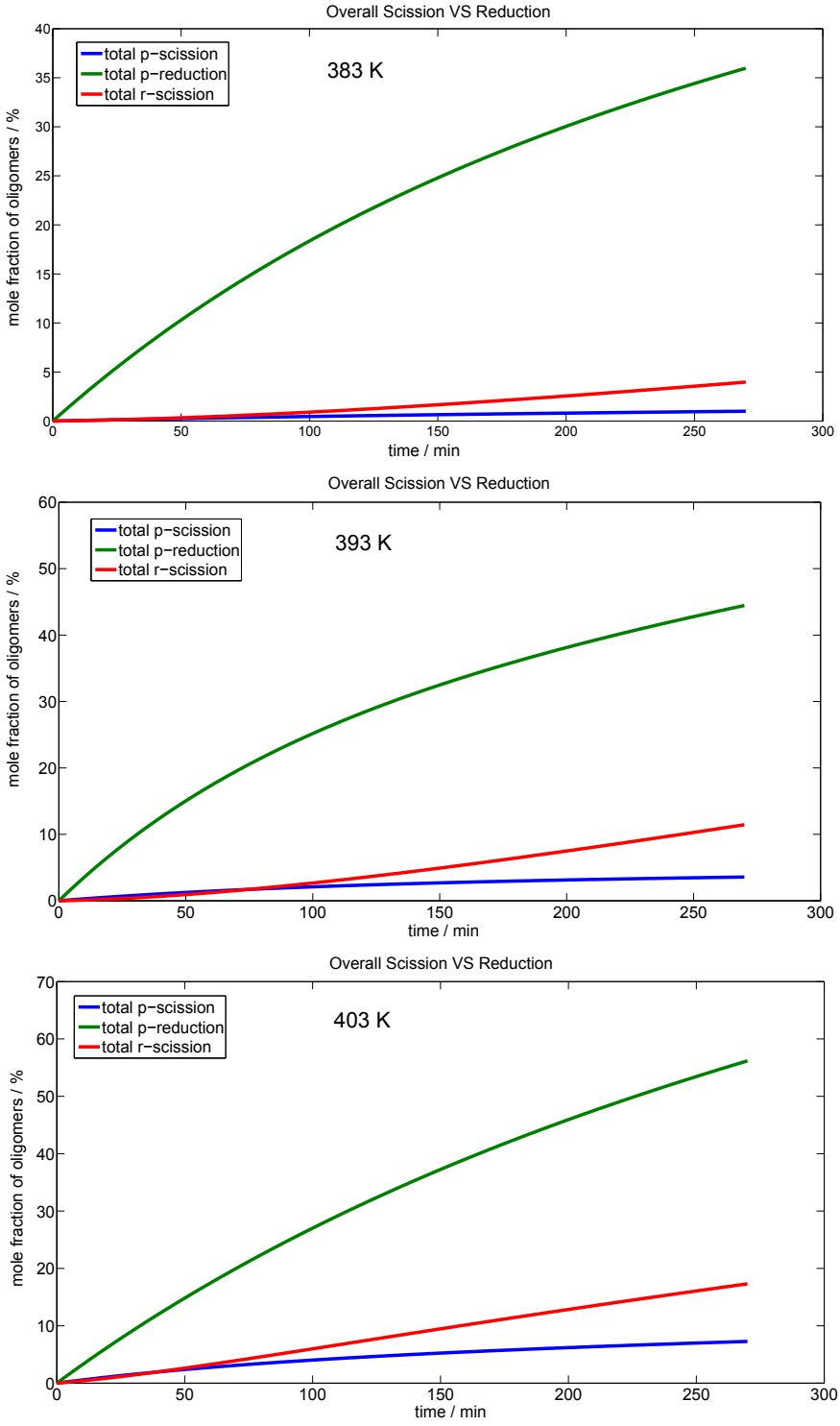

Figure 5.5: Overall comparison of scission versus reduction; Reaction conditions: maltodextrin, 2 mmol; Ru/C, 0.1 g; HPA, 0.2 g; H_2O, 20 cm^3 and 4 MPa H_2 at 383 K, (P=oligosaccharide, R=reduced oligosaccharide).

oligosaccharides. Overall kinetic selectivity of hydrogenation increased with increasing the reaction temperature. Kinetic analysis of the hydrolysis of reduced compounds over hydrolysis of non-reduced compounds showed that the reduced compounds will be hydrolysed in higher kinetic selectivity. The effect of increasing temperature on the hydrolysis of reduced compounds also was higher compared with non-reduced ones.

CHAPTER 6

CONCLUSION

The objective of our research was to study the reaction mechanism and kinetics of hydrolytic hydrogenation of polysaccharides to sorbitol. Due to complex structure of polysaccharides, kinetic study on model compounds of oligosaccharides was carried out. Because of heterogeneous catalytic reaction, mass transfer limitations were verified prior to experiments. Kinetic investigation of disaccharide showed the presence of an alternative pathway in the reaction network. In the presence of molecular acid and supported metal catalyst, disaccharide follows either a hydrolysis to glucose or an alternative pathway through hydrogenation towards reduced disaccharide. In a subsequent reaction, reduced disaccharide will be hydrolyzed to sorbitol and glucose. The selectivity of pathways within the reaction network strongly depends on the reaction conditions. At lower temperatures the hydrogenation pathway is dominant, whereas at higher temperature, hydrolysis becomes favorable. Analysis of empirical data showed that the direct hydrogenation to reduced disaccharide followed by hydrolysis is the more efficient pathway for production of sorbtiol.

In the next step, the kinetics of trisaccharide was examined in order to under-

stand the role of hydrogenation-hydrolysis sequences within a reaction network. Kinetic analysis showed a preferred hydrogenation of trisaccharides over their hydrolysis followed by a facilitated hydrolysis of reduced compound towards sorbitol. This higher selectivity becomes more pronounced at lower reaction temperatures and for longer oligosaccharides.

Finally, a much larger reaction network composed of a mixture of 6 oligosaccharides (di- to heptasaccharide) was studied based on a first-order kinetic model. The overall kinetic selectivity of the hydrogenation over hydrolysis as well as the facilitated hydrolysis of reduced compounds was observed. In summary, a preferential hydrogenation of oligosaccharides followed by hydrolysis to release sorbitol has been proposed as a significant reaction pathway for sorbitol production.

6.1. OUTLOOK

This work was a comprehensive kinetic analysis of oligosaccharides transformation into sorbitol. Some challenges remain which could be addressed for future work.

The results of kinetic modeling suggested that hydrolysis of reduced oligosaccharides is easier than hydrolysis of non-reduced oligosaccharides. It would be worthwhile to obtain the exact difference in the energy of hydrolysis by using of computational chemistry. For this aim, the study of simplest compound of oligosaccharides such as cellobiose or maltose would be helpful.

Analysis of kinetic data for trisaccharides showed that length chain has effect on the hydrolysis and hydrogenation reactions. In this regards, kinetic study of longer chain of oligosaccharides such as penta or heptasaccharides would be desirable to gain further insights concerning sequence of hydrogenation and hy-

drolysis reactions as well as the effect of length chain on both reactions. Finally, study of the effects of reaction conditions such as neutral or weakly acidic conditions on the kinetic selectivity of the hydrogenation and hydrolysis reactions could be considered in future work.

APPENDIX A

EXPERIMENTS

A.1. MATERIALS

Maltooligomers with DP(2-7) (maltose, maltotriose, maltotetraose, etc.) and their reduced forms (maltitol, maltotriitol, maltotetraitol) were purchased from Aldrich. Cellooligomers with DP(3-7) (cellotriose, cellotetraose, etc.) and their reduced forms (cellotriitol, cellotetraitol, etc.) were supplied by Megazyme and cellobiose was purchased from Alfa Aesar. Glucose, sorbitol, heteropoly acid (HPA, silicotungstic acid), and 5 wt.% Ru/C were provided from Aldrich. All above-mentioned chemicals were of analytical grade and used without further purification. The mixture of maltodextrin (DP(4-7)) was purchased from Aldrich and the cellodextrin (DP(2-7)) prepared by mechanocatalytic depolymerization of micro crystalline cellulose (Avicell) was provided from Max Plank Institute für Kohlenforschung. Cellobitol was self-synthesized with purity of 99 % and characterized by ^{13}C NMR spectroscopy.

A.1.1. SYNTHESIS OF CELLOBITOL AND CELLODEXTRIN

For synthesis of cellobitol, autoclave was loaded with 4 g cellobiose, 1 g Ru/C (5 wt.%) and 30 ml of water. The reactor was then purged and vented with N_2 and H_2 at room temperature. The pressure was immediately adjusted to the 60 bar H_2. The autoclave was then preheated under hydrogen pressure to the temperature of 373 K and for 8 h. Then solution was dried under vacuum oven at temperature of 303 K for 24 h. Characterization of cellobitol by NMR spectroscopy can be seen in the Figures A.1 and A.2. In the preparation of cellodextrin, 36 g of micro crystalline cellulose (Avicell) was impregnated with 1.4 mmol H_2SO_4 and mechanocatalytically treated for 2 h. The water solubility of mixture after mechanocatalytic depolymerization was 95 wt.% and mixture was mainly made of sugar oligomers with six monomeric units.

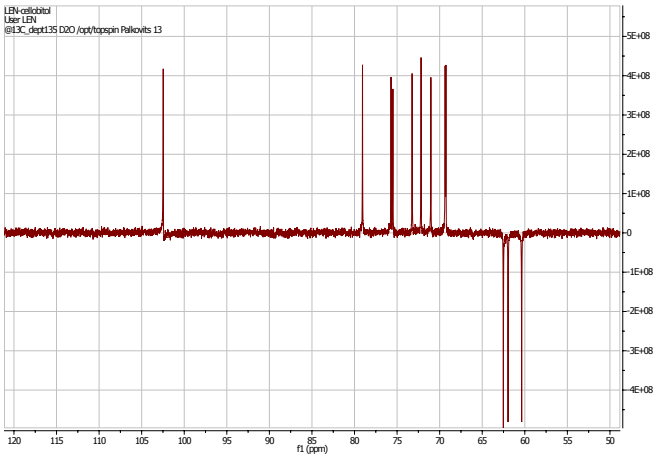

Figure A.1: DEPT 135 spectrum of cellobitol.

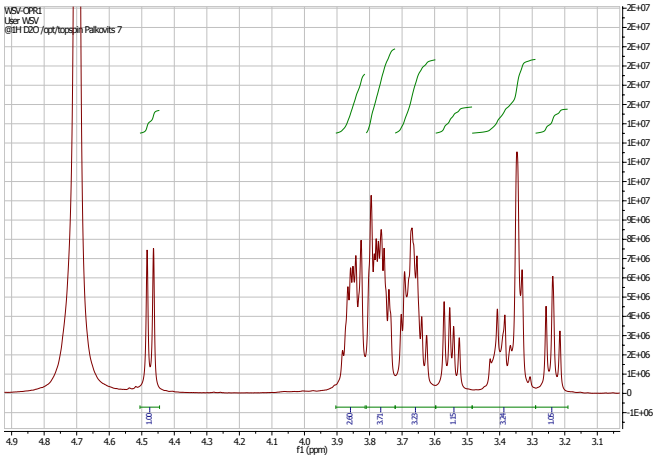

Figure A.2: ^{1}H-NMR of cellobitol.

A.2. ANALYSIS

Different columns were used to analyze the products. In the analysis, the concentration of each compound in the product mixture was determined using calibration curves of pure compounds in the standard solution.

A.2.1. SACCHARIDES ANALYSIS

Disaccharides samples were analyzed using an HPLC (Shimadzu LC-10A) with a RI-detector. Separation of the components was achieved by an organic acid resin column (CS-Chromatographie, Germany, 300 mm x 8.0 mm and 100 mm x 8.0 mm) operated at 313 K. The eluent (154 μL of CF3COOH in 1L of water) was supplied at the 1 ml min^{-1} flow rate. Figure A.3 shows a HPLC separation for hydrolytic hydrogenation of saccharides to sorbitol.

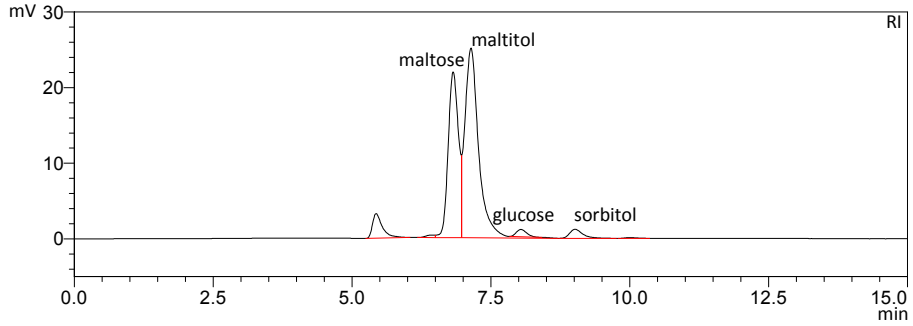

Figure A.3: HPLC separation for conversion of saccharides to sorbitol.

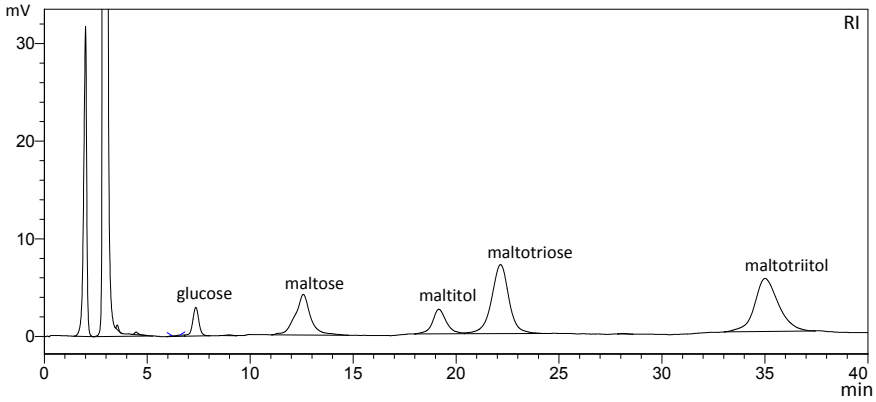

Figure A.4: HPLC separation for conversion of trisaccharides to sorbitol.

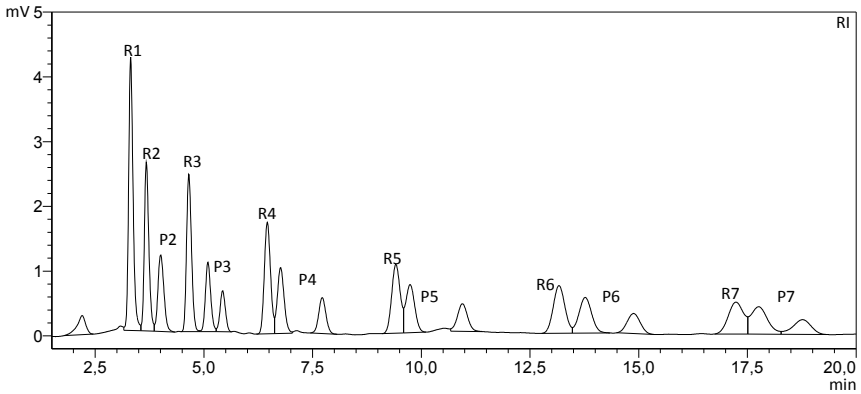

Figure A.5: HPLC separation for conversion of oligosaccharides to sorbitol.

A.2.2. TRISACCHARIDES ANALYSIS

Analyze of trisaccharides were performed using a HPLC system consisting of a ligand exchange column (Shodex sugar SZ5532, 6 mm × 150 mm) and a RI-detector. The eluent was an aqueous solution of acetonitril and water (20/80) at a flow rate of 1 ml min^{-1}. The column was operated at 323 K and the analysis for a sample was complete within 50 minutes. The samples were dissolved in 50 % solution of acetonitril prior to inject into the HPLC system. A HPLC separation for hydrolytic hydrogenation of trisaccharides to sorbitol can be seen in Figure A.4.

A.2.3. OLIGOSACCHARIDES ANALYSIS

The column used for the analysis of oligosaccharides was a hydrosphere ^{18}C column (250 mm × 4.6 mm i.d.), and the eluent was distilled water at a flow rate of 1 ml min^{-1}. The column operated at 293 K and 149 bar and separation of components was complete within 30 minutes. Figure A.5 shows a HPLC separation for hydrolytic hydrogenation of oligosaccharides to sorbitol.

APPENDIX B

MASS TRANSFER EVALUATION

B.1. GAS-LIQUID MASS TRANSFER

Suitable experiments to exclude mass transfer limitations were performed. To study the impact of gas–liquid mass transfer, the stirrer speed was varied between 600 and 1200 rpm. The difference in initial reaction rate was less than

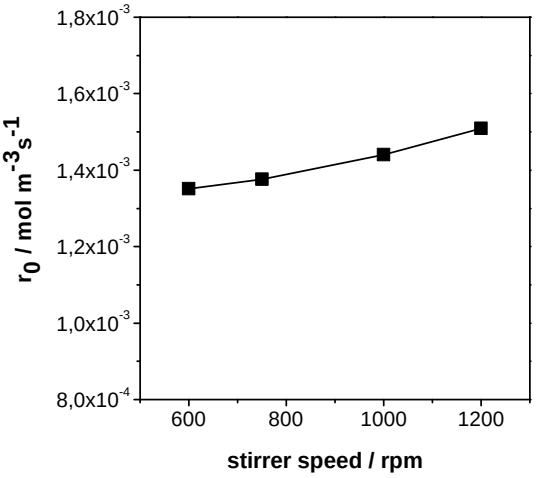

Figure B.1: Effect of stirrig speed on initial rate of cellobiose at 413 K.

5%, indicating the absence of gas–liquid mass transfer limitations (Figure B.1). The influence of hydrogen pressure on the initial reaction rate was investigated by varying the hydrogen pressure between 1 to 7 MPa. An increase in hydrogen pressure improves the reaction rate and its influence on the initial reaction rate can be described by Langmuir-Hinshelwood kinetics (Figure B.2).

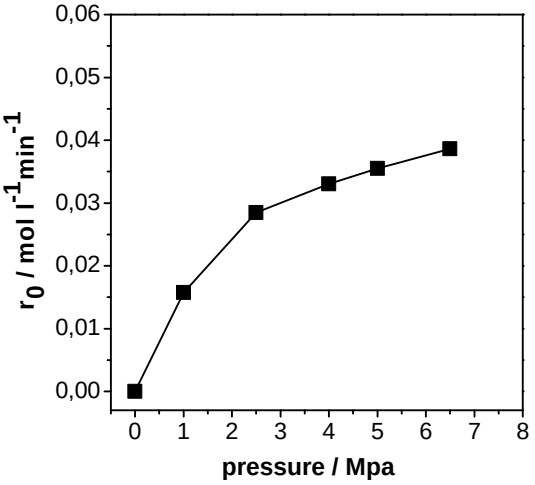

Figure B.2: Initial rate of cellotriose as function of hydrogen pressure at 393 K.

The experimental technique applied to measure the gas–liquid mass transfer coefficient is based on physical absorption of hydrogen in water [72]. In this method, the change of the hydrogen pressure will be followed in time. The reactor is equipped with a pressure transducer in order to record the change in pressure with time. The procedure consisted of the several steps. The reactor is evacuated, and then filled with hydrogen under stirring until equilibrium at known pressure P_0 was reached, then the stirrer was stopped and the reactor was pressurized to a pressure P_1; when a new equilibrium was reached, the stirrer was started and the pressure drop was followed in time until equilibrium pressure P_2 (Figure B.3). Integration between t=0 ($P = P_1$) and P(t) gives the following

equation between gas and liquid phases B.1

$$\frac{(P_2 - P_0)}{(P_1 - P_0)} Ln(\frac{P_1 - P_2}{P(t) - P_2}) = K_L a(t) \tag{B.1}$$

The volumetric gas-liquid mass transfer coefficient ($K_L a$) can be determined from the slope of the resulting plot. The hydrogen solubility ($C^*_{H_2}$) can be taken

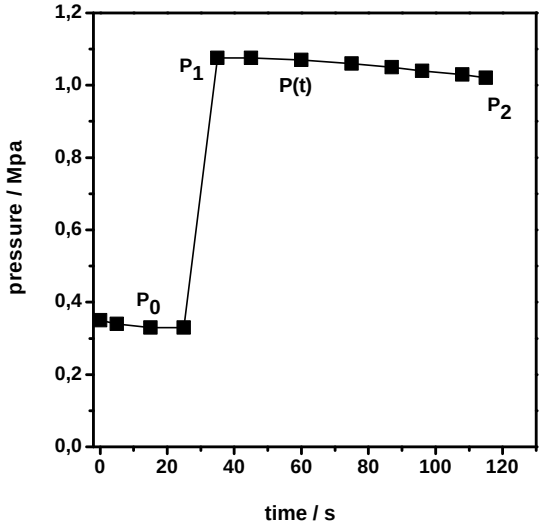

Figure B.3: Determination of volumetric gas-liquid mass transfer coefficient.

based on data published by Pray et al. [71] and also it can be calculated from Henry' law as follows (B.2 and B.3)

$$H_{H_2} = 2.291 \times 10^7 exp(\frac{581.8}{T}) \tag{B.2}$$

$$C_{H_2} = \frac{P_{H_2}}{H_{H_2}} \tag{B.3}$$

Combining these data the influence of mass transfer was estimated for the initial reaction conditions. In all kinetic experiments, a stirrer speed of 750 rpm was used and it was applied to calculate the appropriate ($K_L a$) values to verify gas-liquid mass transfer limitation (Figure B.4). For example, the estimated volumetric gas-liquid mass transfer coefficient at stirring speed of 750 rpm and

393 K was 0.08 s^{-1}. At temperature 393 K, the hydrogen solubility ($C^*_{H_2}$) was estimated to be 50 mol m^{-3} and initial rate of cellobiose was calculated to be 0.0135 mol $m^{-3}s^{-1}$.

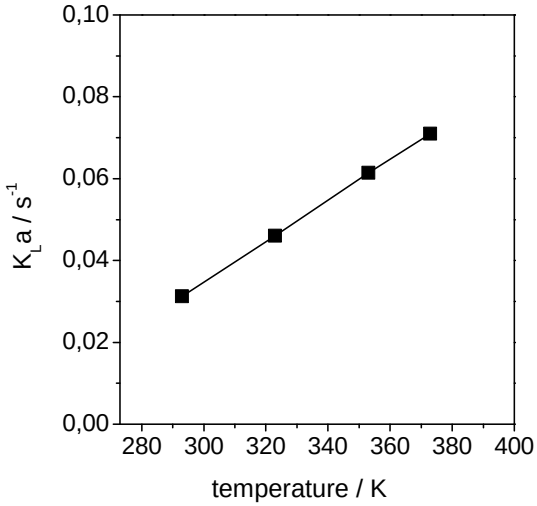

Figure B.4: Volumetric gas-liquid mass transfer coefficient at different temperatures.

B.2. LIQUID-SOLID MASS TRANSFER

Liquid–solid mass transfer coefficient was estimated by Sherwood number Sh which includes Re and Schmidt numbers [73]. The dimensionless numbers were estimated from equations B.4 and B.5.

$$Re = \frac{N_P d_s^5 N_s^3 d_p^4 \rho_L^3}{\mu_L^3 V_L} \tag{B.4}$$

$$Sc = \frac{\mu_L}{\rho_L D} \tag{B.5}$$

In the power number (N_p), p is the power of heating equipment and ρ is the density of liquid (Equation B.6).

$$N_p = \frac{p}{\rho N_s d_p} \tag{B.6}$$

Diffusion coefficient for hydrogen was estimated from the Wilke-Chang correlation (Eq.B.7) [99].

$$D = \frac{1.173 \times 10^{-13}(\phi M)^{0.5} T}{\mu V_m^{0.6}} \tag{B.7}$$

In this correlation, ϕ is association factor for the solvent and V_m is the molar volume of the solute. For estimation of the required liquid-solid mass transfer coefficient, the dimensionless numbers can be estimated based on data for physical properties of H_2 under selected operation conditions (Table B.1).

B.3. INTERNAL MASS TRANSFER

In internal mass transfer evaluation, the average particle diameter for used carbon supported ruthenium catalyst was 19 μm, and for calculations, the hemispherical shape of the catalyst was assumed. For diffusion of hydrogen inside the pores, the Knudsen correlation was used. Knudsen diffusivity is calculated as equation B.8.

$$D_k = 0.097 \times r_p (\frac{T}{M})^{0.5} \tag{B.8}$$

For calculation of effective diffusion D_e, following correlation was applied B.9:

$$D_e = (\frac{\epsilon}{\tau}) D_k \tag{B.9}$$

The porosity (ϵ) and tortuosity (τ) are assumed to be 0.5 and 4, respectively. From calculated values, it can be concluded that the external and internal mass transfer effects on the kinetics can be neglected.

Parameter		value
a	liquid-solid interface area (m^2m^{-3})	45×10^5
C_{H_2}	hydrogen solubility in liquid (cm^3g^{-1})	0.75
C_b	concentration in bulk liquid (mol m^{-3})	33.7
d_p	catalyst particle diameter (m)	1.9^{-5}
d_s	stirring diameter (m)	0.003
D	diffusion coefficient (G-L) (m^2s^{-1})	1.92×10^{-7}
D_k	Knudsen diffusivity (m^2s^{-1})	0.0129
D_e	effective diffusion coefficient (m^2s^{-1})	0.0016
H_{H_2}	Henry constant (Pa l mol^{-1})	50
K_La	volumetric gas–liquid mass transfer coefficient (s^{-1})	0.08
K_Ls	liquid–solid mass transfer coefficient (s^{-1})	0.069
n	reaction order	1
N_s	stirring speed (s^{-1})	12.5
N_p	power number	1.36×10^{19}
r_{obs}	observed reaction rate (mol $(m^3s)^{-1}$)	0.0135
r_p	catalyst particle redius (m)	9.5×10^{-6}
T	temperature (K)	393
V_L	volume of liquid (m^3)	2×10^{-4}
ρ_p	bulk density of catalyst particle (g cm^{-3})	2.1
ρ_L	density of the liquid (kg m^{-3})	985.4
μ_L	dynamic viscosity of the liquid (kg $(ms)^{-1}$)	2.8×10^{-3}
Re	Reynolds number	10^5
Sc	Schmidt number	1.5

Table B.1: Parameters and values used in calculation.

APPENDIX C

MATLAB CODE

C.1. DISACCHARIDES

```
%
clc;
close all;
clear all;
[tdata,Cdata] = ReadExcelFile('.\Excel\Data_matlab.xlsx');
t = tdata;
C = @(K,t)CFunc(K,t,Cdata(1,:,1));
% initial guess for K values
K0 = [0.01,0.01,0.01,0.01,0.01,0.01,0.01,0.01];
[K,resnorm] = FindK(C,tdata(:,:,1),Cdata(:,:,1),K0);
% display results
t2 = 0 : tdata(length(tdata));
C2 = C(K,t2);
S = get(0,'ScreenSize');
figure('OuterPosition',[S(3)/8,S(4)/8,S(3)*3/4,S(4)*3/4])
subplot(2,3,1); plot(t2,C2(:,1),'-k',tdata(:,:,1),Cdata(:,1,1),'sk');
% hold on
%    plot(t2,C2(:,2),'-',tdata(:,:,1),Cdata(:,2,1),'o');
%    plot(t2,C2(:,3),'-',tdata(:,:,1),Cdata(:,3,1),'v');
%    plot(t2,C2(:,4),'-',tdata(:,:,1),Cdata(:,4,1),'s');
%    plot(t2,C2(:,5),'-',tdata(:,:,1),Cdata(:,5,1),'d');
```

```
%    plot(t2,C2(:,6),'-',tdata(:,:,1),Cdata(:,6,1),'*');
% hold off
%legend('model','cellobiose','model','cellobitol','model','glucose',...
%'model','sorbitol','model','sorbitan','model','isosorbide');
%-----------------------------------------------------------------
xlabel('time / min','FontWeight','normal','FontName','Arial','FontSize',14);
ylabel('concentration / M','FontWeight','normal','FontName','Arial','FontSize',14);
title('cellobiose','FontWeight','normal','FontName','Arial','FontSize',14);
%box(subplot(2,3,1),'off');
set(gca,'fontsize',14);
legend('model','data');
set(legend,'FontWeight','normal','FontName','Arial','FontSize',14);
% % -----------------------------------------------------------------
subplot(2,3,2);plot(t2,C2(:,2),'-k',tdata(:,:,1),Cdata(:,2,1),'s k');
xlabel('time / min','FontWeight','normal','FontName','Arial','FontSize',14);
ylabel('concentration / M','FontWeight','normal','FontName','Arial','FontSize',14);
title('cellobitol','FontWeight','normal','FontName','Arial','FontSize',14);
%box(subplot(2,3,2),'off');
set(gca,'fontsize',14);
legend('model','data');
set(legend,'FontWeight','normal','FontName','Arial','FontSize',14);
%-----------------------------------------------------------------
subplot(2,3,3);plot(t2,C2(:,3),'-k',tdata(:,:,1),Cdata(:,3,1),'s k');
xlabel('time / min','FontWeight','normal','FontName','Arial','FontSize',14);
ylabel('concentration / M','FontWeight','normal','FontName','Arial','FontSize',14);
title('glucose','FontWeight','normal','FontName','Arial','FontSize',14);
%box(subplot(2,3,3),'off');
set(gca,'fontsize',14);
legend('model','data');
set(legend,'FontWeight','normal','FontName','Arial','FontSize',14);
% -----------------------------------------------------------------
subplot(2,3,4);plot(t2,C2(:,4),'-k',tdata(:,:,1),Cdata(:,4,1),'s k');
xlabel('time / min','FontWeight','normal','FontName','Arial','FontSize',14);
ylabel('concentration / M','FontWeight','normal','FontName','Arial','FontSize',14);
title('sorbitol','FontWeight','normal','FontName','Arial','FontSize',14);
%box(subplot(2,3,4),'off');
set(gca,'fontsize',14);
legend('model','data');
set(legend,,'Location','NorthWest','FontWeight','normal','FontName','Arial','FontSize',14);
% % % -----------------------------------------------------------------
subplot(2,3,5);plot(t2,C2(:,5),'-k',tdata(:,:,1),Cdata(:,5,1),'s k');
```

```
xlabel('time / min','FontWeight','normal','FontName','Arial','FontSize',14);
ylabel('concentration / M','FontWeight','normal','FontName','Arial','FontSize',14);
title('sorbitan','FontWeight','normal','FontName','Arial','FontSize',14);
%box(subplot(2,3,5),'off');
set(gca,'fontsize',14);
legend('model','data');
set(legend,'Location','NorthWest','FontWeight','normal','FontName','Arial','FontSize',14);
%%%%------------------------------------------------------------------------
 subplot(2,3,6);plot(t2,C2(:,6),'-k',tdata(:,:,1),Cdata(:,6,1),'s k');
 xlabel('time / min','FontWeight','normal','FontName','Arial','FontSize',14);
 ylabel('concentration / M','FontWeight','normal','FontName','Arial','FontSize',14);
 title('isosorbide','FontWeight','normal','FontName','Arial','FontSize',14);
 %box(subplot(2,3,6),'off');
 set(gca,'fontsize',14);
 legend('model','data');
 set(legend,'Location','NorthWest','FontWeight','normal','FontName','Arial','FontSize',14);


function [C,t] = ODESys(F,C0,tm)
% C = ODESys(F,C0) returns the numerical solution to a system of ordinary
% differential equations of the form d/dt C(t) = F(t;C(t)), in terms of
% discrete values of X's where
% F  :: function handle to the nx1 vector function
% C0 :: nx1 vector of initial values at t=0
% tm :: maximum value of t (end time of the reaction)
% C  :: nxm matrix of discrete values of C(t)
% t  :: discretized time domain for values of which C is computed
%
%
n = length(C0);
if (tm <= 0)
    error('tm must be a positive real number!');
end
m = 1000; % numebr of steps + 1
dt = tm/(m-1); % step size (time increment)
t = 0 : dt : tm; % discretized time domain
t = t';
C = zeros(m,n); % matrix of discrete values
C(1,:) = C0;
for i = 2 : m
    C(i,:) = C(i-1,:) + dt*F(t(i),C(i-1,:));
end
```

```
end

function C = CFunc(K,t,C0)
% C = CFunc(K,t,C0) evaluates concentrations C for given kinetic
% constants K, times t and given initial values of C0
% K  :: array of kinetic constants
% t  :: array of time instants for which concentrations are evaluated
% C0 :: array of initial concentrations
%
% See also ODESys
%
F = @(t,C)DC(t,C,K);
tm = t(length(t));
[C2,t2] = ODESys(F,C0,tm);
n = length(t);
m = length(C0);
C = zeros(n,m);
for i = 1:m
    C(:,i) = interp1(t2,C2(:,i),t,'pchip');
end
    function DC = DC(t,C,K)
        n = length(C);
        DC = zeros(1,n);
        DC(1) = -K(1)*C(1)-K(2)*C(1);
        DC(2) = K(2)*C(1)-K(3)*C(2);
        DC(3) = 2*K(1)*C(1)-K(4)*C(3)+ K(3)*C(2);
        DC(4) = K(4)*C(3)+K(3)*C(2)-K(5)*C(4)-K(6)*C(4);
        DC(5) = K(6)*C(4)-K(7)*C(5)-K(8)*C(5);
        DC(6) = K(8)*C(5);
    end
end
```

C.2. OLIGOSACCHARIDES

```
%
clc;
close all;
clear all;
```

```
% logical control constants
see_modeling_results = true;
see_p_results = true;
see_r_results = true;
see_overal_comparison = true;

% initializes constants
rcts_file_path = '.\Excel\Reactions.xlsx'; % contains reaction pathways
data_file_path = '.\Excel\Data_matlab.xlsx'; % contains experimental data
range_of_data = 'A3:O10'; % range of cells containing numerical data
range_of_reactions = 'B3:F42'; % range of cells containing reactions

% read data from excel
[tdata,Cdata] = ReadExcelFile(data_file_path, range_of_data);
t = tdata;
% kintetic function
C = @(K,t)CFunc(K,t,Cdata(1,:,1));

[null, null, rcts] = xlsread(rcts_file_path, 1, range_of_reactions);
[rows, cols] = size(rcts);

dim = rows; % number of K's
clear null rows cols;

% initial guess for K values
% K0 = 10^-1*(ones(1,dim)+rand(1,dim));
K0 = 10^-3*(ones(1,dim));
[K,resnorm] = FindK(C,tdata(:,:,1),Cdata(:,:,1),K0);

%%%%%%%%%%%%%%%%%%%%%%%%%%%%%%%%%%%%%%%%
%                SCISSION VS REDUCTION               %
%%%%%%%%%%%%%%%%%%%%%%%%%%%%%%%%%%%%%%%%
sug.name = {'hepta' 'hexa' 'penta' 'tetra' 'tri' 'bi' 'glucose'};
alc.name = {'heptitol' 'hexitol' 'pentitol' 'tetritol' 'tritol' 'bitol' 'sorbitol'};
% hydrogenation reaction indices
sug.hdgn = {4, 14, 22, 29, 34, 38, 40};
alc.hdgn = {[]};
% hydrolysis reaction indices
sug.hdrl = {(1:3), (11:13), (20:21), (27:28), 33, 37};
alc.hdrl = {(5:10), (15:19), (23:26), (30:32), (35:36), 39};
```

```
t2 = 0 : tdata(length(tdata));
C2 = C(K,t2);

[rows, cols] = size(C2);
r = zeros(rows, cols); % mole of substance (to be obtained by integrating the rates)

for i = 1 : cols
    r(:,i) = integ(C2(:,i), t2);
end

sug.cols = length(sug.name);
sug.scs = zeros(sug.cols, 1); % scission factors
sug.rdn = zeros(sug.cols, 1); % reduction factors

alc.cols = length(alc.hdrl);

for i = 1 : sug.cols
%     idx = 2*i-1;
%     r(:,idx) = integ(C2(:,idx), t2);
    if i ~= sug.cols
        sug.scs(i) = sum(K(sug.hdrl{i}));
    end
    sug.rdn(i) = sum(K(sug.hdgn{i}));
end

%%%%%%%%%%%%%%%%%%%%%%%%%%%%%%%%%%%%%%%%%%%%%%%%%%%%%%%%%%%%%%%%%%%%%%%%%%%%%%%
%                                DISPLAY RESULTS                                %
%%%%%%%%%%%%%%%%%%%%%%%%%%%%%%%%%%%%%%%%%%%%%%%%%%%%%%%%%%%%%%%%%%%%%%%%%%%%%%%
%
% % % % % % % % % % % %       KINETIC MODELING       % % % % % % % % % % % %
%
if see_modeling_results
    S = get(0,'ScreenSize');
    figure('OuterPosition',[S(3)/8,S(4)/8,S(3)*3/4,S(4)*3/4]);
    species = {'hepta' 'heptaitol' 'hexa' 'hexaitol' 'penta' 'pentaitol' ...
    'tetra' 'tetraitol' 'tri' 'tritol' 'bi' 'biotol' 'glucose' 'sorbitol'};
    for i = 1 : 14
        subplot(3,5,i);plot(t2,C2(:,i),'-',tdata(:,:,1),Cdata(:,i,1),'*');
        xlabel('␣time␣(min)','FontWeight','bold','FontName','Arial');
        ylabel('C␣[mol/l]','FontWeight','bold','FontName','Arial');
        title(species(i),'FontWeight','bold','FontName','Arial');
```

```
        %legend('data','model');
        set(legend,'FontWeight','bold','FontName','Arial');
    end
end

%
%%%%%%%%%%%%            SUGARS            %%%%%%%%%%%%
%
if see_p_results
    S = get(0, 'MonitorPosition');
    figure('OuterPosition',[S(3)/8,S(4)/8,S(3)*3/4,S(4)*3/4]);
end

P_SCISS = zeros(rows,1);
P_REDUC = zeros(rows,1);
ps = zeros(rows,1);
pr = zeros(rows,1);

for i = 1 : sug.cols
    idx = 2*i-1;
    ps = sug.scs(i)*r(:,idx);
    pr = sug.rdn(i)*r(:,idx);
    P_SCISS = P_SCISS + ps;
    P_REDUC = P_REDUC + pr;
    if see_p_results
        subplot(2,4,i);plot(t2,ps,'green',t2,pr,'red');
        xlabel(' time (min)','FontWeight','bold','FontName','Arial');
        ylabel('C [mol]','FontWeight','bold','FontName','Arial');
        title(sug.name(i),'FontWeight','bold','FontName','Arial');
        legend('scission','reduction');
        set(legend,'FontWeight','bold','FontName','Arial');
    end
end
%
%%%%%%%%%%%%            ALCOHOLS            %%%%%%%%%%%%
%
if see_r_results
    S = get(0, 'MonitorPosition');
    S(3:4)=0.97*S(3:4);
    rcts(:,2) = {'->'};
    rcts(:,5) = rcts(:,4);
```

```
    rcts(:,4) = {'+'};
    [m,n] = size(rcts);
    for i = 1 : m
        if not(isnan(rcts{i,5}))
            rcts{i,1} = strcat(rcts{i,1:5});
        else
            rcts{i,1} = strcat(rcts{i,1:3});
        end
    end
end

R_SCISS = zeros(rows, 1);

for i = 1 : alc.cols
    idx = 2*i;
    r2 = zeros(rows,length(alc.hdrl{i}));

    for j = 1 : length(alc.hdrl{i})
        r2(:,j) = K(alc.hdrl{i}(j))*r(:,idx);
        R_SCISS = R_SCISS + r2(:,j);
    end

    if see_r_results
        figure('OuterPosition',round([mod(i+2,3)*S(3)/3+S(3)*0.015, ...
            floor(i/4)*S(4)/2+S(4)*0.03, S(3)/3, S(4)/2]));
        plot(t2,r2(:,:));
        xlabel('␣time␣(min)','FontWeight','bold','FontName','Arial');
        ylabel('C␣[mol]','FontWeight','bold','FontName','Arial');
        title(alc.name(i),'FontWeight','bold','FontName','Arial');
        legend(rcts(alc.hdrl{i},1));
        set(legend,'FontWeight','bold','FontName','Arial');
    end
end
%
% % % % % % % % % % % %          COMPARISONS          % % % % % % % % % % % %
%
if see_overal_comparison
    S = get(0, 'MonitorPosition');
    figure('OuterPosition',[S(3)/8,S(4)/8,S(3)*3/4,S(4)*3/4]);
    plot(t2, P_SCISS, t2, P_REDUC, t2, R_SCISS);
    xlabel('␣time␣(min)','FontWeight','bold','FontName','Arial');
```

```
    ylabel('C [mol]','FontWeight','bold','FontName','Arial');
    title('Overall Scission VS Reduction','FontWeight','bold','FontName','Arial');
    legend('total p-scission','total p-reduction', 'total r-scission');
    set(legend,'FontWeight','bold','FontName','Arial');
end

function C = CFunc(K,t,C0)
% C = CFunc(K,t,C0) evaluates concentrations C for given kinetic
% constants K, times t and given initial values of C0
% K  :: array of kinetic constants
% t  :: array of time instants for which concentrations are evaluated
% C0 :: array of initial concentrations
%
% See also ODESys
%
F = @(t,C)DC(t,C,K);
tm = t(length(t));
[C2,t2] = ODESys(F,C0,tm);
n = length(t);
m = length(C0);
C = zeros(n,m);

for i = 1:m
    C(:,i) = interp1(t2,C2(:,i),t,'pchip');
end

function DC = DC(t,C,K)
    n = length(C);
    DC = zeros(1,n);
    DC(1) = -sum(K(1:4))*C(1);
    DC(2) = K(4)*C(1) - sum(K(5:10))*C(2);
    DC(3) = K(1)*C(1) + K(5)*C(2) - sum(K(11:14))*C(3);
    DC(4) = K(10)*C(2) + K(14)*C(3) - sum(K(15:19))*C(4);
    DC(5) = K(2)*C(1) + K(6)*C(2) + K(11)*C(3) + K(15)*C(4) ...
        - sum(K(20:22))*C(5);
    DC(6) = K(9)*C(2) + K(19)*C(4) + K(22)*C(5) - sum(K(23:26))*C(6);
    DC(7) = K(3)*C(1) + K(7)*C(2) + K(12)*C(3) + K(16)*C(4) + K(20)*C(5) ...
        + K(23)*C(6) - sum(K(27:29))*C(7);
    DC(8) = K(8)*C(2) + K(18)*C(4) + K(26)*C(6) + K(29)*C(7) ...
        - sum(K(30:32))*C(8);
    DC(9) = K(3)*C(1) + K(8)*C(2) + 2*K(13)*C(3) + K(17)*C(4) + K(21)*C(5) ...
```

```
        + K(24)*C(6) + K(27)*C(7) + K(30)*C(8) - sum(K(33:34))*C(9);
    DC(10) = K(7)*C(2) + K(17)*C(4) + K(25)*C(6) + K(32)*C(8) + K(34)*C(9) ...
        - sum(K(35:36))*K(10);
    DC(11) = K(2)*C(1) + K(9)*C(2) + K(12)*C(3) + K(18)*C(4) + K(21)*C(5) ...
        + K(25)*C(6) + 2*K(28)*C(7) + K(31)*C(8) + K(33)*C(9) + K(35)*C(10) ...
        - sum(K(37:38))*C(11);
    DC(12) = K(6)*C(2) + K(16)*C(4) + K(24)*C(6) + K(31)*C(8) + K(36)*C(10) ...
        + K(38)*C(11) - K(39)*C(12);
    DC(13) = K(1)*C(1) + K(10)*C(2) + K(11)*C(3) + K(19)*C(4) + K(20)*C(5) ...
         + K(26)*C(6) + K(27)*C(7) + K(32)*C(8) + K(33)*C(9) + K(36)*C(10) ...
         + 2*K(37)*C(11) + K(39)*C(12) - K(40)*C(13);
    DC(14) =  K(5)*C(2) + K(15)*C(4) + K(23)*C(6) + K(30)*C(8) ...
         + K(35)*C(10) + K(39)*C(12) + K(40)*C(13);
end

end
```

APPENDIX D

LIST OF PUBLICATIONS

- L. Negahdar, J. U. Oltmanns, S. Palkovits, and R. Palkovits, Kinetic investigation of the catalytic conversion of cellobiose to sorbitol, Applied Catalysis B: Environmental, 147(0):677–683, 2014.

- L. Negahdar, P. J. C. Hausoul, S. Palkovits, and R. Palkovits, Direct cleavage of sorbitol from oligosaccharides via a sequential hydrogenation–hydrolysis pathway, Applied Catalysis B: Environmental, 160:460–464, 2015.

- P. J. C. Hausoul, L. Negahdar, K. Schute, R. Palkovits, Unravelling the Ru/C-catalyzed Hydrogenation of Cellulosic Biomass, J. Am. Chem. Soc., submitted.

- L. Negahdar, M. G. Al-Shaal, F. J. Holzhäuser and R. Palkovits, Kinetic analysis of the catalytic hydrogenation of alkyl levulinates to gamma-valerolactone, Applied Catalysis A: General, submitted.

- L. Negahdar, I. V. Delidovich and R. Palkovits, Kinetics of cellulose and

hemicelluloses hydrolysis: insight into the reaction mechanism, Chemsuschem, submitted.

Bibliography

[1] P. McKendry. Energy production from biomass (part 1): overview of biomass. *Bioresource Technology*, 83(1):37–46, 2002.

[2] G. W. Huber, S. Iborra, and A. Corma. Synthesis of transportation fuels from biomass: chemistry, catalysts, and engineering. *Chemical Reviews*, 106(9):4044–98, 2006.

[3] B. Kamm, P.R. Gruber, and M. Kamm. *Biorefineries - Industrial Processes and Products*, volume 1. Wiley-VCH Verlag GmbH & Co. KGaA, Weinheim,, 2006.

[4] Roberto Rinaldi and Ferdi Schüth. Acid hydrolysis of cellulose as the entry point into biorefinery schemes. *ChemSusChem*, 2(12):1096–1107, 2009.

[5] Jan A. Geboers, Stijn Van de Vyver, Roselinde Ooms, Beau Op de Beeck, Pierre A. Jacobs, and Bert F. Sels. Chemocatalytic conversion of cellulose: opportunities, advances and pitfalls. *Catalysis Science & Technology*, 1(5):714–726, 2011.

[6] Stijn Van de Vyver, Jan Geboers, Pierre A. Jacobs, and Bert F. Sels. Recent advances in the catalytic conversion of cellulose. *ChemCatChem*, 3(1):82–94, 2011.

[7] Severian Dumitriu. *Polysaccharides : structural diversity and functional versatility*. Marcel Dekker, 2nd edition, 2005.

[8] D. Klemm, B. Heublein, H. P. Fink, and A. Bohn. Cellulose: Fascinating biopolymer and sustainable raw material. *Angewandte Chemie-International Edition*, 44(22):3358–3393, 2005.

[9] J. Bemiller and R. Whistler, editors. *Starch: Chemitry and Technology*. 2009.

[10] Niklas Meine, Roberto Rinaldi, and Ferdi Schüth. Solvent-free catalytic depolymerization of cellulose to water-soluble oligosaccharides. *ChemSusChem*, 5(8):1449–1454, 2012.

[11] Qinghua Zhang and Francois Jerome. Mechanocatalytic deconstruction of cellulose: An emerging entry into biorefinery. *ChemSusChem*, 6(11):2042–2044, 2013.

[12] Roberto Rinaldi, Regina Palkovits, and Ferdi Schüth. Depolymerization of cellulose using solid catalysts in ionic liquids. *Angewandte Chemie International Edition*, 47(42):8047–8050, 2008.

[13] V. Agbor, N. Cicek, R. Sparling, A. Berlin, and D.B. Levin. Biomass pretreatment fundamentals toward application. *Biothechnol. Adv.*, 29:675, 2011.

[14] Michael E. Himmel Shishir P.S. Chundawat, Gregg T. Beckham and Bruce E. Dale. Deconstruction of lignocellulosic biomass to fuels and chemicals. *Annu. Rev. Chem. Biomol. Eng.*, 2:121, 2011.

[15] JunSeok Kim, Y.Y. Lee, and RobertW. Torget. Cellulose hydrolysis under extremely low sulfuric acid and high-temperature conditions. *Applied Biochemistry and Biotechnology*, 91-93(1-9):331–340, 2001.

[16] N. S. Mosier, C. M. Ladisch, and M. R. Ladisch. Characterization of acid catalytic domains for cellulose hydrolysis and glucose degradation. *Biotechnology and Bioengineering*, 79(6):610–618, 2002.

[17] Qian Xiang, Y.Y. Lee, Pär. Pettersson, and RobertW. Torget. Heterogeneous aspects of acid hydrolysis of α-cellulose. pages 505–514, 2003.

[18] D. Fengel and G Wegener. *Wood: Chemistry, Ultrastructure, Reactions*. de Gruyter: Berlin.

[19] J. F. Saeman. Kinetics of wood saccharification - hydrolysis of cellulose and decomposition of sugars in dilute acid at high temperature. *Industrial and Engineering Chemistry*, 37(1):43–52, 1945.

[20] Christophe Blecker, Christian Fougnies, Jean-Claude Van Herck, Jean-Pol Chevalier, and Michel Paquot. Kinetic study of the acid hydrolysis of various oligofructose samples. *Journal of Agricultural and Food Chemistry*, 50(6):1602–1607, 2002.

[21] R Aguilar, J.A Ramirez, G Garrote, and M Vazquez. Kinetic study of the acid hydrolysis of sugar cane bagasse. *Journal of Food Engineering*, 55(4):309 – 318, 2002.

[22] N. Abatzoglov, J. Bouchard, E. Chornet, and R. P. Overend. Dilute acid depolymerization of cellulose in aqueous phase: Experimental evidence of the significant presence of soluble oligomeric intermediates. *The Canadian Journal of Chemical Engineering*, 64(5):781–786, 1986.

[23] R. D. Fagan, Grethlei.He, A. O. Converse, and A. Porteous. Kinetics of acid hydrolysis of cellulose found in paper refuse. *Environmental Science & Technology*, 5(6):545, 1971.

[24] BrightT. Kusema, Gerd Hilmann, Paivi Maki-Arvela, P.ki-Arvela, Stefan Willfor, Bjarne Holmbom, Tapio Salmi, and DmitryYu. Murzin. Selective hydrolysis of arabinogalactan into arabinose and galactose over heterogeneous catalysts. *Catalysis Letters*, 141(3):408–412, 2011.

[25] D. R. Thompson and H. E. Grethlein. Design and evaluation of a plug flow reactor for acid-hydrolysis of cellulose. *Industrial & Engineering Chemistry Product Research and Development*, 18(3):166–169, 1979.

[26] J. P. Franzidis, A. Porteous, and J. Anderson. The acid-hydrolysis of cellulose in refuse in a continuous reactor. *Conservation & Recycling*, 5(4):215–225, 1982.

[27] Green M Shelef G. Malester, I. A. Kinetics of dilute acid hydrolysis of cellulose originating from municipal solid wastes. *Ind. Eng. Chem. Prod. Res. Dev.*, 31:1998, 1992.

[28] Alireza Esteghlalian, Andrew G. Hashimoto, John J. Fenske, and Michael H. Penner. Modeling and optimization of the dilute-sulfuric-acid pretreatment of corn stover, poplar and switchgrass. *Bioresource Technology*, 59(2-3):129 – 136, 1997.

[29] L. Jimenez and J.L. Bonilla. Acid hydrolysis of sunflower residue biomass. *Process Biochemistry*, 28(4):243 – 247, 1993.

[30] S.K. Song and Y.Y. Lee. Acid hydrolysis of wood cellulose under low water condition. *Biomass*, 6(1-2):93 –100, 1984. 2nd Southern Biomass Energy Research Conference.

[31] Rongfu Chen, YoonY. Lee, and Robert Torget. Kinetic and modeling investigation on two-stage reverse-flow reactor as applied to dilute-acid pretreatment of agricultural residues. *Applied Biochemistry and Biotechnology*, 57-58(1):133–146, 1996.

[32] F. Camacho, P. Gonzalez-Tello, E. Jurado, and A. Robles. Microcrystalline-cellulose hydrolysis with concentrated sulphuric acid. *Journal of Chemical Technology & Biotechnology*, 67(4):350–356, 1996.

[33] R. Torget, P. Walter, M. Himmel, and K. Grohmann. Dilute-acid pretreatment of corn residues and short-rotation woody crops. *Applied Biochemistry and Biotechnology*, 28-29(1):75–86, 1991.

[34] A. H. Conner, B. F. Wood, C. G. Hill, and J. F. Harris. Kinetic model for the dilute sulfuric acid saccharification of lignocellulose. *J. Wood Chem. Technol.*, 5:461–489, 1985.

[35] William S. Mok, Michael J. Antal, and Gabor Varhegyi. Productive and parasitic pathways in dilute acid-catalyzed hydrolysis of cellulose. *Industrial & Engineering Chemistry Research*, 31(1):94–100, 1992.

[36] J. Bouchard, G. Garnier, P. Vidal, E. Chornet, and R.P. Overend. Characterization of depolymerized cellulosic residues. *Wood Science and Technology*, 24(2):159–169, 1990.

[37] D. R. Cahela, Y. Y. Lee, and R. P. Chambers. Modeling of percolation process in hemicellulose hydrolysis. *Biotechnology and Bioengineering*, 25(1):3–17, 1983.

[38] J. F. Harris, A. J. Baker, A. J. Conner, T. W. Minor Jeffries, R. C. J. L. Petterson, and Scott R. W. Two-stage, dilute sulfuric acid hydrolysis of wood : an investigation of fundamentals. *Gen. Tech. Rep.*, 1985.

[39] Robert Simha. Kinetics of degradation and size distribution of long chain polymers. *Journal of Applied Physics*, 12(7):569–578, 1941.

[40] Paolo Calvini, Andrea Gorassini, and AntonioLuigi Merlani. On the kinetics of cellulose degradation: looking beyond the pseudo zero order rate equation. *Cellulose*, 15(2):193–203, 2008.

[41] H.-Z. Ding and Z.D. Wang. On the degradation evolution equations of cellulose. *Cellulose*, 15(2):205–224, 2008.

[42] Vadim Mamleev, Serge Bourbigot, Michel Le Bras, Jacques Yvon, and Jeroen Snelders Lefebvre. Model-free method for evaluation of activation energies in modulated thermogravimetry and analysis of cellulose decomposition. *Chemical Engineering Science*, 61(4):1276 – 1292, 2006.

[43] D.K. Shen and S. Gu. The mechanism for thermal decomposition of cellulose and its main products. *Bioresource Technology*, 100(24):6496 – 6504, 2009.

[44] Allan G. W. Bradbury, Yoshio Sakai, and Fred Shafizadeh. A kinetic model for pyrolysis of cellulose. *Journal of Applied Polymer Science*, 23(11):3271–3280, 1979.

[45] Akash Tayal and Saad A. Khan. Degradation of water-soluble polymer: molecular weight changes and chain scission characteristics. *Macromolecules*, 33(26):9488–9493, 2000.

[46] Catherine H. Stephens, Paul M. Whitmore, Hannah R. Morris, and Mark E. Bier. Hydrolysis of the amorphous cellulose in cotton-based paper. *Biomacromolecules*, 9(4):1093–1099, 2008. PMID: 18324778.

[47] Jose-Henrique Q. Pinto and Serge Kaliaguine. A monte carlo analysis of acid hydrolysis of glycosidic bonds in polysaccharides. *AIChE Journal*, 37(6):905–914, 1991.

[48] Dadach Zin-Eddine, Pinto Q. Jose-Henrjque, and Serge Kaliaguine. Acid hydrolysis of cellulose. part ii: Stochastic simulation using a monte carlo technique. *The Canadian Journal of Chemical Engineering*, 72(1):106–112, 1994.

[49] J. N. Bemiller. Acid-catalyzed hydrolysis of glycosides. In L. Wolfrom Melville and R. Stuart Tipson, editors, *Advances in Carbohydrate Chemistry*, volume Volume 22, pages 25–108. Academic Press, 1967.

[50] O. Bobleter, W. Schwald, R. Concin, and H. Binder. Hydrolysis of cellobiose in dilute sulfuric-acid and under hydrothermal conditions. *Journal of Carbohydrate Chemistry*, 5(3):387–399, 1986.

[51] Ortwin Bobleter and Guenther Bonn. The hydrothermolysis of cellobiose and its reaction-product d-glucose. *Carbohydrate Research*, 124(2):185 – 193, 1983.

[52] K. Freudenberg. Hydrolysis and optical rotation of cellulose, starch, and cycloglucans. *J. Polym. Sci*, pages 791–799, 1957.

[53] J. F. Harris M. S. Feather. Partial hydrolysis and acetolysis of cellotriose c14. *J. Am. Chem. Soc.*, 89(22):5661–5664, 1967.

[54] Melvin S. Weintraub and Dexter French. Acid hydrolysis of d-glucans : Part ii. analysis of products from radioactive oligosaccharides. *Carbohydrate Research*, 15(2):251 – 262, 1970.

[55] J. Szejtli J. Hollo, E. Laszlo and G. Zala. Die biosynthesis starke. *Staerke*, 16:211, 1964.

[56] A. M. Ruppert, K. Weinberg, and R. Palkovits. Hydrogenolysis goes bio: From carbohydrates and sugar alcohols to platform chemicals. *Angewandte Chemie-International Edition*, 51(11):2564–2601, 2012.

[57] Marcus Rose and Regina Palkovits. Isosorbide as a renewable platform chemical for versatile applications-quo vadis? *ChemSusChem*, 5(1):167–176, 2012.

[58] R. D. Cortright, R. R. Davda, and J. A. Dumesic. Hydrogen from catalytic reforming of biomass-derived hydrocarbons in liquid water. *Nature*, 418(6901):964–967, 2002.

[59] J. Geboers, S. Van de Vyver, K. Carpentier, K. de Blochouse, P. Jacobs, and B. Sels. Efficient catalytic conversion of concentrated cellulose feeds to hexitols with heteropoly acids and ru on carbon. *Chem Commun (Camb)*, 46(20):3577–9, 2010.

[60] R. Palkovits, K. Tajvidi, J. Procelewska, R. Rinaldi, and A. Ruppert. Hydrogenolysis of cellulose combining mineral acids and hydrogenation catalysts. *Green Chemistry*, 12(6):972–978, 2010.

[61] R. Palkovits, K. Tajvidi, A. M. Ruppert, and J. Procelewska. Heteropoly acids as efficient acid catalysts in the one-step conversion of cellulose to sugar alcohols. *Chem Commun (Camb)*, 47(1):576–8, 2011.

[62] Walter M Kruse and Leon W Wright. Polyhydric alcohol production using ruthenium zeolite catalyst. Google Patents, 1976.

[63] Jan Lolkema. Process for hydrogenation of polysaccharides. Google Patents, 1952.

[64] Utpal K. Singh and M.Albert Vannice. Kinetics of liquid-phase hydrogenation reactions over supported metal catalysts-a review. *Applied Catalysis A: General*, 213(1):1 – 24, 2001.

[65] P. Harriott. *Chemical reactor design*. CRC Press, 2002, 2003.

[66] C. Hinshelwood. *The Kinetics of Chemical Change*. Clarendon Press, 1940.

[67] OA. Hougen and W. K.Watson. *Chemical process principles*. Wiley, 1947.

[68] T. Salmi, D. Y. Murzin, J. P. Mikkola, J. Warna, P. Maki-Arvela, E. Toukoniitty, and S. Toppinen. Advanced kinetic concepts and experimental methods for catalytic three-phase processes. *Industrial & Engineering Chemistry Research*, 43(16):4540–4550, 2004.

[69] F. Kapteijn, J. A. Moulijn, R. A. van Santen, and R. Wever. Chemical kinetics of catalyzed reactions. *Catalysis: An Integrated Approach, Second Ed.*, 123:81–106, 1999.

[70] C. N. Satterfield. Citation classic - mass-transfer in heterogeneous catalysis. *Current Contents/Engineering Technology & Applied Sciences*, (41):E10–E10, 1979.

[71] H. A. Pray, C. E. Schweickert, and B. H. Minnich. Solubility of hydrogen, oxygen, nitrogen, and helium in water - at elevated temperatures. *Industrial and Engineering Chemistry*, 44(5):1146–1151, 1952.

[72] E. Dietrich, C. Mathieu, H. Delmas, and J. Jenck. Raney-nickel catalyzed hydrogenations - gas-liquid mass-transfer in gas-induced stirred slurry reactors. *Chemical Engineering Science*, 47(13-14):3597–3604, 1992.

[73] T. Adachi Y. Sano, N. Yamaguchi. Mass transfer coefficients for suspended particles in agitated vessels and bubble columns. *Journal of Chemical Engineering of Japan*, 7:255, 1974.

[74] Roland Dittmeyer and Gerhard Emig. *Simultaneous Heat and Mass Transfer and Chemical Reaction.* Wiley-VCH Verlag GmbH & Co. KGaA, 2008.

[75] Paresh L Dhepe and Atsushi Fukuoka. Cellulose conversion under heterogeneous catalysis. *ChemSusChem*, 1(12):969–975, 2008.

[76] Atsushi Fukuoka and Paresh L. Dhepe. Catalytic conversion of cellulose into sugar alcohols. *Angewandte Chemie International Edition*, 45(31):5161–5163, 2006.

[77] G. F. Liang, C. Y. Wu, L. M. He, J. Ming, H. Y. Cheng, L. H. Zhuo, and F. Y. Zhao. Selective conversion of concentrated microcrystalline cellulose to isosorbide over ru/c catalyst. *Green Chemistry*, 13(4):839–842, 2011.

[78] Hui Li, Dongsheng Chu, Jun Liu, Minghua Qiao, Weilin Dai, and Hexing Li. A novel ruthenium-phosphorus amorphous alloy catalyst for maltose

hydrogenation to maltitol. *Advanced Synthesis & Catalysis*, 350(6):829–836, 2008.

[79] K van Gorp, E Boerman, C.V Cavenaghi, and P.H Berben. Catalytic hydrogenation of fine chemicals: sorbitol production. *Catalysis Today*, 52(2-3):349 – 361, 1999.

[80] Victor A Sifontes, Daniel Rivero, JohanP. Warana, J.-P. Mikkola, and TapioO. Salmi. Sugar hydrogenation over supported ru/c-kinetics and physical properties. *Topics in Catalysis*, 53(15-18):1278–1281, 2010.

[81] N. Yan, C. Zhao, C. Luo, P. J. Dyson, H. C. Liu, and Y. Kou. One-step conversion of cellobiose to c-6-alcohols using a ruthenium nanocluster catalyst. *Journal of the American Chemical Society*, 128(27):8714–8715, 2006.

[82] W. P. Deng, M. Liu, X. S. Tan, Q. H. Zhang, and Y. Wang. Conversion of cellobiose into sorbitol in neutral water medium over carbon nanotube-supported ruthenium catalysts. *Journal of Catalysis*, 271(1):22–32, 2010.

[83] Jianrong Li, Helena S. M. P. Soares, Jacob A. Moulijn, and Michiel Makkee. Simultaneous hydrolysis and hydrogenation of cellobiose to sorbitol in molten salt hydrate media. *Catalysis Science & Technology*, 3(6):1565, 2013.

[84] B. Kusserow, S. Schimpf, and P. Claus. Hydrogenation of glucose to sorbitol over nickel and ruthenium catalysts (vol 345, pg 289, 2003). *Advanced Synthesis & Catalysis*, 345(9-10):A102–A102, 2003.

[85] Jens Uwe Oltmanns, Stefan Palkovits, and Regina Palkovits. Kinetic investigation of sorbitol and xylitol dehydration catalyzed by silicotungstic acid in water. *Applied Catalysis A: General*, 456(0):168–173, 2013.

[86] E. Crezee. Three-phase hydrogenation of d-glucose over a carbon supported ruthenium catalyst-mass transfer and kinetics. *Applied Catalysis A: General*, 251(1):1–17, 2003.

[87] A. Yamaguchi, N. Hiyoshi, O. Sato, and M. Shirai. Sorbitol dehydration in high temperature liquid water. *Green Chemistry*, 13(4):873–881, 2011.

[88] L. Vanoye, M. Fanselow, J. D. Holbrey, M. P. Atkins, and K. R. Seddon. Kinetic model for the hydrolysis of lignocellulosic biomass in the ionic liquid, 1-ethyl-3-methyl-imidazolium chloride. *Green Chemistry*, 11(3):390–396, 2009.

[89] B. M. Kabyemela, M. Takigawa, T. Adschiri, R. M. Malaluan, and K. Arai. Mechanism and kinetics of cellobiose decomposition in sub- and supercritical water. *Industrial & Engineering Chemistry Research*, 37(2):357–361, 1998.

[90] Y. Kimura S. Adachi R. Matsuno T. Oomori, S. H. Khajavi. Hydrolysis of disaccharides containing glucose residue in subcritical water. *Biochem. Eng. J.*, 18:143–147, 2004.

[91] Leila Negahdar, Jens U. Oltmanns, Stefan Palkovits, and Regina Palkovits. Kinetic investigation of the catalytic conversion of cellobiose to sorbitol. *Applied Catalysis B: Environmental*, 147(0):677–683, 2014.

[92] M. L. Wolfrom and J. C. Dacons. The polymer-homologous series of oligosaccharides from cellulose. *J. Am. Chem. Soc*, 74:5331–5333, 1952.

[93] Daniel T Gillespie. The mathematics of brownian motion and johnson noise. *American Journal of Physics*, 64(3):225–239, 1996.

[94] Daniel T Gillespie. The multivariate langevin and fokker–planck equations. *American Journal of Physics*, 64(10):1246–1257, 1996.

[95] Daniel T Gillespie. Stochastic simulation of chemical kinetics. *Annu. Rev. Phys. Chem.*, 58:35–55, 2007.

[96] Donald A McQuarrie. Stochastic approach to chemical kinetics. *Journal of Applied Probability*, 4(3):413–478, 1967.

[97] Michael A Gibson and Jehoshua Bruck. Efficient exact stochastic simulation of chemical systems with many species and many channels. *The journal of physical chemistry A*, 104(9):1876–1889, 2000.

[98] Anders Nattorp, Martin Graf, Christian Spühler, and Albert Renken. Model for random hydrolysis and end degradation of linear polysaccharides: Application to the thermal treatment of mannan in solution. *Industrial & engineering chemistry research*, 38(8):2919–2926, 1999.

[99] C. R. Wilke and Pin Chang. Correlation of diffusion coefficients in dilute solutions. *AIChE Journal*, 1(2):264–270, 1955.

[100] J. J. Barker and R. E. Treybal. Mass transfer coefficients for solids suspended in agitated liquids. *AIChE Journal*, 6(2):289–295, 1960.

[101] F. B. Bizhanov and R. B. Drozdova. Studies of the kinetics and mechanism of glucose hydrogenation over ruthenium catalysts. *Reaction Kinetics and Catalysis Letters*, 21(1-2):35–39, 1982.

[102] W. E. Cake. The catalytic hydrogenation of dextro glucose. preliminary notice. *Journal of the American Chemical Society*, 44(4):859–861, 1922.

[103] A. Corma, S. Iborra, and A. Velty. Chemical routes for the transformation of biomass into chemicals. *Chemical Reviews*, 107(6):2411–502, 2007.

[104] W. P. Deng, X. S. Tan, W. H. Fang, Q. H. Zhang, and Y. Wang. Conversion of cellulose into sorbitol over carbon nanotube-supported ruthenium catalyst. *Catalysis Letters*, 133(1-2):167–174, 2009.

[105] W. P. Deng, Y. L. Wang, Q. H. Zhang, and Y. Wang. Development of bifunctional catalysts for the conversions of cellulose or cellobiose into polyols and organic acids in water. *Catalysis Surveys from Asia*, 16(2):91–105, 2012.

[106] US Department of Energy. Top value added chemicals from biomass. 2004.

[107] George J Gauthier and John D Miceli. Dual catalyst sequential method for production of sorbitol from hydrolyzed starch solution. Google Patents, 1987.

[108] J. Geboers, S. Van de Vyver, K. Carpentier, P. Jacobs, and B. Sels. Efficient hydrolytic hydrogenation of cellulose in the presence of ru-loaded zeolites and trace amounts of mineral acid. *Chemical Communications*, 47(19):5590–5592, 2011.

[109] Jan Geboers, Stijn Van de Vyver, Kevin Carpentier, Pierre Jacobs, and Bert Sels. Hydrolytic hydrogenation of cellulose with hydrotreated caesium salts of heteropoly acids and ru/c. *Green Chemistry*, 13(8):2167–2174, 2011.

[110] Daniel T Gillespie. A rigorous derivation of the chemical master equation. *Physica A: Statistical Mechanics and its Applications*, 188(1):404–425, 1992.

[111] Daniel T Gillespie. Exact stochastic simulation of coupled chemical reactions. *The journal of physical chemistry*, 81(25):2340–2361, 1977.

[112] Daniel T Gillespie. A general method for numerically simulating the stochastic time evolution of coupled chemical reactions. *Journal of computational physics*, 22(4):403–434, 1976.

[113] Marino Guaita, Oscar Chiantore, and Maria Paola Luda. Monte carlo simulations of polymer degradations. 1. degradations without volatilization. *Macromolecules*, 23(7):2087–2092, 1990.

[114] Jakob Hilgert, Niklas Meine, Roberto Rinaldi, and Ferdi Schüth. Mechanocatalytic depolymerization of cellulose combined with hydrogenolysis as a highly efficient pathway to sugar alcohols. *Energy & Environmental Science*, 6(1):92–96, 2013.

[115] B. Hoffer. The role of the active phase of raney-type ni catalysts in the selective hydrogenation of d-glucose to d-sorbitol. *Applied Catalysis A: General*, 253(2):437–452, 2003.

[116] B. W. Hoffer, P. H. J. Schoenmakers, P. R. M. Mooijman, G. M. Hamminga, R. J. Berger, A. D. van Langeveld, and J. A. Moulijn. Mass transfer and kinetics of the three-phase hydrogenation of a dinitrile over a raney-type nickel catalyst. *Chemical Engineering Science*, 59(2):259–269, 2004.

[117] R. Simon J. Wisniak. *Ind. Eng. Chem. Prod. Res. Dev.*, 18:50, 1979.

[118] B. Kamm, M. Kamm, M. Schmidt, I. Starke, and E. Kleinpeter. Chemical and biochemical generation of carbohydrates from lignocellulose-feedstock (lupinus nootkatensis)–quantification of glucose. *Chemosphere*, 62(1):97–105, Jan 2006.

[119] Leo Kasehagen. Hydrogenation of carbohydrates. Google Patents, 1961.

[120] A. P. G. Kieboom, J. F. De Kreuk, and H. Van Bekkum. Substituent effects in the hydrogenolysis of benzyl alcohol derivatives over palladium. *Journal of Catalysis*, 20(1):58–66, 1971.

[121] John Frank Charles Kingman. *Poisson processes*, volume 3. Oxford university press, 1992.

[122] Hirokazu Kobayashi and Atsushi Fukuoka. Synthesis and utilisation of sugar compounds derived from lignocellulosic biomass. *Green Chemistry*, 15(7):1740–1763, 2013.

[123] H. Kobayashi, Y. Ito, T. Komanoya, Y. Hosaka, P. L. Dhepe, K. Kasai, K. Hara, and A. Fukuoka. Synthesis of sugar alcohols by hydrolytic hydrogenation of cellulose over supported metal catalysts. *Green Chemistry*, 13(2):326–333, 2011.

[124] Cornelis Martians Hendrik Kool. Process of manufacturing polyhydric. Google Patents, 1956.

[125] A. Y. Kovalevsky, L. Hanson, S. Z. Fisher, M. Mustyakimov, S. A. Mason, V. T. Forsyth, M. P. Blakeley, D. A. Keen, T. Wagner, H. L. Carrell, A. K. Katz, J. P. Glusker, and P. Langan. Metal ion roles and the movement of hydrogen during reaction catalyzed by d-xylose isomerase: a joint x-ray and neutron diffraction study. *Structure*, 18(6):688–99, 2010.

[126] Ning Li and George W. Huber. Aqueous-phase hydrodeoxygenation of sorbitol with pt/sio2-al2o3: Identification of reaction intermediates. *Journal of Catalysis*, 270(1):48–59, 2010.

[127] Michiel Makkee, Antonius P. G. Kieboom, and Herman van Bekkum. Hydrogenation of d-fructose and d-fructose/d-glucose mixtures. *Carbohydrate Research*, 138(2):225–236, 1985.

[128] L. C. A. Maranhao, F. G. Sales, J. A. F. R. Pereira, and C. A. M. Abreu. Kinetic evaluation of polyol production by three-phase catalytic hydrogenation of saccharides. *Reaction Kinetics and Catalysis Letters*, 81(1):169–175, 2004.

[129] P. McKendry. Energy production from biomass (part 3): gasification technologies. *Bioresource Technology*, 83(1):55–63, 2002.

[130] David R. Morris, Lietai Yang, Frank Giraudeau, Xiadong Sun, and Frank R. Steward. Henry's law constant for hydrogen in natural water and deuterium in heavy water. *Physical Chemistry Chemical Physics*, 3(6):1043–1046, 2001.

[131] Beau Op de Beeck, Jan Geboers, Stijn Van de Vyver, Jonas Van Lishout, Jeroen Snelders, Wouter J. J. Huijgen, Christophe M. Courtin, Pierre A. Jacobs, and Bert F. Sels. Conversion of (ligno)cellulose feeds to isosorbide with heteropoly acids and ru on carbon. *ChemSusChem*, 6(1):199–208, 2013.

[132] Y. Roman-Leshkov, M. Moliner, J. A. Labinger, and M. E. Davis. Mechanism of glucose isomerization using a solid lewis acid catalyst in water. *Angewandte Chemie. International Edition in English*, 49(47):8954–7, 2010.

[133] Jane F. Ruddlesden, Allan Stewart, David J. Thompson, and Russell Whelan. Diastereoselective control in ketose hydrogenations with supported copper and nickel catalysts. *Faraday Discussions of the Chemical Society*, 72(0):397–411, 1981.

[134] Clarissa O. da Silva, Benedetta Mennucci, and Thom Vreven. Density functional study of the optical rotation of glucose in aqueous solution. *The Journal of Organic Chemistry*, 69(23):8161–8164, 2004/11/01 2004.

[135] Abraham Tamir. *Applications of Markov chains in chemical engineering*. Elsevier, 1998.

[136] J. B. Taylor and J. S. Rowlinson. The thermodynamic properties of aqueous solutions of glucose. *Transactions of the Faraday Society*, 51:1183, 1955.

[137] N. A. Vasyunina and G. S. Barysheva. Hydrolytic hydrogenation of saccharose. *Bulletin of the Academy of Sciences of the USSR, Division of chemical science*, 23(7):1506–1508, 1974.

[138] Gert de Wit, Jan J. de Vlieger, Alida C. Kock-van Dalen, Roelf Heus, Rob Laroy, Antonius J. van Hengstum, Antonius P. G. Kieboom, and Herman van Bekkum. Catalytic dehydrogenation of reducing sugars in alkaline solution. *Carbohydrate Research*, 91(2):125–138, 1981.

[139] Mizuho Yabushita, Hirokazu Kobayashi, and Atsushi Fukuoka. Catalytic transformation of cellulose into platform chemicals. *Applied Catalysis B: Environmental*, 145(0):1–9, 2014.

[140] Joseph Zakzeski, Anna L. Jongerius, Pieter C. A. Bruijnincx, and Bert M. Weckhuysen. Catalytic lignin valorization process for the production of aromatic chemicals and hydrogen. *ChemSusChem*, 5(8):1602–1609, 2012.

[141] Yi-Heng Percival Zhang, Shi-You Ding, Jonathan R. Mielenz, Jing-Biao Cui, Richard T. Elander, Mark Laser, Michael E. Himmel, James R. McMillan, and Lee R. Lynd. Fractionating recalcitrant lignocellulose at modest reaction conditions. *Biotechnology and Bioengineering*, 97(2):214–223, 2007.